SLAC-PUB-1595
June 1975
(T/E)

LARGE TRANSVERSE MOMENTUM PROCESSES*

Dennis Sivers, Stanley J. Brodsky, and Richard Blankenbecler
Stanford Linear Accelerator Center
Stanford University, Stanford, California 94305

(Submitted to Physics Reports)

*Work supported by the U. S. Energy Research and Development Administration.

ABSTRACT

We present a comprehensive survey of experimental and theoretical work on large transverse momentum processes. Exclusive data and single particle inclusive measurements are summarized and some discussion of multiparticle inclusive data is included. We review many of the predictions of nonparton models including the geometrical, statistical, eikonal and bootstrap approaches. A more detailed discussion is given of the structure of models based on the hard scattering of constituents. The predictions for hadronic and electromagnetic processes based on quark counting rules and the constituent interchange model (CIM) are summarized. We present numerous comparisons with experiment and indicate the framework for the comparison with new experimental data. Recent theoretical progress in the problem of relating short distance structure of hadrons with the asymptotic behavior of form factors and fixed angle amplitudes is also reviewed. We include a brief discussion of the possible influence of new hadronic degrees of freedom on large-p_T phenomena. Finally, we attempt to anticipate the type of experiments which will prove decisive in the understanding of this subject.

TABLE OF CONTENTS

LIST OF TABLES

I. INTRODUCTION

A. Large Transverse Momentum Reactions and the Structure of Hadrons

It has long been known that the average hadron-hadron collision produces particles with low transverse momentum. A few years ago, early experiments at the CERN-ISR indicated that the probability of producing a particle with large transverse momentum, though quite small, is actually several orders of magnitude higher than might have been expected on the basis of a simple extrapolation of the low transverse momentum data. While these experimental results were not as dramatic as the famous Rutherford α-particle scattering experiments (Rutherford, 1911), they may have the same sort of significance. It is apparent that it is not feasible to conceive of hadronic collision processes as occurring between structureless matter distributions but that there is an effective nonuniformity characterized by a small distance scale or perhaps by pointlike constituents.

In the past decade, the observation of scale-invariant electron and muon scattering at large momentum transfer has demonstrated that hadrons have an effective pointlike constituent structure. These experimental data have been well explained in terms of the quark-parton model, in which the carriers of the currents are structureless but yet carry a finite fraction of the hadron's momentum. Thus one expects that hadrons can scatter to large transverse momentum via hard, large angle scattering processes involving their constituents. The possibility that the large transverse momentum processes involving only hadrons are directly related to the deep inelastic lepton induced reactions has attracted a great deal of attention. We will devote the major portion of this review exploring and pursuing the consequences of this type of connection.

In contrast, there have been numerous attempts to explain the large transverse momentum processes without invoking partons. These models lack some of the attractive features of quark-parton models in that they do not make the kind of unification between hadron spectroscopy, electroproduction and hadronic scattering possible in the quark model. They are important, however, in order to see how far we can go without invoking quarks and in order to define what constitutes a definitive test of the application of quark-parton ideas to hadronic scattering.

Even if granted the basic postulates of the quark-parton picture of hadronic structure, one must still admit that the violent collision of hadrons is a more difficult way to probe that structure than deep inelastic lepton-hadron since both the beam and target particles possess unknown complexity. To use an analogy due to Feynman, studying hadron-hadron collisions is like smashing two watches together and watching the gears fly out! Pursuing this analogy we see that the production of large p_T hadrons in such a collision provides a unique way to studying the, possibly fundamental, "gear-gear" interaction. The ultimate goal is to understand both lepton and hadron-induced reactions within the same basic framework and to unravel the essential dynamical degrees of freedom of the hadrons. The variety of information on violent hadronic interactions which is experimentally accessible is large and there are many opportunities for testing and refining our theoretical ideas. The extra complexity in the hadron-hadron interaction, if it can be handled, offers the possibility of a richer lode of information. Conceivably, such information could help illuminate the central mystery of quark-parton models: the mechanism of confinement which prevents quarks from being observed singly.

In this review we will attempt to summarize what is known experimentally about large transverse momentum reactions as well as to examine the current theoretical speculations. This summary will be as current as possible but the nature of the field is such that there may be substantial new information and possible "surprises" from new experiments that we have not been able to cover. The cutoff date on experimental information is roughly January 1, 1975.

Our review is organized as follows. The remainder of the introduction will present some general theoretical concepts and should serve to warn the careful reader of our personal prejudices. We also outline here the main implications of the data for various theories, the connection between small-p_T and large-p_T phenomena, and the interelation between large p_T inclusive production and exclusive large-angle scattering. In Section II we discuss in further detail the main experiments and try to extract the phenomenological features of the data. In Section III we review model approaches to large transverse momentum which do not involve partons including eikonal, bootstrap, fireball and thermodynamic models. Interestingly enough, we find that many features of the data can be understood in these purely hadronic terms. In Section IV we return to a more careful treatment of hard collision models. Particular emphasis is placed on the separation of short-distance and large-distance phenomena, the dimensional counting ansatz and specific features of the constituent interchange model. We also include a review of recent theoretical treatments of the elastic form factor. In Section V we conclude with a discussion of how experiments may be able to discriminate between models. The appendices include a derivation of the basic equation of the hard scattering model and a comparison of different techniques for calculations. We also discuss areas ripe for more theoretical work. Large

transverse momentum physics is just at its infancy and this review can only be a small step toward illuminating a crucial new area of hadronic physics.

B. Implications of Power-Law Scaling for Inclusive Cross Sections

The fact that the observed inclusive spectrum of hadrons produced at large transverse momentum at the CERN-ISR was much larger than an extrapolation of the form $\exp(-6p_T)$ based on the Hagedorn thermodynamic model suggests that the data can be explained in a hard scattering model. In these models, because of the assumed structureless nature of the constituents the general form of the invariant cross section for $A+B \rightarrow C+\text{ANYTHING}$ is predicted to be

$$\frac{d^3\sigma}{d^3p/E}(s,t,\mathcal{M}^2) \underset{p_T^2 \gg m^2}{\longrightarrow} \frac{1}{\left(p_T^2\right)^N} f(t/s,\mathcal{M}^2/s) \qquad \text{(IB. 1)}$$

where $p_T^2 \cong tu/s$ and $\mathcal{M}$ is the missing mass. We call this factorization of the cross section into a power times a function of the dimensionless "scaling" parameters power law scaling. For two-body exclusive processes $A+B \rightarrow C+D$ at fixed θ_{CM} the analogous scaling form is

$$\frac{d\sigma}{dt}(s,t) \underset{p_T^2 \gg m^2}{\longrightarrow} \frac{1}{\left(p_T^2\right)^N} f(t/s) \qquad \text{(IB. 2)}$$

This latter scaling law also implies the power law falloff for the electromagnetic form factors of hadrons. In general, the value of N in (IB. 1) and (IB. 2) depends on the particles involved.

There is substantial experimental evidence for the approximate validity of (IB. 1) and (IB. 2) which we will examine in more detail later. The one thing we want to note here is that a simple parametrization of the inclusive cross section

$pp \to \pi^0$ anything (see Fig. I. 1), can be written (Busser et al., 1973)

$$\frac{d^3\sigma}{d^3p/E}(pp \to \pi^0 X) \cong \frac{120\ \mathrm{mb/GeV}^2}{\left[p_T^2 + 1\ \mathrm{GeV}^2\right]^4} e^{-13x_T} \qquad 0.1 < x_T < 0.4 \qquad \text{(IB. 3)}$$

where $x_T = p_T/p_T\,\mathrm{max} \cong 2p_T/\sqrt{s}$. Charged pion data at FNAL (for $0.3 < x_T < 0.7$) seems to fall even more rapidly with p_T, roughly as p_T^{-12} (Cronin et al., 1973) .

It is interesting to compare this empirical formula with the observation of Bjorken scaling for deep inelastic lepton production. We can write the invariant cross section as

$$\frac{d^3\sigma}{d^3p/E}(ep \to eX) = \frac{4\pi\alpha^2}{t^2} f(t/s, \mathcal{M}^2/s)$$
$$s \gg m^2,\ \mathcal{M}^2/s,\ t/s \text{ fixed} \qquad \text{(IB. 4)}$$

which is equivalent to

$$\frac{d^3\sigma}{d^3p/E}(ep \to eX) \propto \frac{1}{p_T^4} \tilde{f}\left(\theta_{cm}, \mathcal{M}^2/s\right) \qquad \text{(IB. 5)}$$

This formula displays the scale-invariance of the lepton inclusive cross section. There is apparently no relevant mass involved in this reaction. To the extent that scale invariance is valid experimentally, we can deduce (in the one-photon approximation) that the usual structure functions $W_1(p\cdot q, q^2)$ and $\nu W_2(p\cdot q, q^2)$ are functions only of the variable $x = -t/(\mathcal{M}^2 - t)$.

Since the data now imply that the electromagnetic interactions within hadrons are essentially scale-invariant, it is evident that the exchange of one photon will lead to a scale invariant cross section for hadron-hadron collisions. This fact has been emphasized by Berman, Bjorken and Kogut (1971). The cross section for one-photon exchange for hadrons is, however, everywhere more than four orders of magnitude smaller than the current data (see Fig. I. 2). Using (IB. 3)

to extrapolate, we can surmise that one-photon exchange may be important at $\sqrt{s} \cong 2000$ GeV and $p_T \cong 45$ GeV/c which is near the upper limits of the range of possible future Isabelle experiments. At very high p_T we might also have a contribution from the weak interactions of hadrons. The kinematic range where all three types of interactions are potentially important is likely to be full of surprises.

In view of the form predicted for one-photon exchange, a natural ansatz for violent hadron-hadron collisions proposed by Berman, Bjorken and Kogut (1971) and in a different form by Berman and Jacob (1970) is that there is a contribution due to the carriers of the electromagnetic current interacting through vector gluon exchange. It is conventional to assume that the coupling constant which characterizes this interaction is dimensionless, as in QED, in order to have a renormalizable theory. This, in turn, leads to a scale-invariant cross section $Ed^3\sigma/d^3p \propto p_T^{-4} f(t/s, \mathcal{M}^2/s)$ in contrast to the parametrization (IB.3). Within the context of this model, however, the observed p_T behavior might be interpreted as implying that the matrix element is not dimensionless.

One of the major problems in understanding the relevance of quark-parton ideas to violent hadron-hadron collisions is then the apparent absence of this p_T^{-4} contribution. One simple possibility is just to assume a super-renormalizable theory such as an underlying $g\phi^3$ theory in order that the coupling constant possesses units of mass. As discussed by scalar exchange will give the observed p_T^{-8} behavior. Another possibility is that, due to kinematic requirements and the absence of observable quarks, a particle with form factor $F(t) \sim (1-t/m^2)^{-1}$ is always involved in the interaction. This contribution is important in the Constituent Interchange Model (CIM) of Blankenbecler, Brodsky and Gunion (1972a, b), the related model of Landshoff and Polkinghorne (1973a), and, as discussed by Ellis (1974a, b) contributes to a "semi-inclusive" mode of the parton gluon model.

It is not clear, however, that merely removing the possible p_T^{-4} term solves all the problems. Data from the Chicago-Princeton group on $pp \rightarrow \pi^{\pm}X$ and Fermilab indicates the situation is more complicated in that a single term of the form (IB. 1) apparently cannot fit all the data since the effective power of N in (IB. 1) is different in different kinematic regions. The most natural ways of reconciling all the data is to assume that a sum of power law scaling terms is needed or that N depends on x_T. Correlation experiments can tell these options apart, as we shall see.

A sum of terms is actually predicted in the constituent interchange model (CIM) of Blankenbecler, Brodsky and Gunion and in the massive quark model of Preparata (1974a, b). One finds that different terms with different powers of p_T dominate in different parts of the CP experiment. A quite acceptable fit to the FNAL and ISR data can be achieved with a two-term parametrization although, in principle, there is no reason to exclude more terms. The soft gluon model of Fried, Gaisser and Kirby (1973) predicts that N increases with x_T (Fried, 1974).

In the former vein, Bander, Barnett and Silverman (1974) and Ellis (1974a) suggest that three types of mechanisms can be important—each dominant within its own regime in x_T. At small x_T quark-quark scattering is important, at intermediate x_T quark-hadron processes become more important, and as one moves toward the exclusive boundary only hadron-hadron contributions may be important. Experimentally, this is still very much a possibility as long as the p_T^{-4} contribution is small. Within the context of asymptotically free gauge theories there might be some reasons for this type of suppression (Cahalan, Geer, Kogut, and Susskind, 1974).

As noted by Ellis (1974a) the production of "jets", many hadrons with a total transverse momentum of p_T, may show a p_T^{-4} scaling law even though the

production of a single hadron, at ISR energies, falls off more rapidly. Similarly, in a model due to Preparata (1974a, b), a scale invariant form will not arise until $q\bar{q} \rightarrow$ two "fireballs" becomes possible. We will discuss the predictions of all these distinct models for inclusive spectra in more detail and see to what extent current or projected experimental data will allow us to distinguish models. In any event the apparent absence of a scale-invariant quark-quark contribution in current data is of enormous theoretical importance from a quark-parton viewpoint and is one of the most striking indications that there are important aspects of hadron structure not seen in deep inelastic lepton scattering but which can be studied in large-p_T hadronic collisions.

C. Further Implications of the Large-Transverse-Momentum Data—Feynman Scaling

The different kinematic regions of the inclusive process $AB \rightarrow C + \text{anything}$ are defined in the Peyrou plot shown in Fig. I.3 . The invariant cross section is described in terms of the center-of-mass variables, p_T, θ_{CM} and ϵ,

$$\begin{aligned} p_T^2 &= tu/s \\ -t/s &\cong \frac{1}{2}(1-\cos\theta_{CM}) \\ -u/s &\cong \frac{1}{2}(1+\cos\theta_{CM}) \\ \epsilon = \mathcal{M}^2/s &\cong 1-x_R = 1-\left(x_T^2+x_L^2\right)^{1/2} \end{aligned} \qquad \text{(IC. 1)}$$

where $\mathcal{M}$ is the missing mass, $x_T = p_T/p_{CM}^{max}$ and $x_L = p_L/p_{CM}^{max}$. The radial distance from the perimeter of the Peyrou plot is measured by ϵ.

The small-p_T region where $x_T \cong 0$ contains the bulk of the data. By convention it is further subdivided at high energy into the "central" region, $x_L \cong 0$, the "triple-Regge" region, $x_L \cong 1$, and the "fragmentation" region consisting

of all intermediate values of x_L. The large-p_T or "deep" region is the one in which we are primarily interested here. It extends from $p_T > 2$–3 GeV/c right out to $\epsilon = 0$, the exclusive limit. Since the deep region shares boundaries with each of the others, important constraints on hadronic theories can be obtained by requiring a smooth connection between this and the other kinematic regions.

One important feature of the inclusive cross section data is the approximate validity of Feynman scaling. For small transverse momentum this means we can write

$$\frac{d^3\sigma}{d^3p/E}(s, p_T, x_L) \sim f(p_T, x_L) \qquad \text{(IC. 2)}$$

This approximate asymptotic energy independence is expected theoretically to be valid to within logarithmic factors. These factors are important in the discussion of the asymptotic behavior of total cross sections but they will be neglected here.

As one continues out into the deep region, Feynman scaling is expected to generalize. One possible simple generalization is to write

$$\frac{d^3\sigma}{d^3p/E}(s, p_T, x_R) \sim f(p_T, x_R) \quad . \qquad \text{(IC. 3)}$$

At fixed p_T, $x_T \cong 2p_T/\sqrt{s}$ goes to zero as $s \to \infty$ and we expect some energy dependence of the cross section associated with this fact. This does not mean that Feynman scaling fails at large p_T, it merely means that correction terms depend on p_T so that scaling is approached more slowly at large p_T. One can argue that the approach to scaling is largely kinematic in that the energy behavior of $pp \to \bar{p}$ and the energy behavior of $pp \to \pi$ are very similar if they are compared at the same value of "effective mass", $\sqrt{m^2+p_T^2}$. This point is emphasized in Fig. I. 4 taken from the review of Walker (1973).

If we view hadrons as composite or complex systems, it is interesting to ask what the effective energy of the fundamental interactions in a collision might be. For ordinary production processes most of the energy is radiated as hadronic "bremsstrahlung" down the beam direction. High energy alone is not sufficient to study high-energy interactions since, for example, in a multiperipheral chain we can go to high total energy without any subenergies becoming large. When we observe a high-p_T particle, however, we are guaranteed that there is a violent subprocess which occurs at a minimum effective energy squared of

$$s_{eff} \gtrsim 4p_T^2 \quad . \tag{IC.5}$$

The structure of an interaction with a hard component is illustrated schematically in Fig. I.5. In much of the discussion of this review we are investigating the possibility that this hard component may represent a simple or even a fundamental interaction. If we can find a prescription for stripping away the effects of the outer bremsstrahlung, then we can see whether we can fairly compare this core subprocess with some annihilation cross section, such as, for example, $\sigma_{e^+e^-} \to$ hadrons at $s_{e^+e^-} \gtrsim 4p_T^2$. The division of the process illustrated in the diagram of Fig. I.5 is quite universal; virtually all the models which have been proposed turn out to have this structure in common. If we assume the absence of important interference effects, the inclusive cross section corresponding to Fig. I.5 can be written in a simple form involving probabilities. We define the distribution

$$G_{b/B}(x) = \frac{dN_{b/B}}{dx} \; ; \qquad 0 \leq x \leq 1 \tag{IC.6}$$

for hadron B to contain an offshell fragment b with the longitudinal fraction $x = p_L^b = p_L^B$ of the initial momentum. There is an implied integration over the

transverse momentum which is assumed to be rapidly convergent. The conservation of momentum implies the constraint

$$1 = \sum_b \int_0^1 x dx \, G_{b/B}(x) \quad . \tag{IC.7}$$

Notice that there is a term in $G_{b/B}(x)$ which corresponds to the "elastic" propagation of B without bremsstrahlung

$$G_{B/B}(x) \simeq Z\,\delta(1-x) \quad . \tag{IC.8}$$

The quark-parton model for deep inelastic scattering gives the familiar relation

$$F_{2B}(x) = \nu W_2(x) = \sum_a \lambda_a^2 x \, G_{q_a/B}(x) \tag{IC.9}$$

where $G_{q_a/B}$ is now the infinite momentum frame probability function for a quark-parton of charge λ_a within hadron B. Within the same spirit, the inclusive hadron-hadron reactions can, at large-p_T, be written in the form

$$\frac{d^3\sigma}{d^3p/E}(AB \to CX) = \sum_{\substack{a \in A \\ b \in B}} \int_0^1 dx_a \int_0^1 dx_b \, G_{a/A}(x_a)\, G_{b/B}(x_b) \frac{d^3\sigma^I}{d^3p/E}(ab \to CX) \tag{IC.10}$$

where $d\sigma^I/(d^3p/E)$ $(ab \to CX)$ is hadron irreducible since the initial bremsstrahlung is contained in the G's. A derivation of (IC. 10) is given in Appendix A. The "violent" subprocess, $ab \to CX$ occurs at reduced $s_{eff} = x_a x_b s \gtrsim 4p_T^2$. If the integration over transverse momentum (which is implied in Eq. (IC. 10)) is not performed, for example, we can study azimuthal correlations in two-particle inclusives. With a specific choice of elementary scattering, Eq. (IC. 10) and Fig. I.5 were originally given by Berman, Bjorken and Kogut (1971). It has been rederived and generalized in various forms using infinite momentum frame techniques (Blankenbecler et al., 1972), Sudakov variables (Landshoff

and Polkinghorne, 1973) and an analysis of the multiperipheral model (Amati, Testa and Caneschi, 1973; Levin and Ryskin, 1973). The interrelations between these approaches are discussed in Appendix B. Possible off-shell effects in the hard subprocess $d\sigma^I/\left(d^3p/E\right)(ab \to CX)$ are not explicitly included in Eq. (IC.10). The fact that $G_{b/B}(x)$ becomes a function independent of $|\vec{p}_B|$ for $|\vec{p}_B| \to \infty$, can be derived in super-renormalizable elementary field theories and bound state calculations.

Other examples of reactions which have the same general form as Eq. (IC. 10) include the Drell-Yan formula (Drell and Yan, 1971) for the process $hh \to \mu^+\mu^- X$ via $\bar{q}q$ annihilation and the two-photon process $ee \to ee$ + hadrons.

It is important to note the connection between the behavior of G(x) near x=0 and the Regge behavior of total cross sections. If $\sigma_{\bar{a}A} \sim s^{\alpha-1}$ one readily finds (modulo logarithmic factors) (Feynman, 1972; Landshoff, Polkinghorne and Short, 1971; Abarbanel et al., 1969)

$$G_{a/A}(x) \sim Cx^{-\alpha} \tag{IC. 11}$$

Inserting this into (IC. 10) we see that Pomeron exchange, α=1, gives Feynman scaling for the inclusive cross section, Eq. (IC. 4).

D. Relations Among Cross Sections in Hard Scattering Models

It is interesting to note that many of the properties of cross sections in hard-scattering models can be determined directly from the underlying basic assumption. Consider any model in which we can write in the limit $s, t, u \gg (\text{masses})^2$ the exclusive cross section as

$$\frac{d\sigma}{dt}(AB \to CD) = \left(F^b_{BD}(t)\right)^2 K^c_{Ab}(s, t, u) \tag{ID. 1}$$

and the inclusive cross section in the triple-Regge region as

$$\frac{Ed^3\sigma}{d^3p}(AB \to CX)\Big|_{T.R.} = \frac{s}{s+u} F_{b/B}(x)\, K^c_{Ab}(xs, t, xu) \qquad \text{(ID. 2)}$$

where $x = -t/(s+u) = -t/\mathcal{M}^2 - t$ is the Bjorken scaling variable. The hadronic from factor $F^b_{BD}(t)$ reflects the probability of the transition $B \to D$ with D remaining intact and $F_{b/B}(x)$ is the generalized structure function describing the breakup of the target B due to the projectile b. These equations are the analogs of the usual electron scattering formulae and include the assumption that the large momentum transfer is achieved in a single factorizable impulse. A sum over the internal index b of such separable terms can be considered as well but we will not write this sum explicitly.

The expressions (ID. 1) and (ID. 2) are connected in the limit of small missing mass by a relation of the Drell-Yan-West type (Drell and Yan, 1970; West, 1970). The $x \to 1$ limit of the inclusive cross section can be written

$$\lim_{x \to 1} \frac{d\sigma}{dt\, d\mathcal{M}^2} = \frac{1}{\mathcal{M}^2}\left[(1-x)\, F_{b/B}(x)\right] K^c_{Ab}(s, t, u) \quad . \qquad \text{(ID. 3)}$$

If this is to join smoothly onto exclusive scattering for $\mathcal{M}^2 = m_D^2$, then for $(1-x) \cong m_D^2/\left(m_D^2 - t\right)$ we must have

$$(1-x)\, F_{b/B}(x) \propto \left(F^b_{BD}(t)\right)^2 \qquad \text{(ID. 4)}$$

Hence,

$$F^b_{BD}(t) \sim (-t)^{1-n} \iff F_{b/B}(x) \sim (1-x)^{2n-1} \qquad \text{(ID. 5)}$$

This is a simple extension of the Drell-Yan-West relation but one has not assumed that the hadronic form factors have the same t-behavior of the electromagnetic form factor.

From (ID. 1), we see that in general the function K falls off less rapidly at fixed angle than the exclusive cross section itself. If

$$\frac{d\sigma}{dt}(AB \to CD)\Big|_{\text{fixed } t} \sim \beta^2(t)\, s^{2\alpha(t)-2} \tag{ID. 6}$$

then

$$K^c_{Ab}(s,t,u)\Big|_{\text{fixed } t} \sim \bar{\beta}^2(t)\, s^{2\alpha(t)-2} \tag{ID. 7}$$

with

$$\beta(t) = F^b_{BD}(t)\, \bar{\beta}(t) \tag{ID. 8}$$

Therefore, in the limit $s \gg \mathcal{M}^2 \gg |t|$ (the triple-Regge region with $x \cong 0$) the inclusive cross section can be written

$$\frac{Ed^3\sigma}{d^3p}(AB \to CX) \sim (-t)^{2\alpha(t)-2}\, \bar{\beta}^2(t)\, F_{b/B}(0) \left(\frac{\mathcal{M}^2-t}{s}\right)^{1-2\alpha(t)} \tag{ID. 9}$$

If this term is to contribute to Feynman scaling we must require $F_{b/B}(0) \neq 0$. A more general parametrization of $F_{b/B}(x)$ near $x=0$

$$F_{b/B}(x) \sim f_{b/B}\, x^a \tag{ID. 10}$$

results in the behavior

$$\frac{Ed^3\sigma}{d^3p}(AB \to CX) \sim (-t)^{2\alpha(t)-2}\, \bar{\beta}^2(t)\, f_{b/B}(-t/s)^a \left(\frac{\mathcal{M}^2-t}{s}\right)^{1-a-2\alpha(t)} \tag{ID. 11}$$

The usual triple-Regge formula is independent of the $x \to 1$ behavior of $F_{b/B}(x)$, however, if we want to guarantee that it connects smoothly onto the exclusive limit it is important that we continue away from $x=0$ with the appropriate form of $F_{b/B}(x)$ obeying (ID. 4). This simple correction to the triple-Regge formula becomes important for decreasing missing mass.

If we want to generalize the expression (ID. 2) to describe the inclusive cross section in the central region we must consider the fragmentation of the projectile A. If we write the probability of finding fragment a of particle A with longitudinal momentum fraction x_a as $G_{a/A}(x_a) = x_a^{-1} F_{a/A}(x_a)$ it is suggestive to write the cross section in the explicitly symmetric form

$$\frac{Ed^3\sigma}{d^3p}(AB \to CX) = \int dx_a dx_b \, \delta\left(x_a x_b s + x_a t + x_b u - m_a^2 - m_b^2 - m_c^2 - m_a^2\right)$$

$$F_{a/A}(x_a) \, F_{b/B}(x_b) \, K_{ab}^c\left(x_a x_b s, x_a t, x_b u\right) \qquad \text{(ID. 12)}$$

where a sum over a and b is again understood. Comparing this form with Eq. (IC. 10) we see we have isolated a restricted subset of possible internal processes in the most general hard scattering model where the internal subprocess is a 2-2 scattering leading to particle c.

By a simple change of variable, Eq. (ID. 12) can be rewritten as an angular integral of the form

$$\frac{Ed\sigma}{d^3p} \simeq \int_{-(1-2x_1)}^{(1-2x_2)} \frac{dz}{(1-z^2)} F_{a/A}\left(\frac{2x_1}{1+z}\right) F_{b/B}\left(\frac{2x_2}{1-z}\right) K_{ab}^c\left(s = \frac{4p_T^2}{1-z^2}, z\right) \qquad \text{(ID. 13)}$$

where K can be identified with $\frac{2}{\pi} d\sigma/dt$ (ab $\to$ cd). In the limit of large p_T^2 at fixed x_1 and x_2, the dependence on p_T^2 is given in terms of the fixed angle behavior of the basic process described by K_{ab}^c. For example, for the process $pp \to \pi X$, an estimate of the contribution from the pion intermediate state can be made by using the empirical result that $\pi p \to \pi p$ varies as s^{-8} at fixed angle $F_p(t) \sim (-t)^{-2}$, and hence $K \sim s^{-4}$. This contribution to the inclusive cross section therefore varies as $\left(p_T^2\right)^{-4}$. It is possible to make a much better estimate by a more detailed estimate of K(s, t, u) but this will be postponed until specific models are discussed. We see that many different models will yield

formulas of the above structure; they must be judged, therefore, on their detailed predictions for $F_{BD}(t)$, $F_{b/B}(x)$, and $K(s,b,u)$, on their range of applicability, and their simplicity. A further generalization of (ID. 13) allows for final state fragmentation of c into C.

E. What are the Important Internal Mechanisms?

Given that the underlying structure of current models is roughly determined by the form of diagram I.5, the differences between the various approaches consist of assumptions concerning the question of what the important internal mechanisms, $ab \rightarrow CX$ in Eq. (IC. 10), can be. The possibilities include the following.

Quark-quark scattering

This is the mechanism originally discussed by Berman and Jacob (1970) and made explicit in the pioneering paper of BBK. The large-angle quark-quark scattering is followed by the scale-invariant fragmentation of one of the quarks into the hadron C. If the fundamental quark-quark interaction is scale-invariant this leads to $Ed\sigma/d^3p$ scaling as p_T^{-4} as discussed earlier. The implications of this model for particle ratios and for two-particle production have been explored by Ellis and Kislinger (1974) and by Bjorken (1973a, b, c). More complicated phenomenological forms for the quark-quark cross section, constrained to agree with fixed-angle exclusive hadronic processes, are used in the calculations of Horn and Moshe (1973).

Quark-quark scattering is in many senses, the most attractive hard collision model because of its simple connection with ideas found useful in deep inelastic lepton production and the amount of work done on the many alternatives is due largely to the apparent absence of the p_T^{-4} behavior. The specific predictions for the phase-space structure of events and for particle ratios are important predictions which merit testing in spite of this failure.

Quark-hadron scattering

These are the dominant contributions of the constituent interchange model of BBG. The basic hypothesis is that the quark-quark scattering contributions are suppressed leaving other types of internal subprocesses involving quarks and hadrons (perhaps because the dominant interaction is between quarks and their containers). One important example of such a contribution is $qM \rightarrow qM$ (quark-meson scattering). Here we can either detect the hard-scattering meson directly or the quark or meson can fragment into a hadron. Since the fragmentation functions are assumed scale invariant, the power of p_T in the power law scaling, Eq. (IB. 1), directly reflects the fixed angle energy dependence of the subprocess. A simple ansatz for the scaling laws of exclusive processes is given by the dimensional counting rules of Brodsky and Farrar (1973) and Matveev, Maradyan, and Tavkhelidze (1973). We will discuss in considerable detail in Section IV. C how these rules are derived and their implications for several processes. The nontrivial extension to the general case and to inclusive scattering was given by Blankenbecler and Brodsky (1974) and will also be covered in considerable detail.

The quark-hadron mechanism has also been discussed in detail by Landshoff and Polkinghorne (1973a, b, c; 1974) where there is special emphasis on the fusion mechanism $q\bar{q} \rightarrow MM$. A related approach can also be found in the work of Kinoshita (1974) and collaborators.

Hadron-hadron scattering

In the multiperipheral model of Amati, Caneschi and Testa (1973) and Levin and Ryskin (1973), the diagram of Fig. I. 5 is still relevant if we think of the central collision as the two-body process $MM \rightarrow MM$ where the M is the elementary scalar in a $g\phi^3$ field theory. This model has been thoroughly discussed by

Levin and Ryskin (1974). It leads asymptotically to a strict p_T^{-8} scaling law for the inclusive cross section but there are serious difficulties in making connections with deep inelastic reactions and large angle exclusive processes. In its simplest form the model predicts limited multiplicities in the recoil system opposite a high-p_T hadron.

A more general approach has been discussed by Teper (1974b) who merely assumes that the violent subprocess is a purely hadronic large angle scattering process. Quarks or partons are thus never explicitly mentioned. If we adopt either the constituent counting rules or empirical fits for various exclusive large-angle processes this can provide interesting lower bounds on the behavior of the inclusive cross section. Experimentally, exclusive meson-baryon scattering is roughly consistent with the scaling law

$$\frac{d\sigma}{dt}(MB \rightarrow MB) \sim \frac{1}{s^8} f(\theta_{CM}) \tag{IE. 1}$$

Thus, using Eq. (IC. 10), we see that we must have a contribution proportional to

$$\frac{Ed^3\sigma}{d^3p} \gtrsim \frac{1}{p_T^{16}} f(\theta_{CM}, \epsilon) \tag{IE. 2}$$

both for $pp \rightarrow BX$ and $pp \rightarrow \pi X$. These contributions are also present in the CIM but they are usually assumed to be dominated by terms involving quarks at sufficiently large values of p_T (at fixed x_T). Similarly, the assumed behavior

$$\frac{d\sigma}{dt}(MM \rightarrow MM) \sim \frac{1}{s^6} f(\theta_{CM}) \tag{IE. 3}$$

given by the dimensional counting rules can lead to a contribution

$$\frac{Ed\sigma}{d^3p}(pp \rightarrow \pi X) \geq \frac{1}{p_T^{12}} f(\theta_{CM}, \epsilon) \tag{IE. 4}$$

It is a virtue of the assumption that the violent subprocess involves hadrons that it allows us to use the structure of Eq. (IC. 10) directly with experimental data on large-angle exclusive scattering in order to calculate inclusive cross sections. To the extent that we can neglect off-mass-shell effects and coherence, this should provide important normalization checks. The approach should also predict simply particle ratios for small x_T where the fragmentation functions are proportional to total cross sections. Since it is not clear whether a point-like power-law falloff or a exponential falloff associated with a mass scale is required for large-angle exclusive cross sections, the advantage of dealing directly with data is obvious.

If we discuss the violent subprocess in Fig. I. 5 in purely hadronic terms the motion of a "fireball" or high-mass excited hadronic state becomes important. For example, in the early model of Berman and Jacob (1970) the internal heavy vector gluon exchange leads to the excitation of baryonic fireballs. A version of this model was discussed by Berger and Branson (1973). In its direct form, the model require that a baryon be found with large transverse momentum on each side of the collision axis along the direction of the scattered fireballs. There may also be problems with Feynman scaling or crossing symmetry in the particular versions of the model discussed so far.

Another approach to diagram I. 5 is to assume the core subprocess consists of the production of a single heavy fireball. In order to be different from the fireballs in the statistical bootstrap approach in Hagedorn (1963) and Frautschi (1971), this new heavy fireball must have some unusual characteristics associated with it. If it possessed the usual cascade decay mode found in bootstrap models, then the invariant cross section would be approximately given by a Boltzmann factor e^{-p_T/kT_0} although Bouquet, Letessier and Tounsi (1974)

have shown that modifications due to a large recoil momentum building up after several decays can broaden the p_T distribution. With one or more new mass scales in addition to the usual $kT_0 \cong m_\pi$ of the statistical bootstrap theory we can obviously reproduce single particle distributions but there may be some problems in getting reasonable two-particle distributions and multiplicities from a cascade decay mode. Within the context of one fireball model, it is difficult to treat quantum number constraints correctly so that, for example, a nontrivial K^+/K^- particle ratio can be obtained.

Another possibility is that this new type of heavy fireball possesses a non-negligible fission decay mode, $F^*(M) \rightarrow F^*(M/2)\, F^*(M/2)$, in order to give the final state a distribution in phase space more like the jet structure of the parton model. Obviously, to a certain accuracy, we can then reproduce many parton-model results.

F. <u>The Structure of High-p_T Events</u>

One of the potentially most interesting pieces of information that can be obtained concerning large transverse momentum phenomena is the structure of events in phase space. When a high-p_T particle is produced we would like to know how many other particles are produced and what regions of phase-space they populate. A spectacular possibility is that completely new and unexpected types of matter, such as colored or charmed hadrons, weak bosons, or heavy leptons, may be preferentially produced in association with large transverse momentum particles. In any case, the measurement of correlations and associated multiplicities can provide severe restraints on models for the underlying production mechanism.

An essential characteristic of hard-collision models typified by Fig. I.6 is the development of some sort of jet structure. It is easy to see how this arises

within the context of these models. The fragmentation of the initial hadrons and possible fragmentation of the scattered constituents is assumed to be a gentle process which preserves the direction of all hadronic momenta within fluctuations of typical size $\langle p_T \rangle \sim 0.3 - 0.4$ GeV/c. In the case that one of the scattered particles is a quark parton this entails a belief that as in models for deep inelastic scattering the final state interactions which neutralize quark quantum numbers are of this same gentle nature. The coplanarity of the internal hard-scattering process is therefore approximately maintained in the regions of phase space in which final state hadrons are found. Event-by-event there will be fragmentation prodcts along both beam directions and along the direction of the scattered large-p_T constituents. This structure is shown in Fig. I.6. The fact that the two large-p_T jets emerge approximately coplanar but not collinear is due to the center-of-mass motion of a and b.

The observation of jet structure would be a success for hard-scattering models while the measurement of jet-jet cross sections would offer the potential of looking back "inside" an event and deducing the fundamental quark-quark or quark-hadron cross section. However, there is some evidence from recent measurements of azimuthal correlations associated with large-p_T by the CCR group that the deviations from coplanarity in large-p_T events are significantly greater than what is expected on the basis of the simple arguments (Bjorken, 1974). The spread in hadron momenta around a jet axis is more like 1.2 GeV/c than 0.35 GeV/c. It may be possible that hard-scattering models, since they prefer p_T distributions that fall rather slowly (as powers), will be able to accommodate this fact but the situation is not as clear as it might have been (Gunion, 1974b, c).

An important point to remember is that if one of the scattered constituents is a quark, the multiplicity and distribution of hadrons in the jet associated with that quark should be identical to that of the system which balances the transverse momentum of a deeply-inelastic-scattered lepton. This connection, involving particle ratios, etc., can be tested experimentally in order to quantify our presumption that quarks represent an important dynamical degree of freedom in large-p_T hadronic processes.

If the basic hard process is quark-quark scattering, the usual assumption is that in a given event all the available phase space regions shaded in Fig. I.6 are approximately uniformly populated. However, if the quarks scatter through a single elementary exchange then the middle regions will usually be empty of hadrons. Further details on multiplicities and the phase space-geography of the parton model are discussed by Bjorken (1974), Savit (1973), and by Ellis and Kislinger (1974).

Let us briefly compare several models. In the hadronic multiperipheral model, the active process is just meson-meson scattering and the average high-p_T jets consist of only a limited number of particles. The fusion process $q\bar{q} \rightarrow MM$ is assumed to dominate in the covariant parton model of Landshoff and Polkinghorne (1974). In the simplest version of this model we would again expect a typical jet to contain a fixed number of particles. In the CIM another important process is $qM \rightarrow qM$ which leads to an asymmetric situation where the average multiplicity on the quark side grows with increasing p_T while the multiplicity on the other side stays fixed. Since there are potentially many different processes important in the CIM and each can have different characteristics, the average phase space population is probably more like the simple parton model.

An important prediction in the fireball model of Berman and Jacob (1970) and Berger and Branson (1973) is that one expects baryon number one in each jet.

LIST OF FIGURES FOR SECTION I

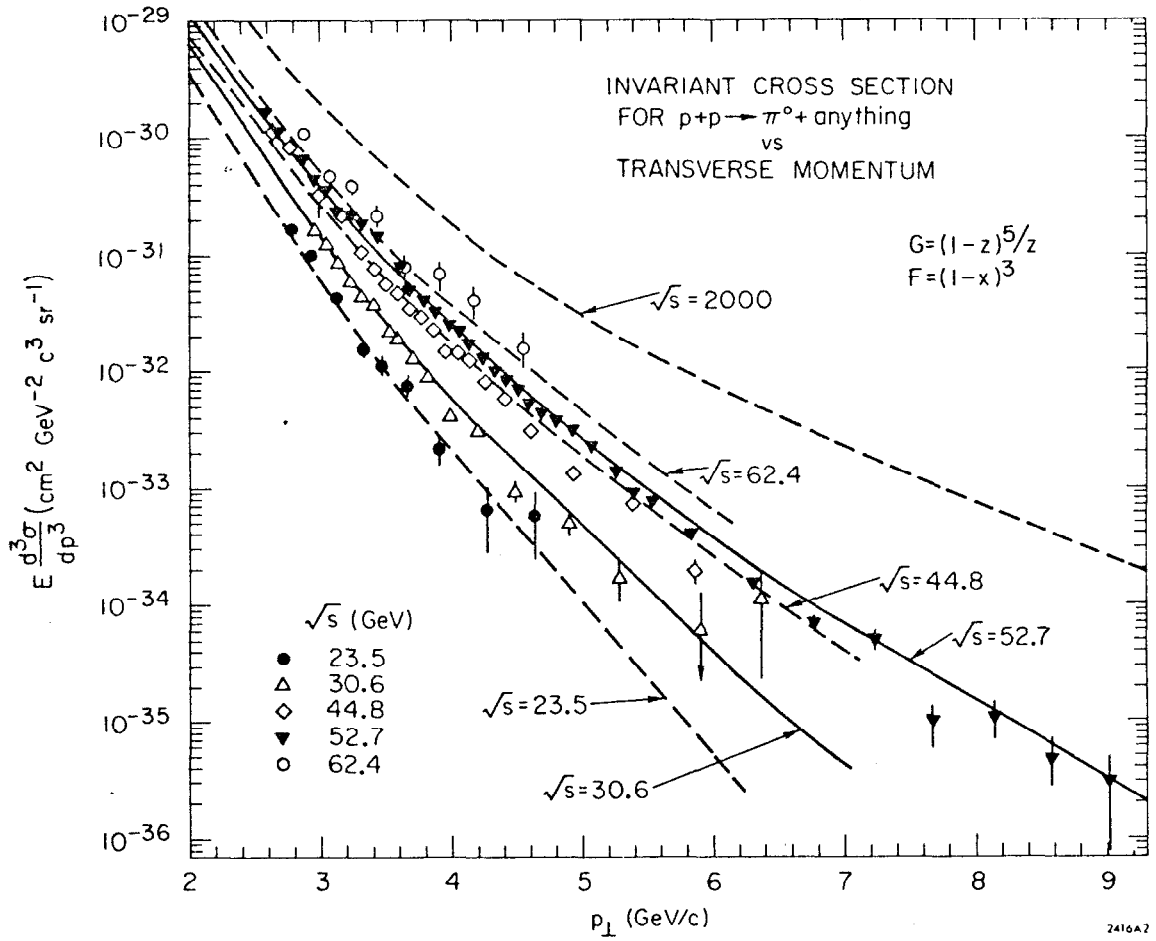
INVARIANT CROSS SECTION
FOR p+p → π°+ anything
vs
TRANSVERSE MOMENTUM
G=(1-z)^5/z
F=(1-x)^3
√s = 2000
√s=62.4
√s=44.8
√s=52.7
√s=23.5
√s=30.6
√s (GeV)
23.5
30.6
44.8
52.7
62.4
E d³σ/dp³ (cm² GeV⁻² c³ sr⁻¹)
p⊥ (GeV/c)
2416A2

FIG. I.1

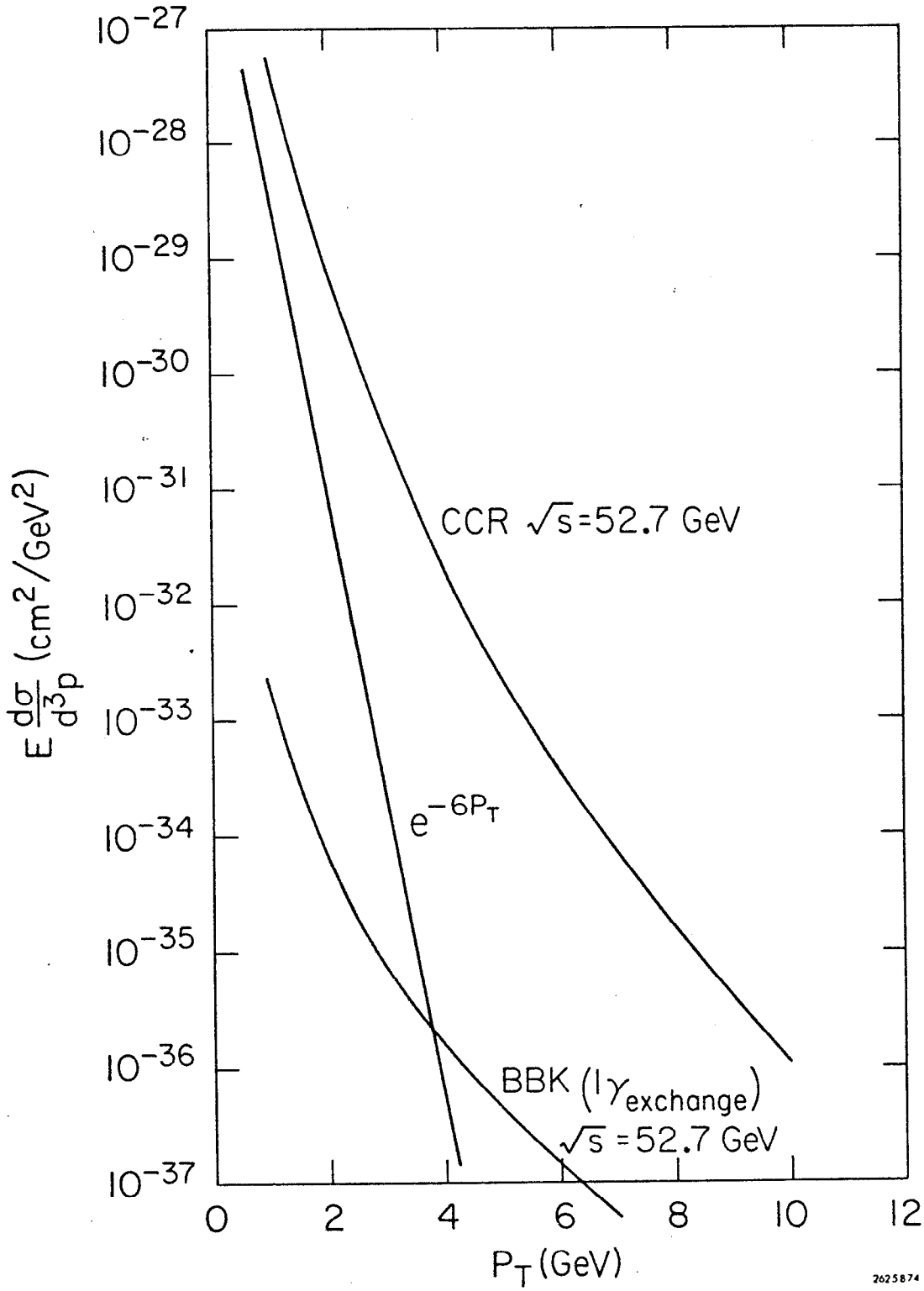
10^{-27}
10^{-28}
10^{-29}
10^{-30}
10^{-31}
10^{-32}
10^{-33}
10^{-34}
10^{-35}
10^{-36}
10^{-37}
$E\frac{d\sigma}{d^3p}$ (cm^2/GeV^2)
CCR $\sqrt{s}$=52.7 GeV
e^{-6P_T}
BBK ($1\gamma_{exchange}$)
$\sqrt{s}$ = 52.7 GeV
0
2
4
6
8
10
12
P_T (GeV)
2625874

FIG. I.2

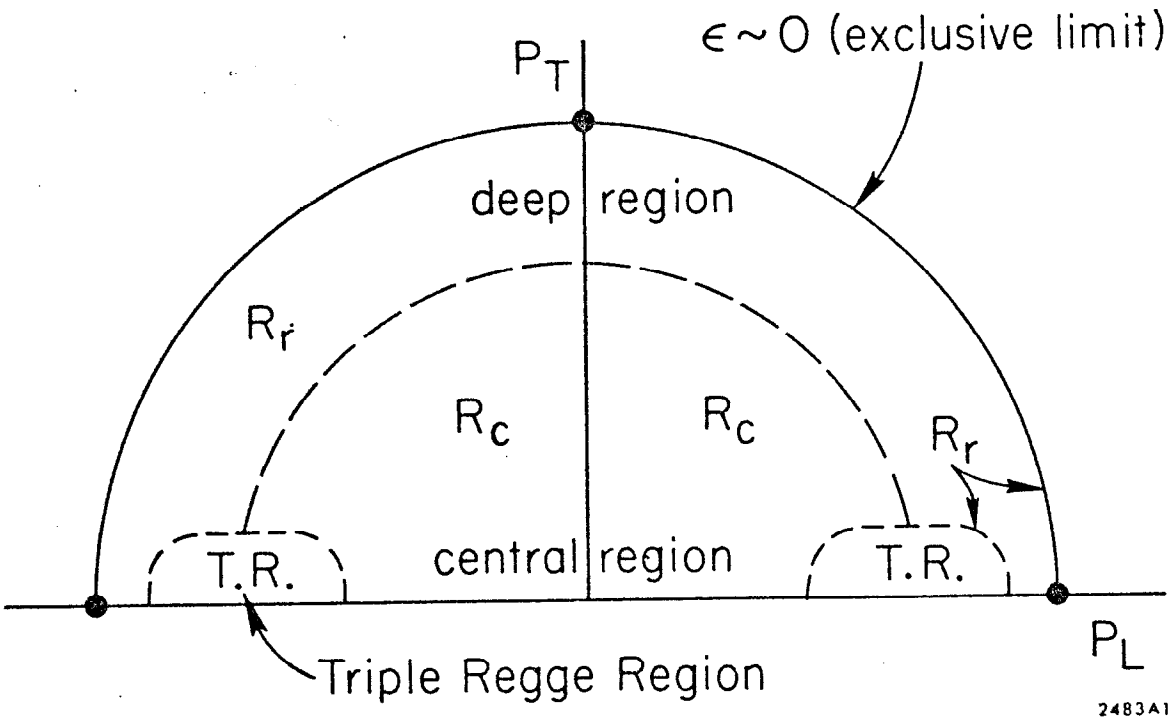
$\epsilon \sim 0$ (exclusive limit)
P_T
deep region
R_r
R_c
R_c
R_r
T.R.
central region
T.R.
Triple Regge Region
P_L
2483A1

FIG. I.3

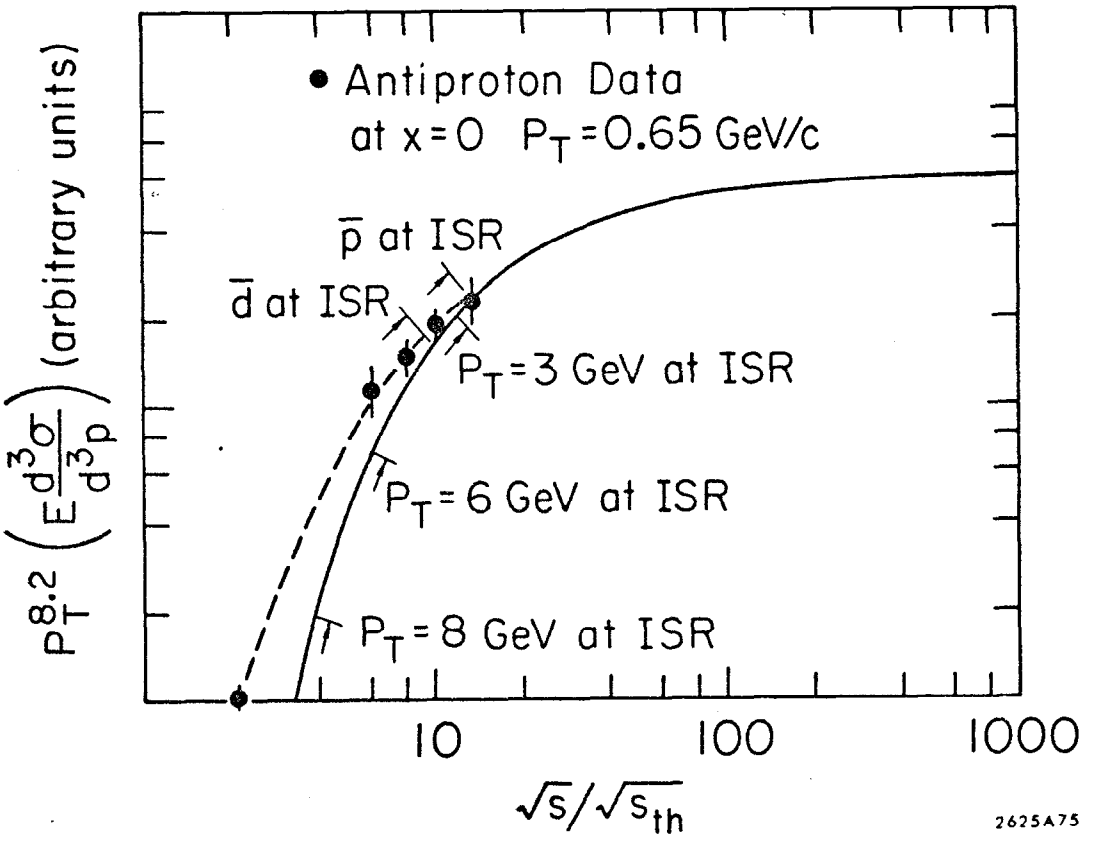
• Antiproton Data
at x = 0 P_T = 0.65 GeV/c
$\bar{p}$ at ISR
$\bar{d}$ at ISR
P_T = 3 GeV at ISR
P_T = 6 GeV at ISR
P_T = 8 GeV at ISR
$P_T^{8.2}\left(E\frac{d^3\sigma}{d^3p}\right)$ (arbitrary units)
10
100
1000
$\sqrt{s}/\sqrt{s_{th}}$
2625A75

FIG. I.4

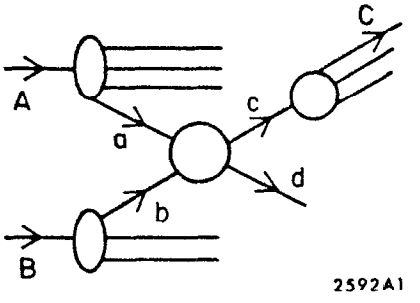

FIG. I.5

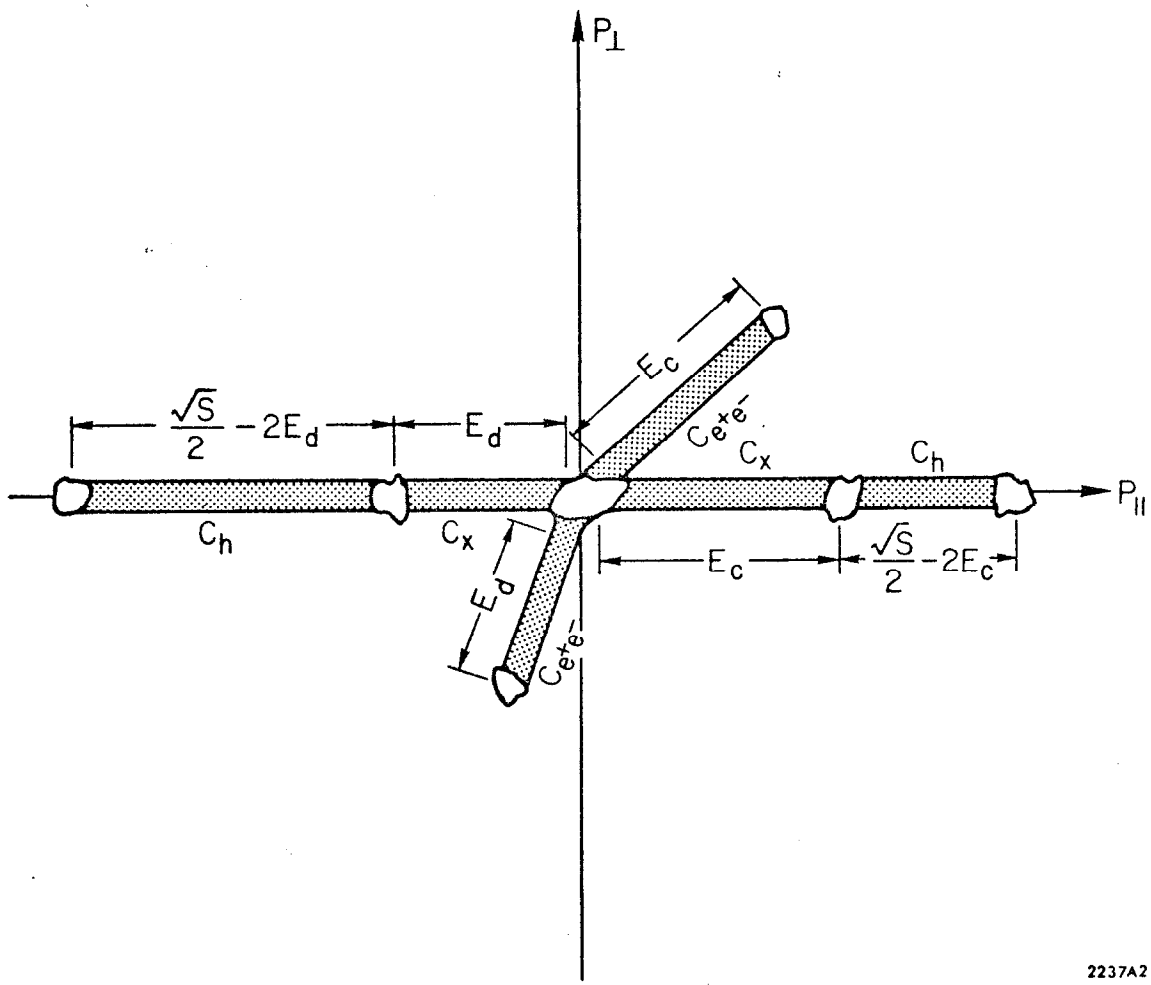
P⊥
P∥
$\frac{\sqrt{S}}{2} - 2E_d$
E_d
E_c
$C_{e^+e^-}$
C_x
C_h
C_h
C_x
E_d
$C_{e^+e^-}$
E_c
$\frac{\sqrt{S}}{2} - 2E_c$
2237A2

FIG. I.6

II. EXPERIMENTAL SUMMARY

The production of particles with large transverse momentum in hadronic collisions is a subject of intrinsic experimental interest. Even if it were clear that the results could be fit by mundane extensions of ideas valid at small transverse momentums, the experiments would be valuable in order to explore and define the short-distance boundary of the strong interactions. Of course, the experiments done so far have not been mundane but have produced some big surprises. This make physics interesting and it is the interest generated by those surprises which triggered the large amount of work which now justifies this review.

In this section we attempt to summarize the available experimental data with a minimum of theoretical input. Theoretical prejudice will not be absent since it will influence what subjects we include and since it has a large effect on how we or the original authors of the papers reviewed here choose to plot data. We hope that this summary of those data which bear directly or indirectly on the nature of hadronic interactions at short distance may prove valuable a source material to those with new untried-theoretical ideas or that it can provide an entry into the original literature for those interested in more details of the experimental situation.

The data we review here includes two-body exclusive scattering through large angles, single-particle inclusive spectra, and two-or-more particle inclusive correlations. We conclude with a partial list of experiments which have been proposed and which may produce results in the near future.

Previous reviews or experimental summary talks which can be consulted for more data include Lundby (1973), Walker (1973), Ellis and Thun (1974), Brodsky (1973, 1974a,b), Landshoff (1974), Cronin (1974), Darriulat (1974), and Jacob (1974).

A. Exclusive Scattering at Large Angles

Data on exclusive 2-2 scattering processes have accumulated steadily over the years. In the forward and backward directions differential cross sections can be described by Regge parametrizations of the form

$$\frac{d\sigma}{dt}(AB \rightarrow CD)\Big|_{s\rightarrow\infty} \sim \beta(w)\ s^{2\alpha(w)-2} \quad , \qquad \text{(IIA. 1)}$$

where w = t or u. The size and energy dependence of these peripheral peaks is correlated dramatically with the quantum numbers exchanged in the t or the u channel. Figure IIA. 1, taken from Chiu (1972), indicates one aspect of this correlation which supports (IIA. 1). The bulk of the existing data lies within the peripheral peaks and it is therefore not surprising that most of the theoretical attention has been directed towards this Regge region.

We are primarily interested here in the scattering of hadrons through large angles. Away from the peripheral peaks, the one thing common to all reactions is that the differential cross sections fall rapidly with energy, requiring experiments with high beam intensity and/or long running time. The kinematic range in which measurements have been made reflects this counting-rate restriction but accentuated theoretical interest in the topic may help justify the considerable experimental effort and machine time necessary to extend the coverage of this kinematic region.

Differential cross sections at p_{LAB} = 5 GeV/c for pp, $\bar{p}p$, $\pi^{\pm}p$, $K^{\pm}p$ elastic scattering are shown in Fig. IIA. 2. In Fig. IIA. 3 $\pi^{-}p$ elastic scattering is compared with $\pi^{+}p \rightarrow K^{+}\Sigma^{+}$ and $\pi^{-}p \rightarrow \eta^{o}n$. Except for pp scattering, all the other large angle cross sections are remarkably similar in magnitude at this energy. There appears to be no solid explanation for the special role of pp but the striking similarity in size of the other cross sections at 90° compared

with the large differences in the size of the peripheral peaks indicated in Fig. IIA.1 is worth noting. Evidence discussed below suggests that the pp cross section falls with energy more rapidly than the others so there may be an energy regime where they are all comparable.

When considering the energy dependence of the large-angle differential cross sections, it is important to note the fact that low-energy non-diffractive cross sections in the forward and backward regions exhibit a rapid falloff with energy before the emergence of the peripheral peaks. This fact has been emphasized by Lundby (1973). Figure IIA.4 shows backward $K^{\pm}p$ elastic cross sections as a function of laboratory momentum. Both reactions initially exhibit a rapid falloff at low energies which, for $K^{+}p$, is replaced above $s = 4\ GeV^2$ by a slower energy dependence as the peripheral peak emerges. No backward peak is observed in $K^{-}p$ scattering until even higher energies and for this reaction the initial energy dependence is maintained much longer. Figure IIA.5 demonstrates this same point. The data for backward $\bar{p}p$ scattering show another reaction where, in an exotic-exchange channel, the typically rapid low-energy falloff of the cross section continues to a fairly high energy. A possible connection of the low-energy mechanism which is responsible for this rapid falloff with the dynamic mechanism responsible for the high-energy fixed-angle cross section will be discussed in Section IV.E. This may be an interesting point to explore further since behavior of the low-energy cross sections is usually attributed to specific properties of the low-lying direct channel resonances.

One corollary of this observation is that it is possible to extrapolate the large-angle cross sections from low energies to high energies without encounting the type of dramatic break observed in Fig. IIA.5 for backward $K^{+}p$. As an

example the K^+p elastic cross section as measured by Baglin et al. (1973a, b), Danysz et al. (1972), Akerloff et al. (1967) and Yuta et al. (1974) is shown in Fig. IIA.6.

Of course, the best reaction for a detailed study of the energy dependence of the differential cross section at large angles is $pp \rightarrow pp$ where we have good data over a large range of energy. The pp differential cross section at 60°, 70°, 80°, and 90° is shown as a function of ln s in Fig. IIA.7. The lines drawn through the data indicate the possibility of dip structure in the cross section at these large angles. This structure, as well as fits to the data based on current models will be discussed in more detail later. One feature in the data which is notable is the absence of any large shrinkage effects—the cross section at different angles is falling at approximately the same rate. This indicates the possibility of approximately factorizing the cross section at large angles into a form

$$\frac{d\sigma}{dt}(s, \cos\theta)\Big|_{\cos\theta \neq \pm 1} \cong f(s)\, g(\cos\theta) \qquad \text{(IIA.2)}$$

This factorization is indicated more clearly in Fig. IIA.8 where the pp cross section data at different energies normalized to the 90° cross section and plotted as a function of $\cos\theta$. It is interesting to investigate possible corrections to Eq. (IIA.2) but we will defer this until we can discuss the implications of various possible models for the cross section.

The systematics of differential cross section measurements are important but if we are to deduce amplitude structure for the various processes it is necessary to have more information. Polarization measurements are obviously important but, because of the small counting rates, there have been very few polarization experiments extending to large angles. The data of Abshire et al. (1974) include polarization measurements for pp elastic scattering out to

$t=-6$ GeV^2. This data is shown combined with some small-t polarization measurements in Fig. IIA.9 . Two features are notable. The polarization does not vanish at large t at this energy and there is evidence for some structure, perhaps double zeros at $t \cong -1, -2.5, -4$ GeV^2. We can conclude that a single spin amplitude does not dominate in this range of momentum transfer and that the different amplitudes have potentially complicated behavior at large momentum transfer.

Another type of structure which may be important at large t consists of rapid fluctuations of amplitudes with energy or with angle. This behavior, known as Ericson Fluctuations (Ericson, 1963), is familiar in nuclear physics. Experiments designed to look for Ericson fluctuations in pp elastic scattering have not reported any evidence for the phenomenon. Allaby et al. (1966) examined $pp \rightarrow pp$ at 16.9 GeV/c over a range of angles and Akerlof et al. (1967) looked at $\theta_{CM} = 90^o$ over a range of energies without seeing any sharp structure. F. Schmidt et al. (1973), motivated in part by a prediction of Frautschi (1972), have looked at $\pi^{\pm}p \rightarrow \pi^{\pm}p$ at 5 GeV/c. The incident beam possessed at a momentum spread $\Delta p = 120$ MeV/c but the final state scattering angles were measured with sufficient accuracy to calculate the incident momentum of a given event to $\Delta p = 14$-20 MeV/c. This allowed the data to be divided into two bins with momentum greater than or less than average. At each t, an asymmetry parameter was defined by

$$A = \frac{N(+) - N(-)}{N(+) + N(-)} \qquad \text{(IIA.3)}$$

Data on A are shown in Fig. IIA.10. The large asymmetry, particularly indicates that, in some t bins, the cross section may change by a factor of 3 when the incident energy varies by 36 MeV. It would be interesting to verify

this result in other experiments and look for these fluctuations in different reactions and at different energies.

In summary, the main features which can be extracted from the data on large angle exclusive scattering are quite simple. The falloff with energy of differential cross sections is roughly like $s^{-8} - s^{-10}$ in contrast with the $s^{0} - s^{-2}$ observed in high energy peripheral peaks. There is the possibility that this rapid falloff is connected to the energy dependence of cross sections close to threshold so at large angles we have a smooth continuation from high energies to low energies. The pp elastic cross section is much higher than $\pi^{\pm}p$, $K^{\pm}p$ and $\bar{p}p$ elastic but may be falling more rapidly. There are some indications from new data on polarization and Ericson fluctuations that large angle amplitudes are not completely smooth and featureless. The question of whether all these features of the data can be a accommodated within the framework of existing theoretical ideas is very interesting and we will address this problem in some detail below.

LIST OF FIGURES FOR SECTION IIA

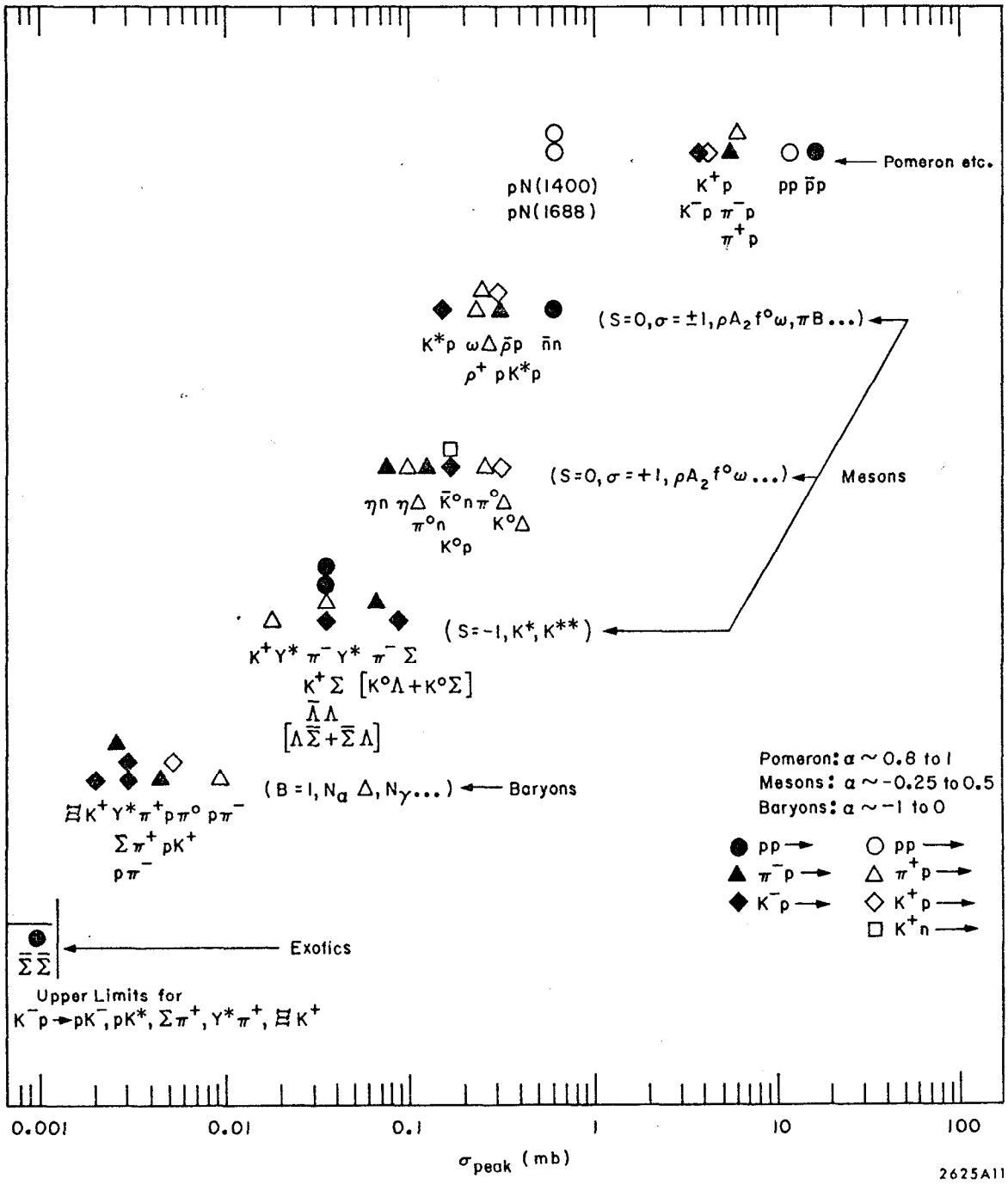
pN(1400)
pN(1688)
K+p
K−p π−p
π+p
pp p̄p
Pomeron etc.
K*p ωΔp̄p n̄n
ρ+ pK*p
(S=0, σ=±1, ρA2 f°ω, πB...)
ηn ηΔ K̄°n π°Δ
π°n K°Δ
K°p
(S=0, σ=+1, ρA2 f°ω...)
Mesons
K+Y* π− Y* π− Σ
K+Σ [K°Λ+K°Σ]
Λ̄Λ
[ΛΣ̄+Σ̄Λ]
(S=−1, K*, K**)
Ξ K+ Y*π+ pπ° pπ−
Σπ+ pK+
pπ−
(B=1, Nα Δ, Nγ...)
Baryons
Pomeron: α ~ 0.8 to 1
Mesons: α ~ −0.25 to 0.5
Baryons: α ~ −1 to 0
pp
π−p
K−p
pp
π+p
K+p
K+n
Exotics
Upper Limits for
K−p→pK−, pK*, Σπ+, Y*π+, ΞK+
0.001
0.01
0.1
1
10
100
σpeak (mb)
2625A11

FIG. IIA. 1

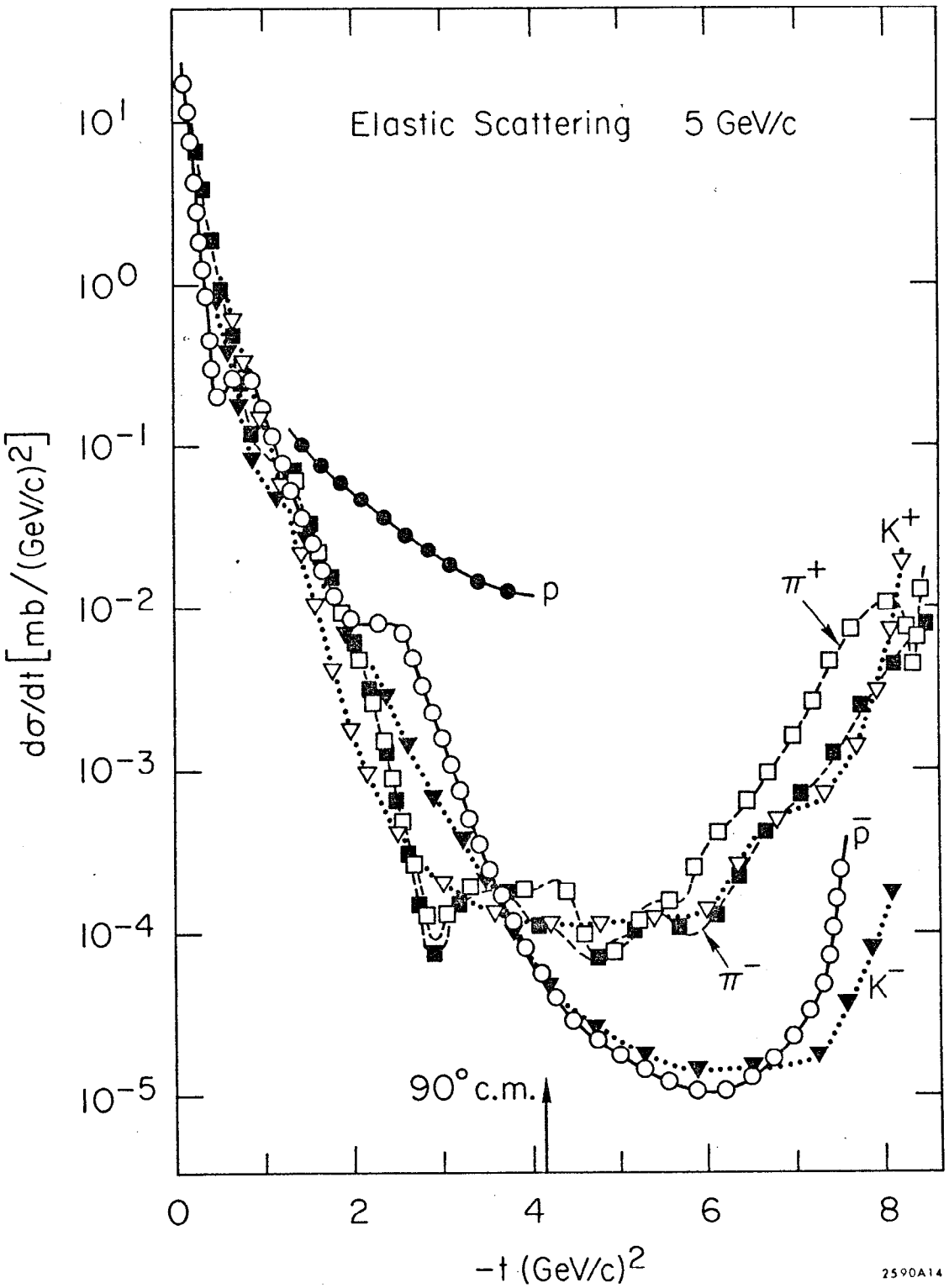
Elastic Scattering 5 GeV/c
10^1
10^0
10^{-1}
10^{-2}
10^{-3}
10^{-4}
10^{-5}
$d\sigma/dt\,[mb/(GeV/c)^2]$
p
π^+
K^+
$\bar{p}$
π^-
K^-
90° c.m.
0
2
4
6
8
$-t\ (GeV/c)^2$
2590A14

FIG. IIA.2

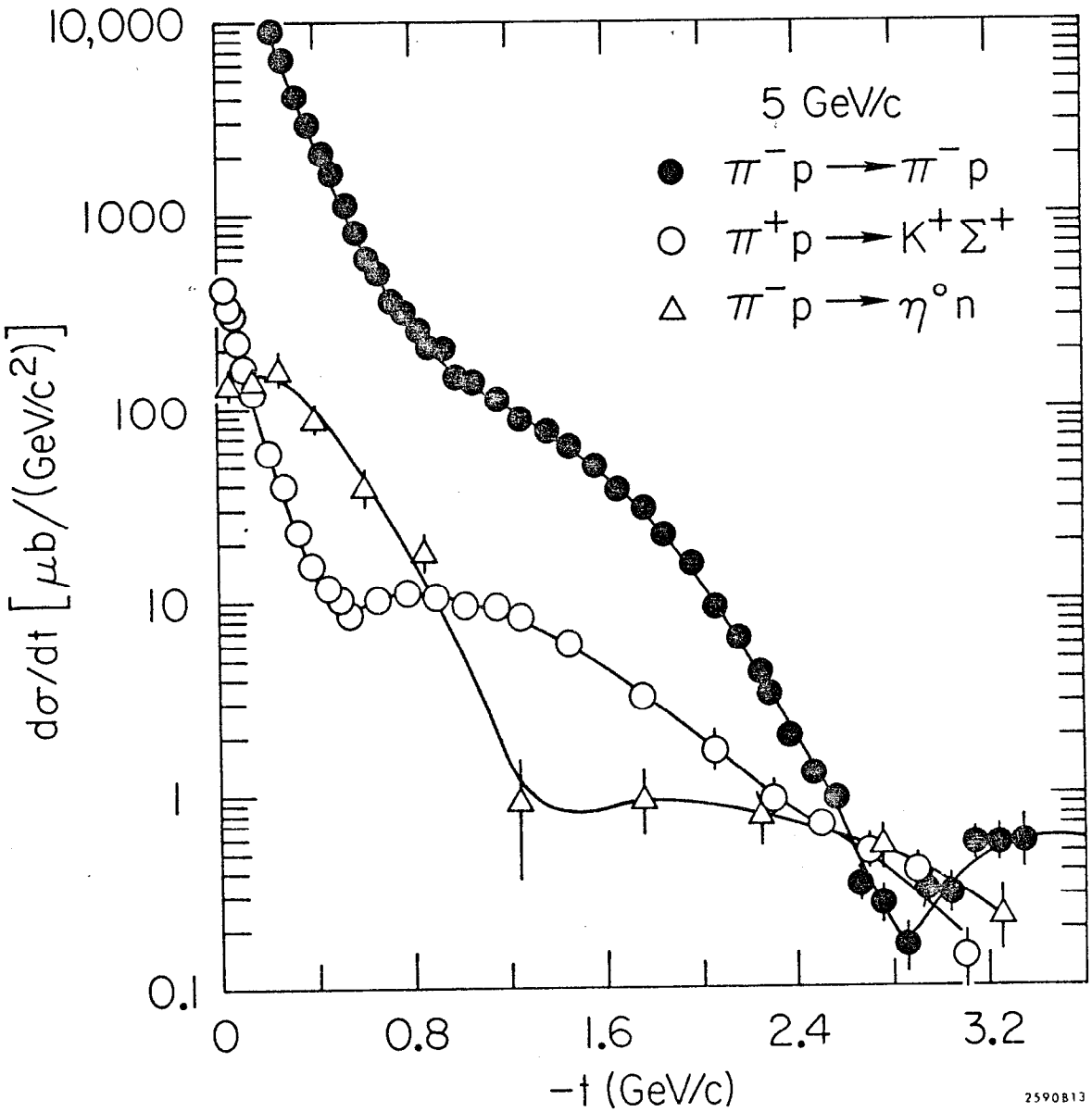
10,000
1000
100
10
1
0.1
dσ/dt [μb/(GeV/c²)]
0
0.8
1.6
2.4
3.2
−t (GeV/c)
5 GeV/c
π⁻p → π⁻p
π⁺p → K⁺Σ⁺
π⁻p → η°n
2590B13

FIG. IIA.3

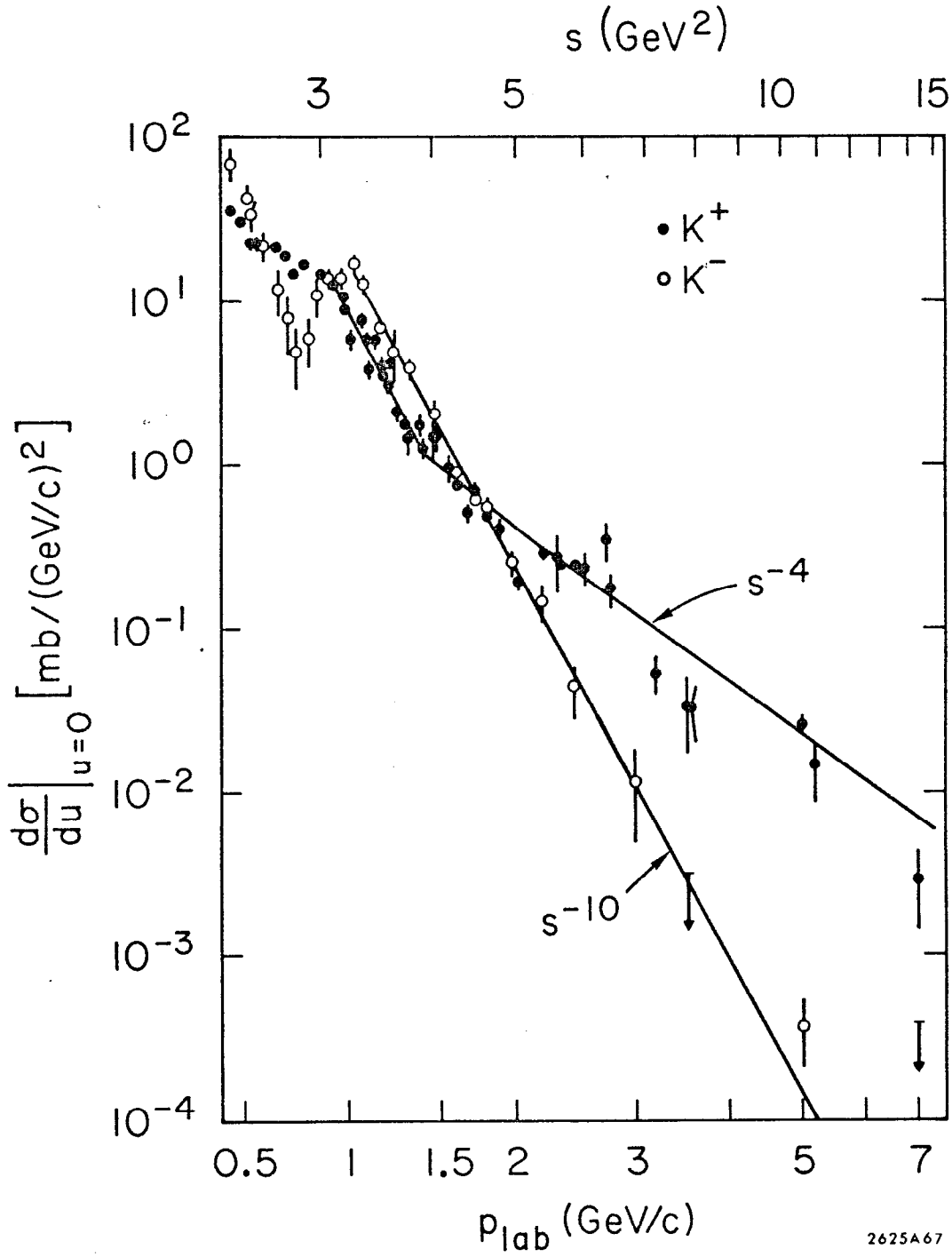
s (GeV²)
3
5
10
15
10²
10¹
10⁰
10⁻¹
10⁻²
10⁻³
10⁻⁴
• K⁺
○ K⁻
s⁻⁴
s⁻¹⁰
dσ/du |u=0 [mb/(GeV/c)²]
0.5
1
1.5
2
3
5
7
p_lab (GeV/c)
2625A67

FIG. IIA.4

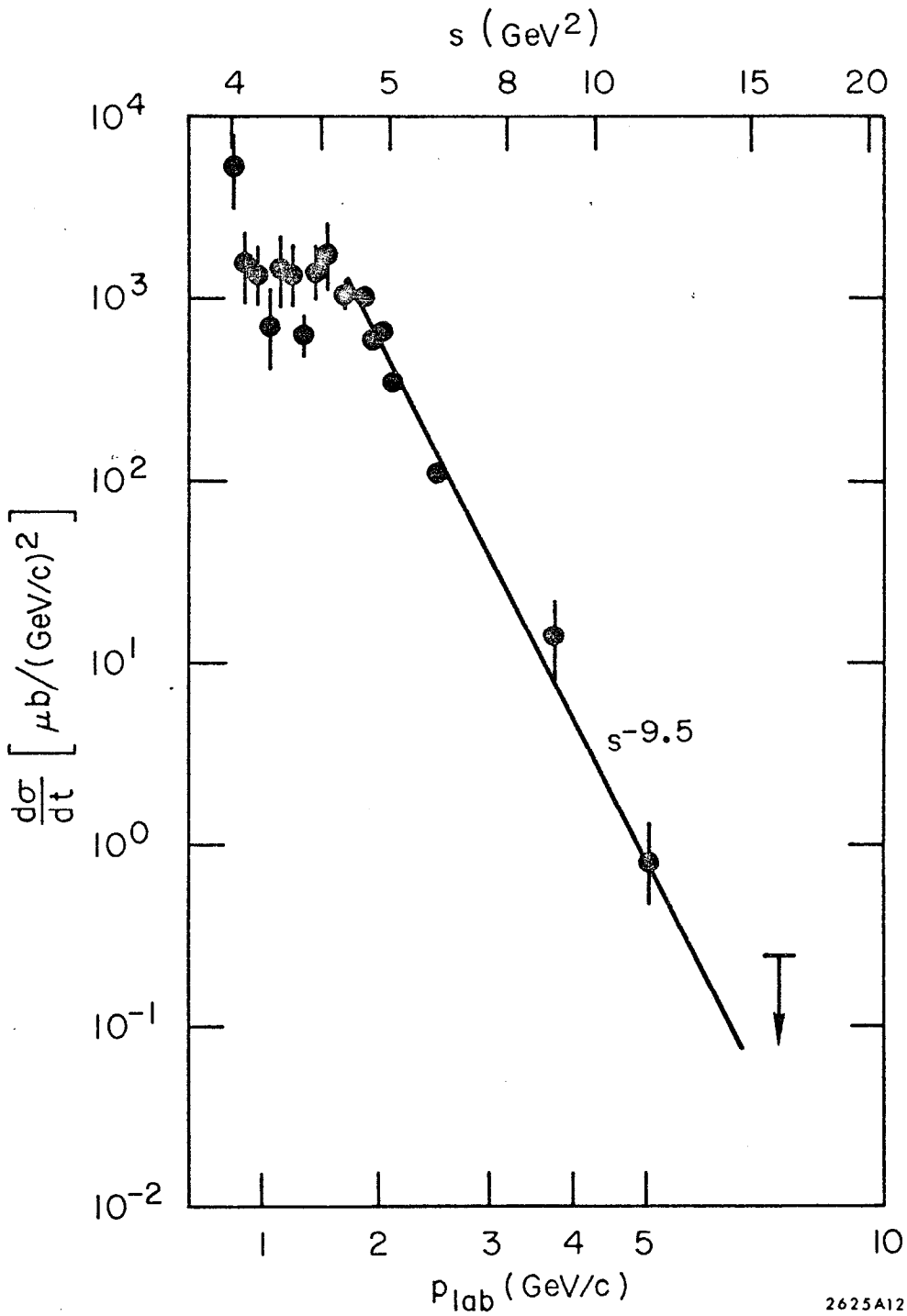
s (GeV^2)
4
5
8
10
15
20
10^4
10^3
10^2
10^1
10^0
10^{-1}
10^{-2}
$\frac{d\sigma}{dt}$ [μb/(GeV/c)^2]
$s^{-9.5}$
1
2
3
4
5
10
p_{lab} (GeV/c)
2625A12

FIG. IIA.5

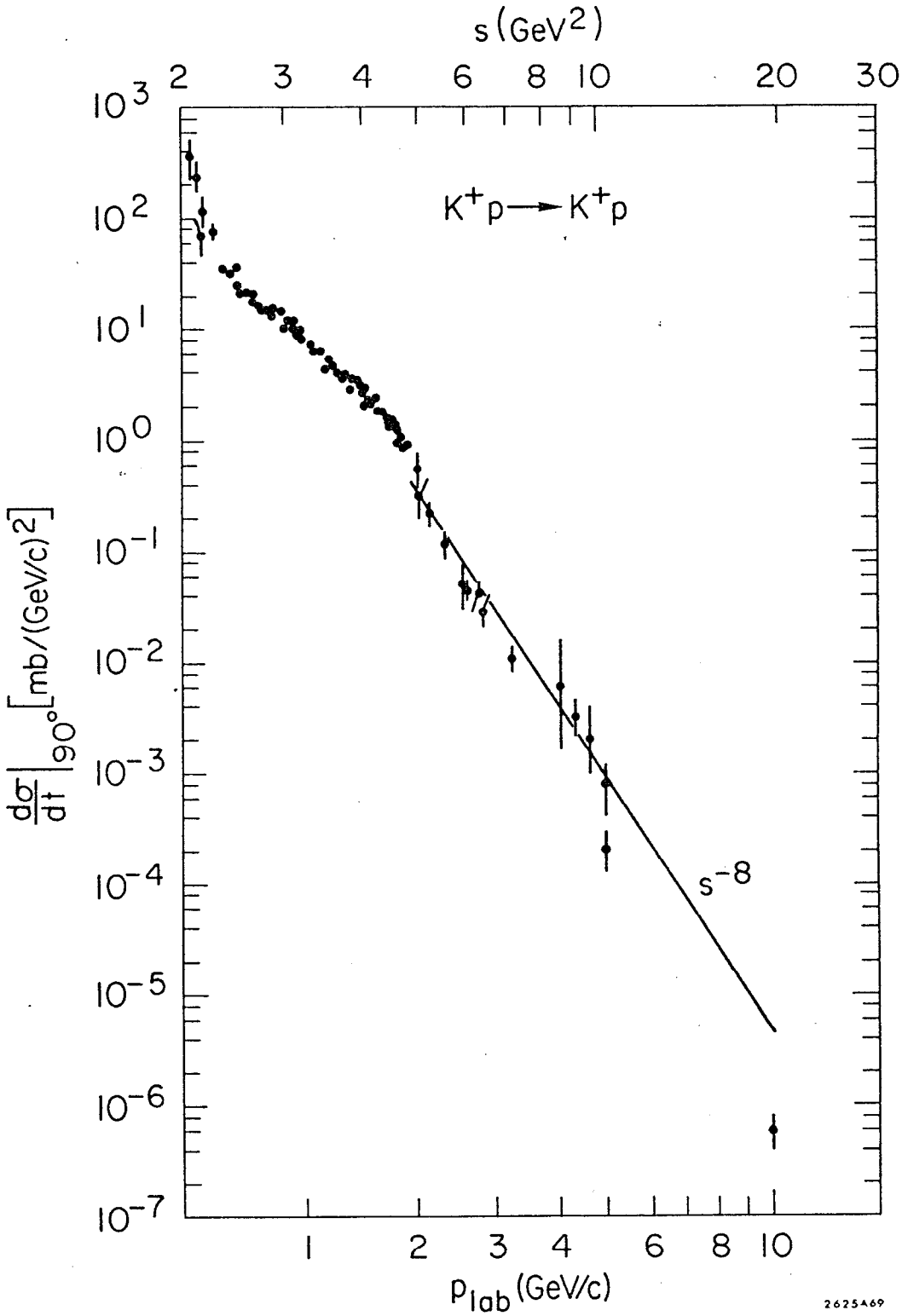
s (GeV²)
2
3
4
6
8
10
20
30
10³
10²
10¹
10⁰
10⁻¹
10⁻²
10⁻³
10⁻⁴
10⁻⁵
10⁻⁶
10⁻⁷
K⁺p → K⁺p
s⁻⁸
dσ/dt |90° [mb/(GeV/c)²]
1
2
3
4
6
8
10
p_lab (GeV/c)
2625A69

FIG. IIA.6

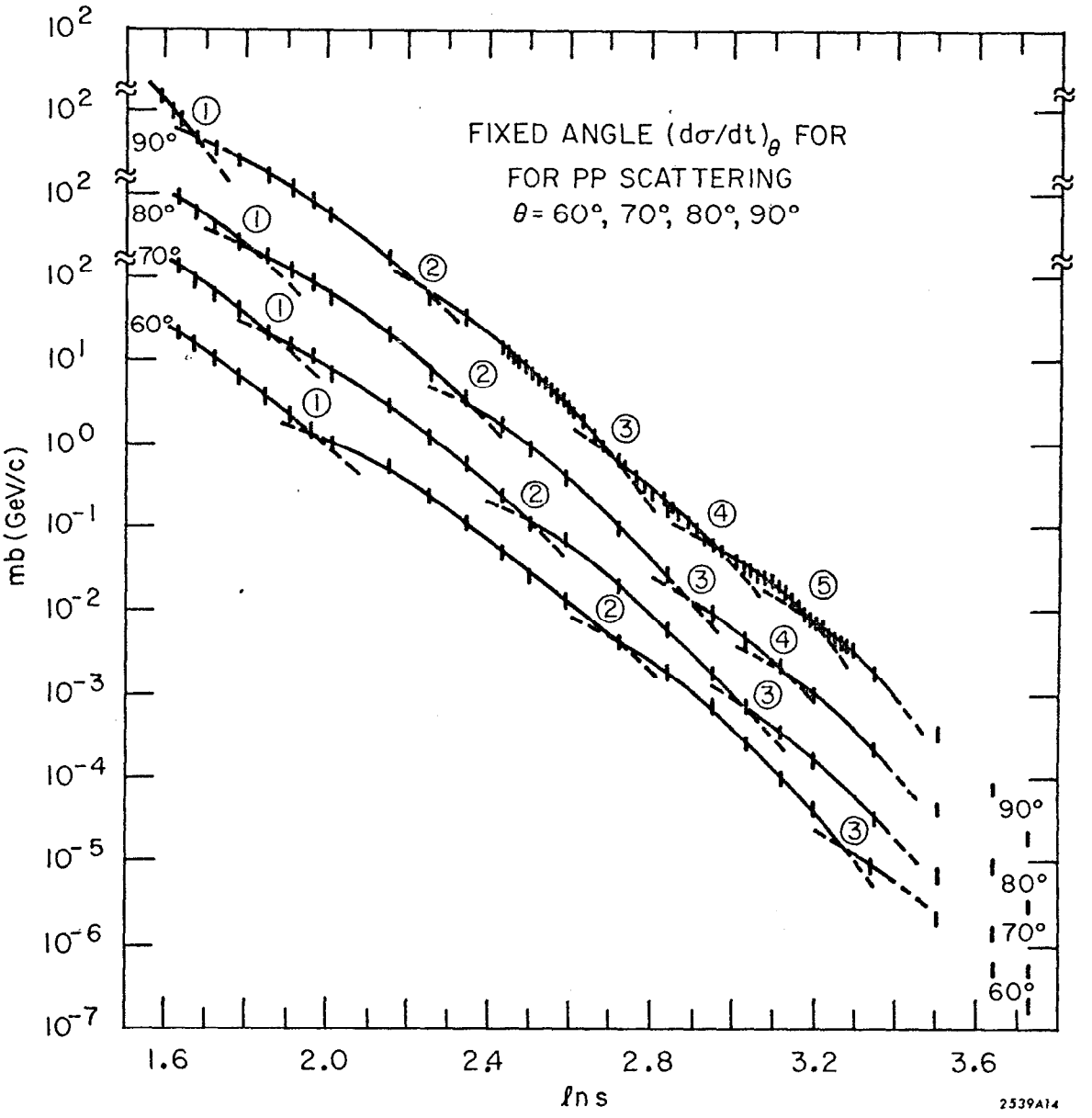
FIXED ANGLE $(d\sigma/dt)_\theta$ FOR
FOR PP SCATTERING
θ = 60°, 70°, 80°, 90°
mb (GeV/c)
$\ell n\, s$
90°
80°
70°
60°
2539A14

FIG. IIA.7

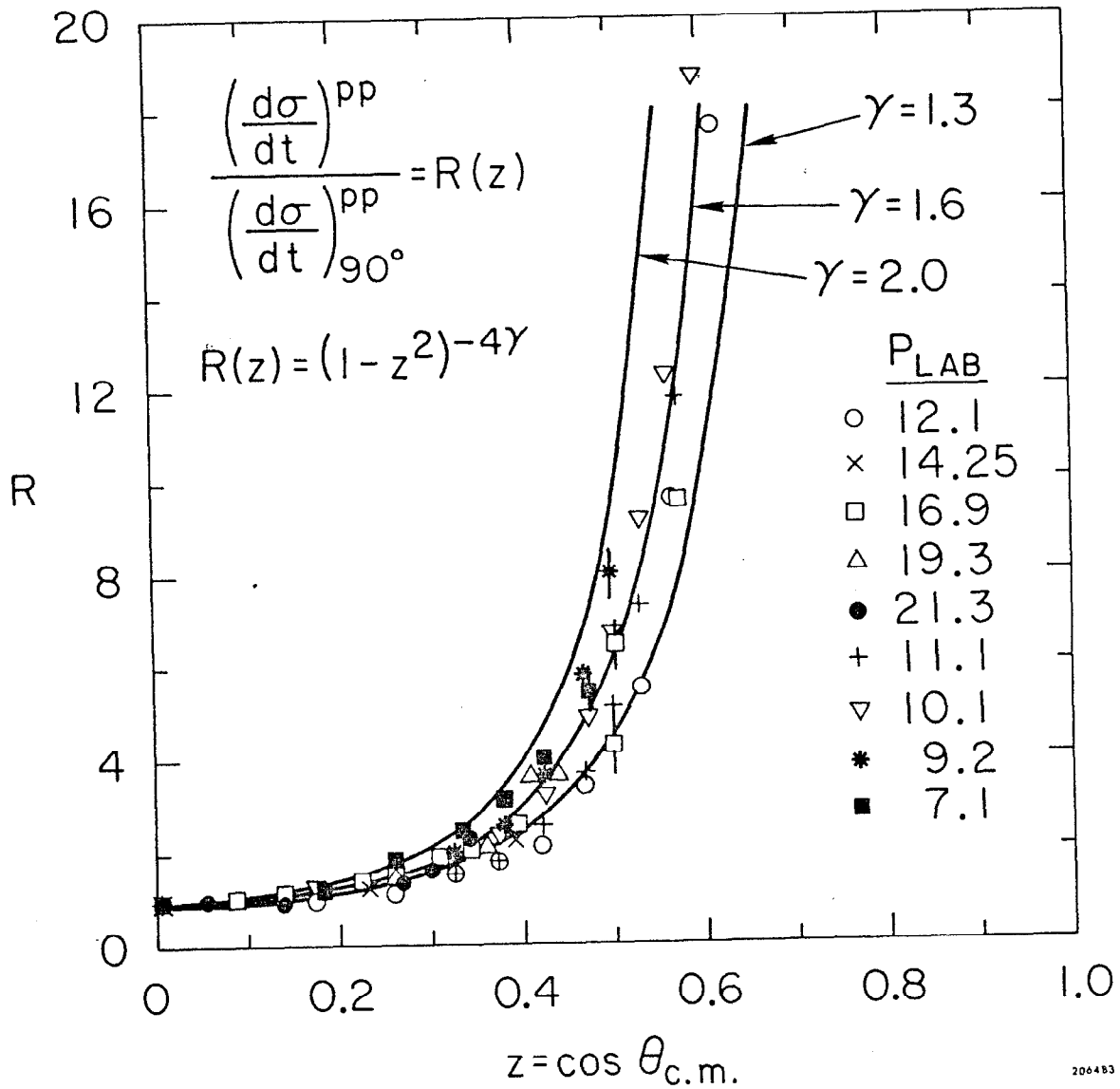
$\left(\frac{d\sigma}{dt}\right)^{pp} \Big/ \left(\frac{d\sigma}{dt}\right)^{pp}_{90°} = R(z)$
$R(z) = (1 - z^2)^{-4\gamma}$
$\gamma = 1.3$
$\gamma = 1.6$
$\gamma = 2.0$
P_{LAB}
12.1
14.25
16.9
19.3
21.3
11.1
10.1
9.2
7.1
R
0
4
8
12
16
20
0
0.2
0.4
0.6
0.8
1.0
$z = \cos\theta_{c.m.}$
206483

FIG. IIA. 8

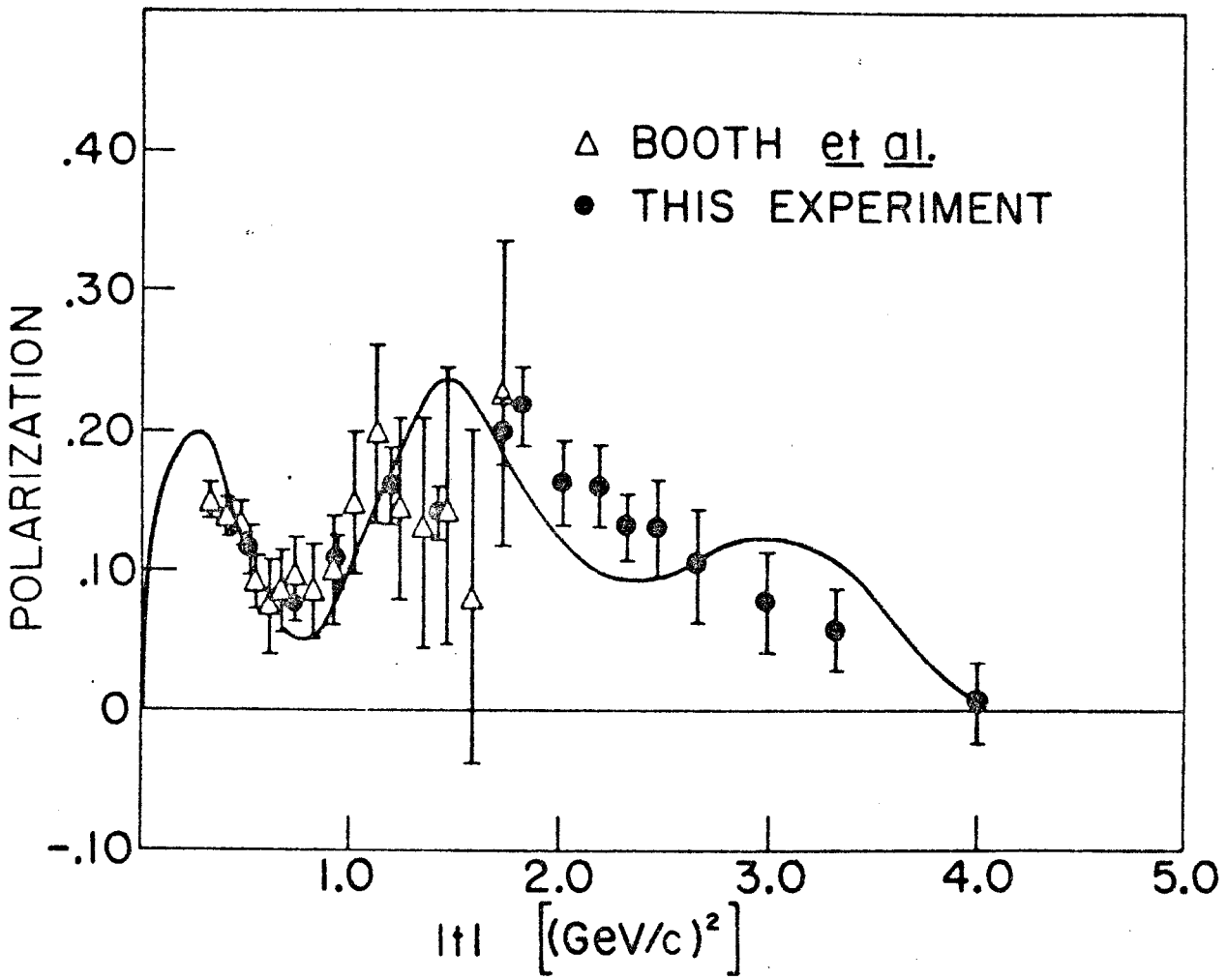
△ BOOTH et al.
● THIS EXPERIMENT
POLARIZATION
.40
.30
.20
.10
0
-.10
1.0
2.0
3.0
4.0
5.0
|t| [(GeV/c)²]

FIG. IIA.9

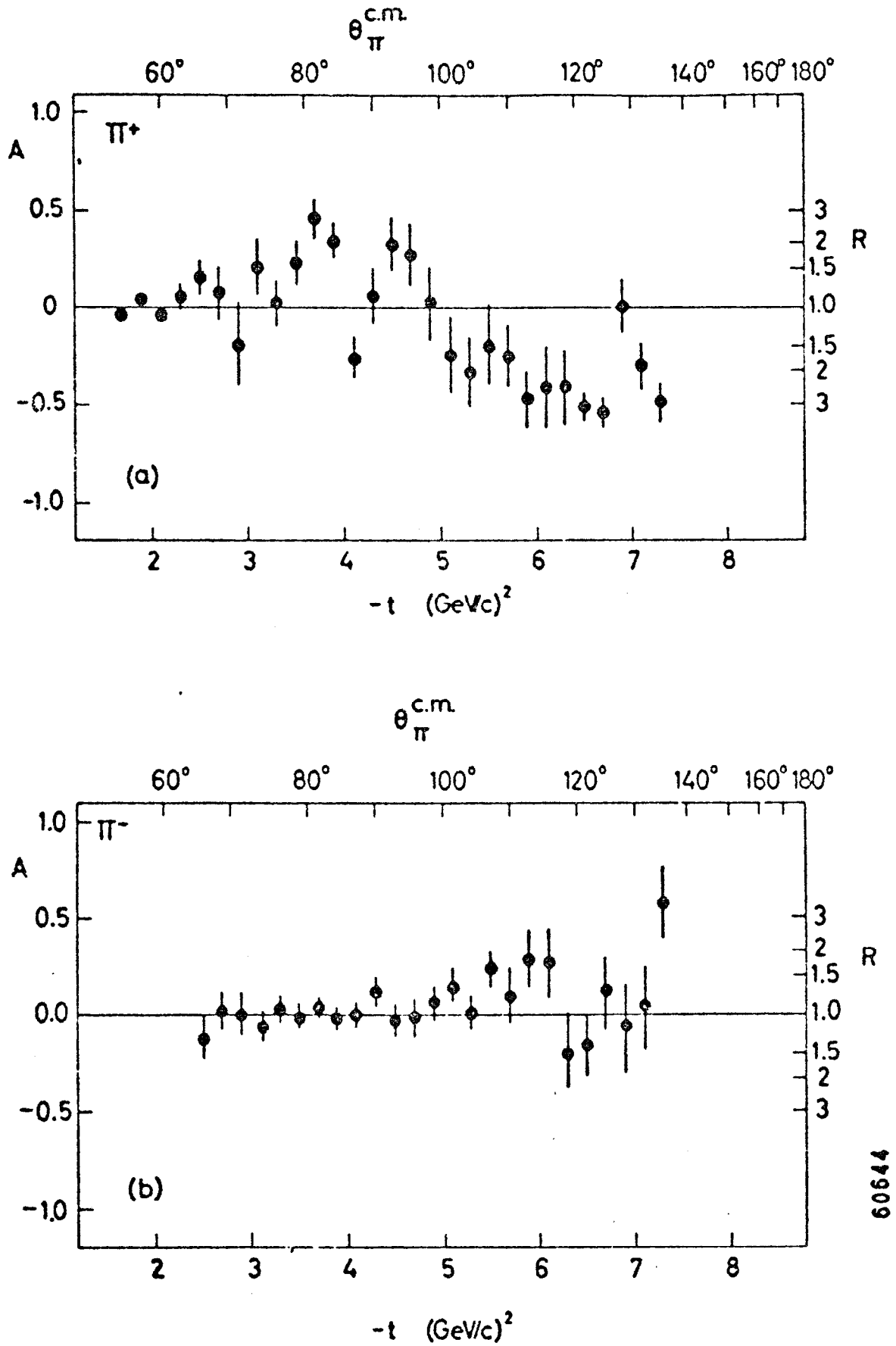

60644

FIG. IIA. 10

B. Single Particle Inclusive Experiments

In this section we discuss experimental data on the single-particle inclusive process

$$AB \rightarrow C + \text{anything} \qquad \text{(IIB.1)}$$

where the detected particle is observed to have large transverse momentum. The important features of the data include the shape and energy dependence of the inclusive spectra, particle ratios, and the connection of the high-p_T spectra to those measured at low p_T.

The first high-p_T single-particle inclusive measurements at the CERN-ISR reported a yield much larger than had previously been expected. As shown in Fig. IIB. 1, the invariant cross section for producing hadrons with $p_T = 5$ GeV/c is approximately 10^5 times larger than the value given by a simple extrapolation of the e^{-6p_T} dependence found to be valid in the region $0.15 \lesssim p_T \lesssim 1.0$ GeV/c. The current high energy experiments with substantial data for the production of particles with $p_T > 2.0$ GeV/c are listed in Table II. 1 along with some of the important experimental characteristics. This table is an updated version of a similar listing given by Ellis and Thun (1974). The fact that the number of completed experiments is still small enough so that they can be included in this table is important as a reminder of how new this subject really is.

A notable fact of Table II. 1 is that all the experiments we will discuss here measure proton-nucleon collisions. Experiments with pion or other types of secondary beams are still only in the preliminary stage. As we go through the following outline of results it is important to keep in mind that the various experiments are in substantial overall agreement. There are some problems concerning the relative normalization of the data from different experiments but these are minor in view of the fact that, with the steeply falling cross

TABLE II. 1

Measurements of Inclusive Single-Particle Cross Sections at Large p_T

Experiment	Reaction	Detector	c.m. energy (GeV)	p_T range (GeV/c)	c.m. angle (Degrees)
CERN-Columbia-Rockefeller (ISR) Busser et al. (1973)	$pp \rightarrow \pi^0$ + anything	Lead-glass	23.5 30.6 44.8 52.7 62.4	2.8-4.6 3.0-6.4 2.6-5.9 2.6-9.0 2.9-4.6	90 30
Saclay-Strasbourg (ISR) Banner et al. (1973)	$pp \rightarrow X^{\pm}$ + anything (X not identified) $pp \rightarrow \pi^{\pm}$ + anything $pp \rightarrow \gamma$ + anything	Magnetic spectrometer and shower counter	23.2, 30.4 44.4, 52.7 44.4, 52.7 44.4, 52.7	1.0-3.0 3.0-5.0 1.0-3.0	90
British-Scandinavian (ISR) Alper et al. (1973, 1974a, b)	$pp \rightarrow \pi^{\pm}$ $pp \rightarrow K^{\pm}$ + anything $p\bar{p}$	Single-arm spectrometer with two magnets Cerenkov counters added?	44 53 23-62 44 53	1.3-3.2 1.3-5.0 1.5-4.7 1.5-4.6	59 39° 59 90 90
Chicago-Princeton Fermilab Cronin et al. (1973)	$pW \rightarrow \pi^{\pm}$ $pW \rightarrow K^{\pm}$ $pBe \rightarrow p, \bar{p}$ $d\bar{d}$ +anything	Magnetic spectrometer	19.4 23.8 27.3	0.8-7.3 0.8-7.6 0.8-7.2	77 89 96
Fermilab Carey et al. (1974a, b)	$pp \rightarrow \gamma$ + anything	Lead-glass	9.8-27.4	0.2-3.0	Fixed angle in lab = 100 mrad
Columbia-Fermilab Appe et al. (1974a)	$pp \rightarrow \pi^0$ + anything $pp \rightarrow h^-$ + anything	Lead-glass			
CERN-Paris-Heidelberg Karlsruhe Cottrell et al. (1975)	$pp \rightarrow h^+$ + anything	ISR split field magnet facility	52.5	2-4	9-21°

sections, a 10% error in measuring the absolute value of the transverse momentum can lead to more than a factor of two in the absolute value of the cross section.

The CERN-Columbia-Rockefeller collaboration (CCR), have measured π^o production at the CERN-ISR. Gamma rays from the decay of a π^o are detected in an array of lead-glass counters. The two photons from the decay of a π^o are not spatially resolved and the total photon energy is measured. The contamination in the signal at large p_T from η production is suppressed since the decay of an η would lead to photons in different counters and would be counted as two π^o's with lower transverse momentum. A more recent experiment shows that η^o/π^o ratio = 0.55 ± .11 for p_T in the interval 3 to 5.6 GeV/c (Busser et al., 1975). Due to the large kinematic region spanned by this experiment, the global dependence of the data is extremely important. The claim is that all the data can be fit to the empirical form

$$\frac{Ed^3\sigma}{d^3p} = \frac{A}{p_T^n} e^{-bx_T} \qquad \text{(IIB.2)}$$

(see Eq. (IB.3) in the Introduction) where $x_T = 2p_T/\sqrt{s}$, A = 15.4 mb, n = 8.24 ± 0.05 and b = 13.05 ± 0.25. Because of the systematic errors the data are consistent with n=8 which was the power predicted by the constituent interchange model (Blankenbecler, Brodsky and Gunion, 1972) for this process.

Three other experiments have measured γ-ray yields. The Saclay-Strasbourg collaboration (SS) have data on pp $\rightarrow\gamma$ for values of $p_T \lesssim 3.0$ GeV/c. These measurements can be converted to π^o spectra assuming there is no other major source of high energy photons so that the interpretation of the data requires suppression of η production. The SS results generally support the p_T and

energy-dependence of the CCR data in the region of overlap except that an overall normalization factor of approximately 0.7 is needed which brings (IIB.2) into agreement with the SS rate (see Busser et al., 1974).

The FNI collaboration (D. Carey et al., 1974) measured $pp \rightarrow \gamma +$ anything at Fermilab for fixed lab angles of 80, 100, and 120 mrad. For incident proton energies from 50 to 400 GeV/c. This translates to a range of θ_{CM} from 40° to 110°. Converting to a π^o invariant cross section they fit their data at all angles to the form

$$\frac{E\, d^3\sigma}{d^3p}(pp \rightarrow \pi^o X) \propto (1-x_R)^4 \left(p_T^2 + 0.86\right)^{-4.5} \qquad \text{(IIB.3)}$$

where $x_R = p^*/p_{max}$ is the radial scaling variable. Since the bulk of the data is at a lower energy than either CCR or SS, it is difficult to make a direct comparison. There appears to be no direct conflict but the form (IIB.3) when extrapolated does not agree with other data.

The final γ experiment we will be discussing here, a Columbia-Fermilab collaboration (CF) (J. Appel et al., 1974a), used a beryllium target. When converted to produce the cross section per nucleon the experimental results indicate a good agreement with a modification of the CCR fit designed to fit smoothly onto the low-p_T data. The quoted parametrization, given in Eq. (IB.3), gives some support to the results of CCR but there are some normalization problems associated with the nuclear target which we will discuss below.

The inclusive production of charged particles in proton-nucleon collisions has been measured by three groups, the Saclay-Strasbourg collaboration (SS) and the British Scandinavian collaboration (BS) at the CERN-ISR and the Chicago-Princeton (CP) group at Fermilab.

The Saclay-Strasbourg group (M. Banner et al., 1973) measured both charged particles and π^o's. One of the first high p_T experiments, their original results are consistent with the more detailed results reported since.

The CP experiment (J. W. Cronin et al., 1973, 1974) has measured the production of charged hadrons at p_{LAB}=200, 300, 400 GeV/c at Fermilab. The measurements were taken at fixed laboratory angles but these were chosen to be near 90° CM in the energy range scanned (77°, 89°, 96°, respectively). The experiment was run with nuclear tungsten target. At 300 GeV/c the measurements were repeated with other targets in an attempt to understand the nuclear effects. The first result, indicated in Fig. IIB.2, is that the variation of the invariant cross section for π production with the atomic number A is approximately linear for large p_T. This suggests the approximate validity of the impulse or single-scattering approximation inherent in the parton model. At small p_T the cross section is supposed to scale more like $A_{eff} = \sigma_{abs}/\sigma_p$. The fact that the large p_T cross section is closer to being proportional to $A^{1.1}$ than $A^{1.0}$ and that particle ratios depend on A in a nontrivial way at large p_T, indicates there may be some additional rescattering effects but these will not be considered further here.

One important aspect of this experiment is the large values of $x_T = 2p_T/\sqrt{s}$ at which cross sections are measured. For $\pi^\pm$ production they measure out to an x_T of 0.72 while the CCR measurements for π^o are all taken below $x_T = 0.35$. This means that CP are sensitive to the x_T dependence of the data in spite of their comparatively small range of $\sqrt{s}$. For $x_T \geq 0.4$, the pion data can be parametrized by a form

$$\frac{E\, d^3\sigma}{d^3p} \propto s^{-5.5\pm0.2} \exp\left\{-(36.0 \pm 0.4)\, x_T\right\} . \qquad \text{(IIB.4)}$$

For $x_T < 0.35$ the data agree with the CCR experiment. The effective power of s in the CP data (see Cronin, 1974) is shown in Fig. IIB.3 plotted against x_T. For low x_T, the power of s in this type of parametrization is sensitive to finite mass effects and, for $x_T = 0$, must equal zero in order to agree with Feynman scaling.

Particle ratios in the CP experiment are shown as a function of p_T in Figs. IIB.4 and IIB.5. In view of the evidence that there might be some nuclear effects which are important in the particle ratios, it is important to look at the particle composition from pp collisions. The British Scandinavian data on particle composition at $\sqrt{s} = 52.8$ GeV is shown as a function of p_T in Fig. IIB.6 The overall agreement is quite good. It is notable that the ratio K^+/π^+ appears to approach an asymptotic constant while K^-/π^- and $\bar{p}/\pi^-$ are falling. It is interesting that $\bar{p}/p \cong 1$ near $p_T = 1\text{-}1/2$ GeV/c.

Another important measurement from these two groups is the detection of heavy particles. The CP data on deuteron and antideuteron production are shown in Fig. IIB.5. In the momentum interval $2 < p_T < 5$ GeV/c the BS collaboration report a ratio

$$\bar{p}/\bar{D} = 1.2 \times 10^3 \qquad \text{(IIB.5)}$$

and a ratio

$$d/\bar{d} = 3.5 \pm 1.5 \qquad \text{(IIB.6)}$$

Comparison with the deuteron-antideuteron ratio of CP shows that the ratio (IIB.6) is strongly s-dependent and consistent with approaching 1 at small p_T.

To study the global dependence of single particle inclusive data the plots in Figs. IIB.7 and IIB.8 due to Cronin (1974) are valuable. These graphs show the cross section on a logarithmic scale plotted against ℓn s. The lines drawn in are contours of constant p_T and constant x_T. These figures clearly show the

absence of and importance of data extending to large values of x_T in the CERN-AGS-Serpukhov energy regimes. In view of the smoothness with which exclusive cross sections at large angle continue down to low energy it would be extremely interesting to see the "low-energy" behavior of the large p_T cross sections observed at Fermilab and the CERN-ISR. What low-energy data does exist joins smoothly onto the large p_T-large s data and, on this plot, there does not appear to be a sharp distinction between the large p_T and the low p_T regimes. An interesting fact (Walker, 1973) is that the energy dependence of the large p_T π-production data is similar to the energy dependence of $\bar{p}$ production at low p_T. This is illustrated in Fig. I.4, reinforcing the feeling of continuity between the large p_T and small p_T regimes. Perhaps the initial conclusions emphasizing the difference of the two regimes based on an extrapolation of the exp $(-6p_T)$ form were not well founded.

The single particle inclusive spectra presented here will soon be supplemented by new data in other kinematic regions and with other beams. We will return to expectations for this data based on fits with current models to the existing data in Section V.

LIST OF FIGURES FOR SECTION IIB

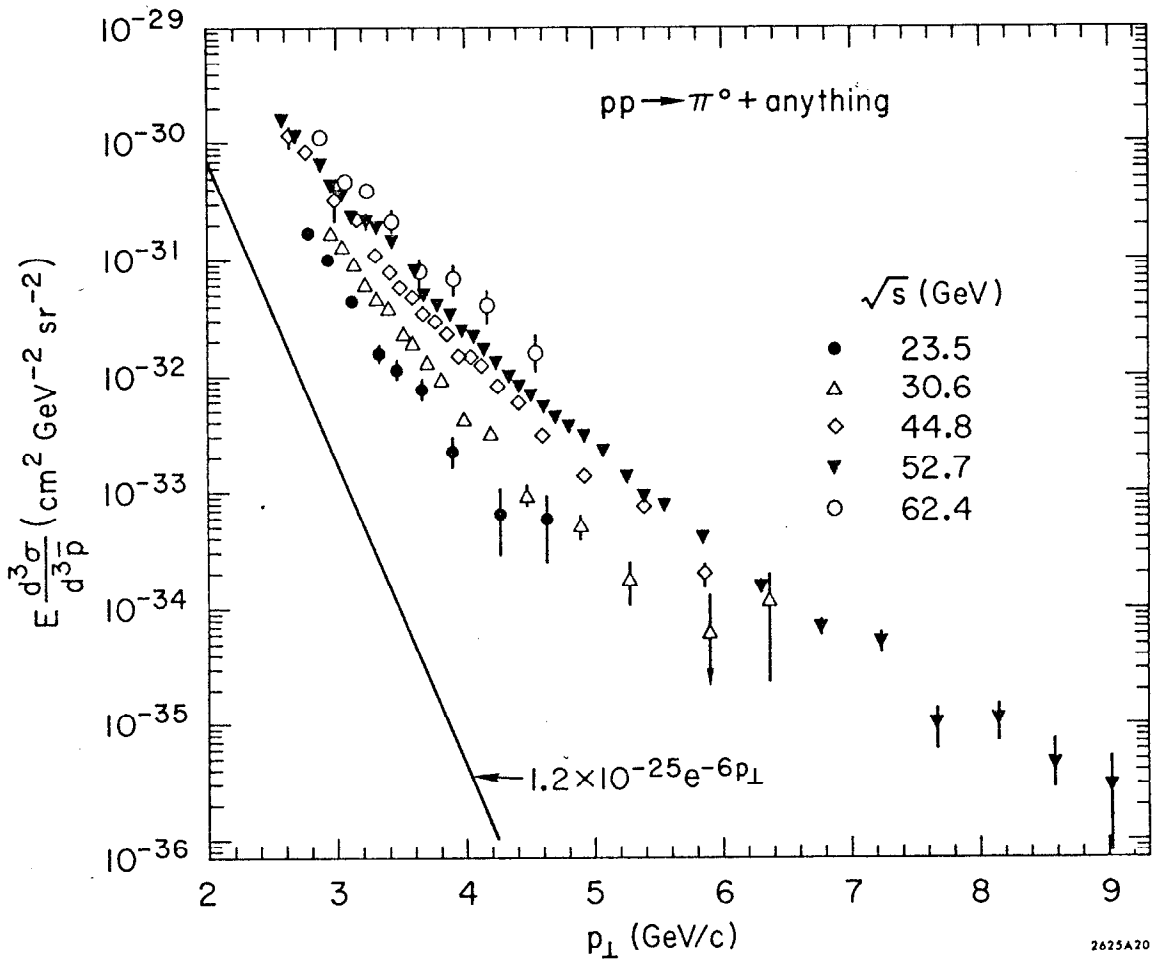
pp → π° + anything
√s (GeV)
23.5
30.6
44.8
52.7
62.4
1.2×10⁻²⁵e⁻⁶ᵖ⊥
E d³σ/d³p̄ (cm² GeV⁻² sr⁻²)
p⊥ (GeV/c)
2625A20

FIG. IIB. 1

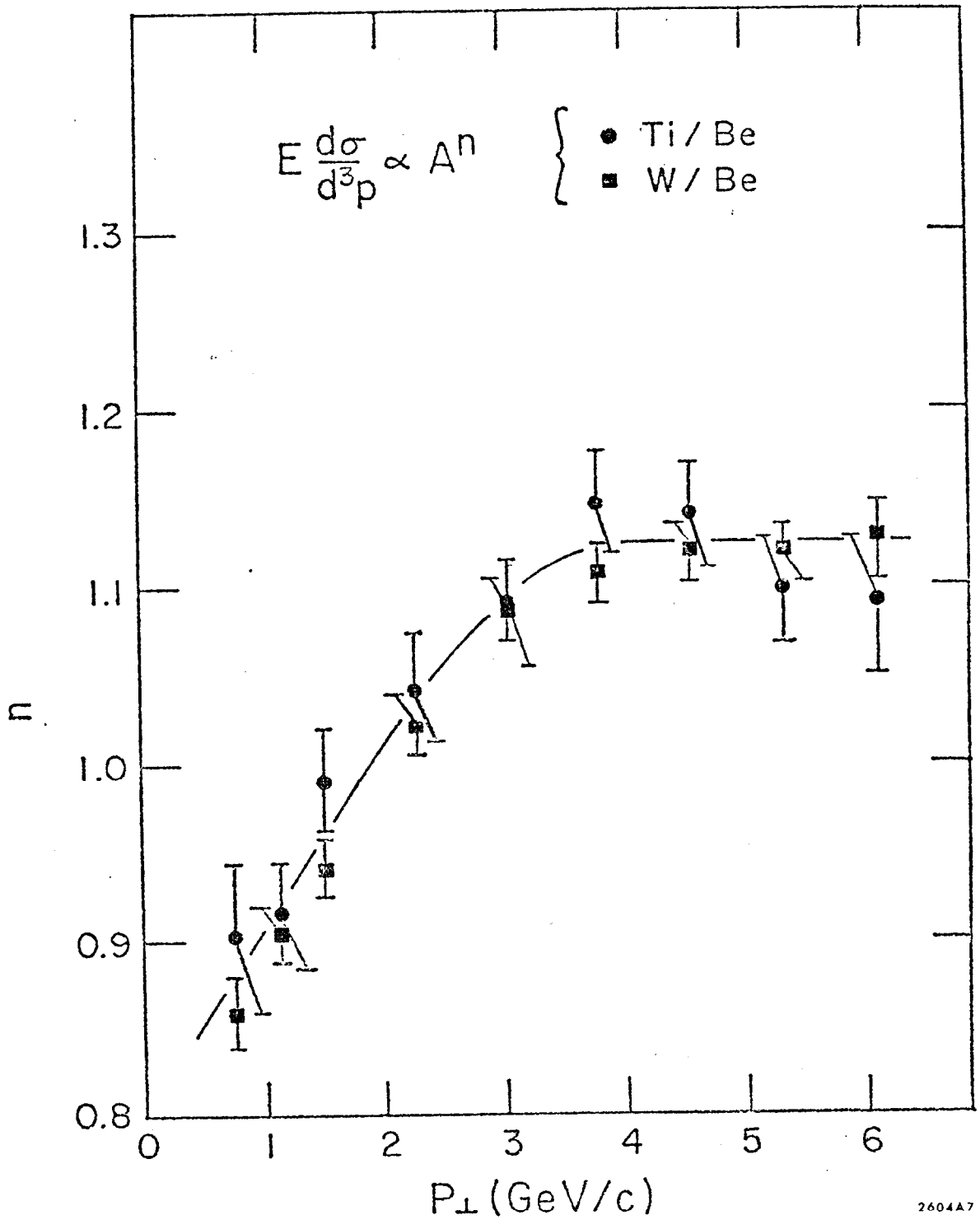
$E\frac{d\sigma}{d^3p} \propto A^n$
Ti / Be
W / Be
1.3
1.2
1.1
1.0
0.9
0.8
n
0
1
2
3
4
5
6
$P_\perp$ (GeV/c)
2604A7

FIG. IIB.2

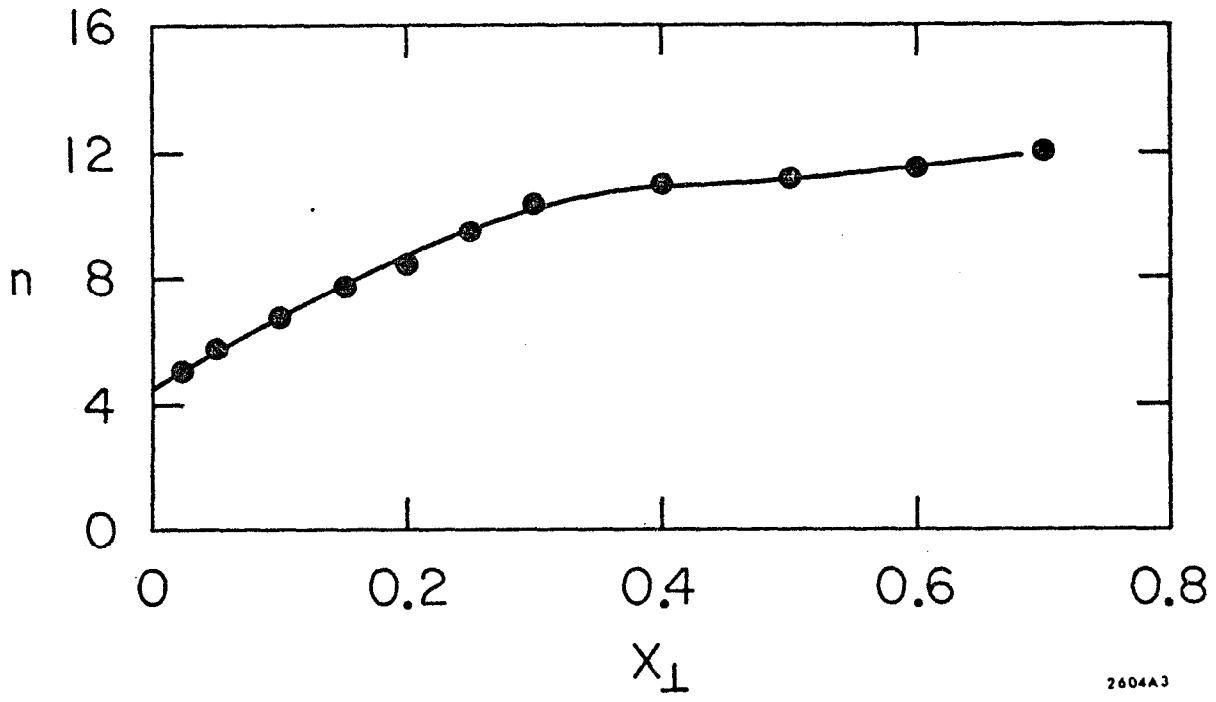

FIG. IIB.3

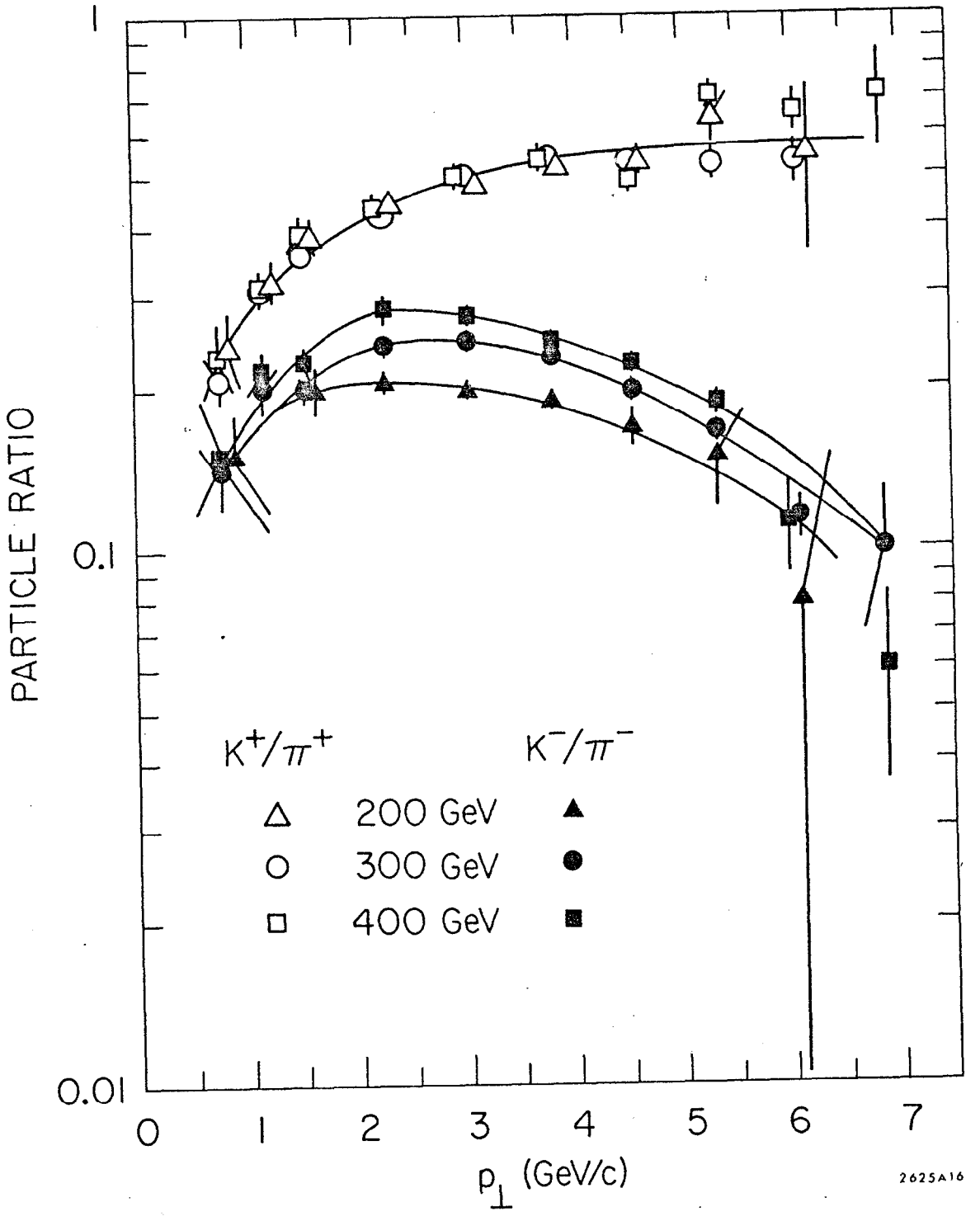
PARTICLE RATIO
1
0.1
0.01
0
1
2
3
4
5
6
7
$p_\perp$ (GeV/c)
K^+/π^+
K^-/π^-
200 GeV
300 GeV
400 GeV
2625A16

FIG. IIB.4

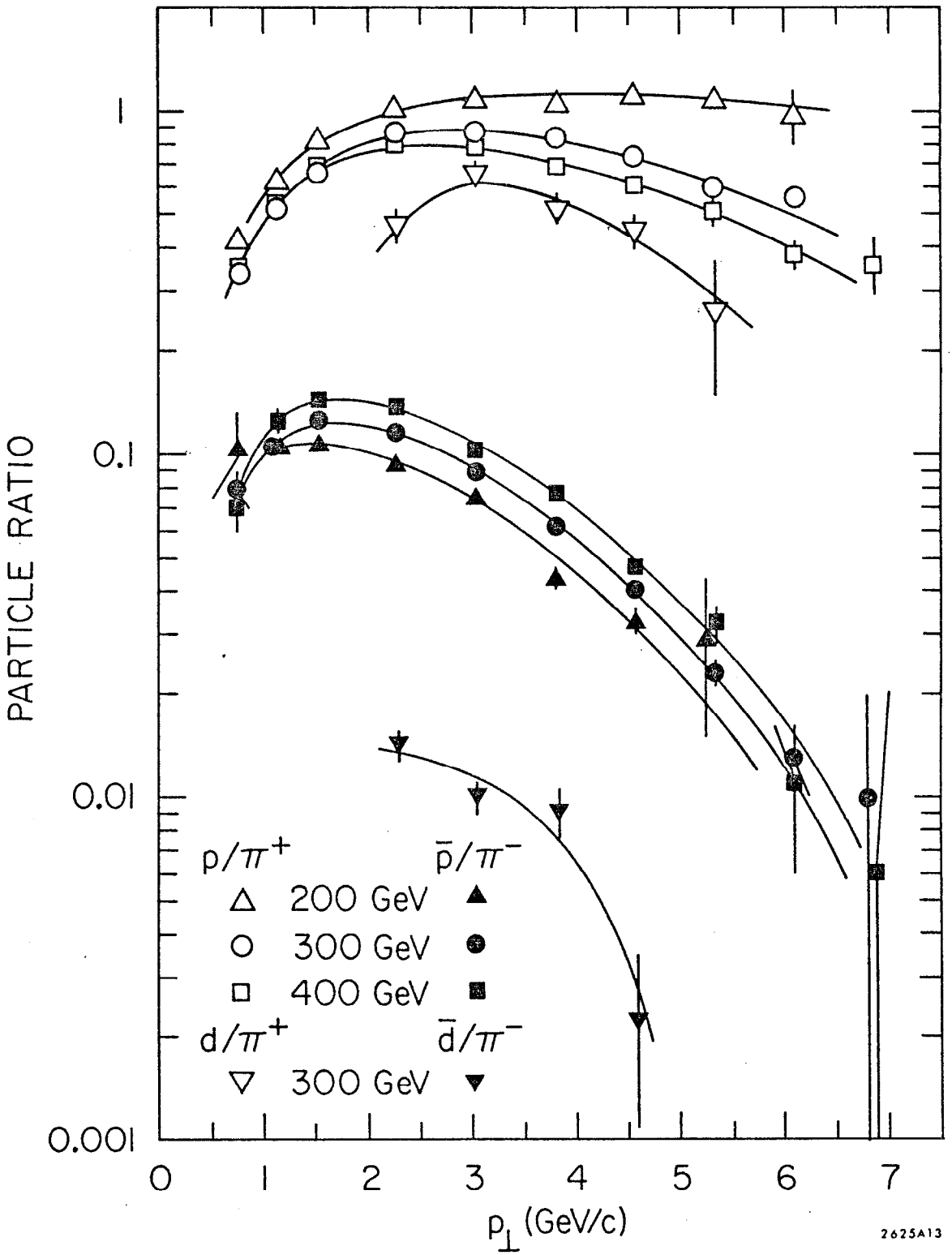
PARTICLE RATIO
1
0.1
0.01
0.001
0
1
2
3
4
5
6
7
$p_\perp$ (GeV/c)
p/π^+
$\bar{p}/\pi^-$
200 GeV
300 GeV
400 GeV
d/π^+
$\bar{d}/\pi^-$
300 GeV
2625A13

FIG. IIB.5

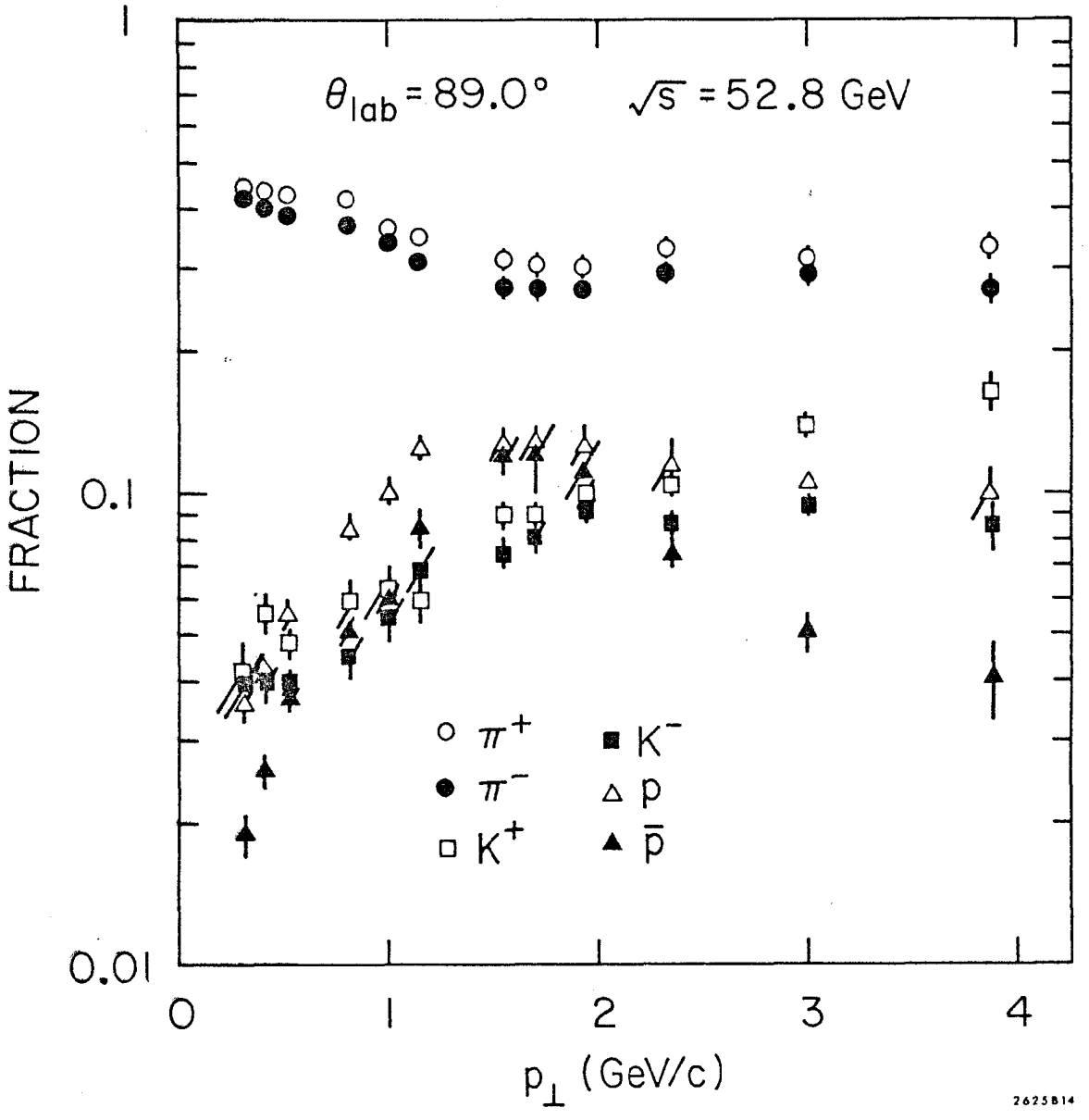
$\theta_{lab} = 89.0°$
$\sqrt{s} = 52.8$ GeV
FRACTION
1
0.1
0.01
0
1
2
3
4
$p_\perp$ (GeV/c)
π^+
π^-
K^+
K^-
p
$\bar{p}$
2625B14

FIG. IIB.6

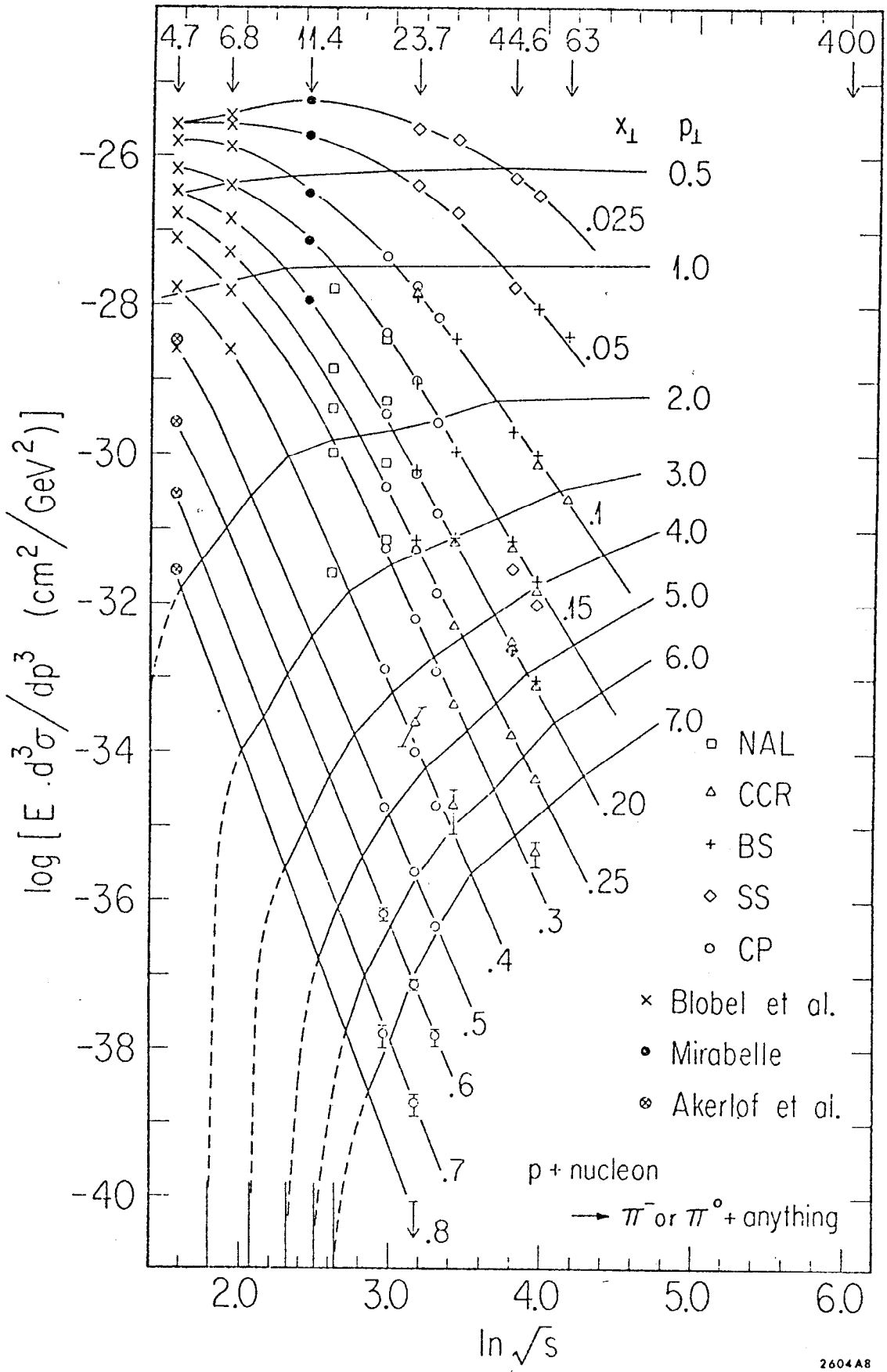
4.7
6.8
11.4
23.7
44.6
63
400
$x_\perp$
$p_\perp$
0.5
1.0
2.0
3.0
4.0
5.0
6.0
7.0
.025
.05
.1
.15
.20
.25
.3
.4
.5
.6
.7
.8
NAL
CCR
BS
SS
CP
Blobel et al.
Mirabelle
Akerlof et al.
p + nucleon
$\rightarrow \pi^-$ or π^0 + anything
$\log [E \cdot d^3\sigma/dp^3 \ (cm^2/GeV^2)]$
-26
-28
-30
-32
-34
-36
-38
-40
2.0
3.0
4.0
5.0
6.0
$\ln \sqrt{s}$
2604A8

FIG. IIB.7

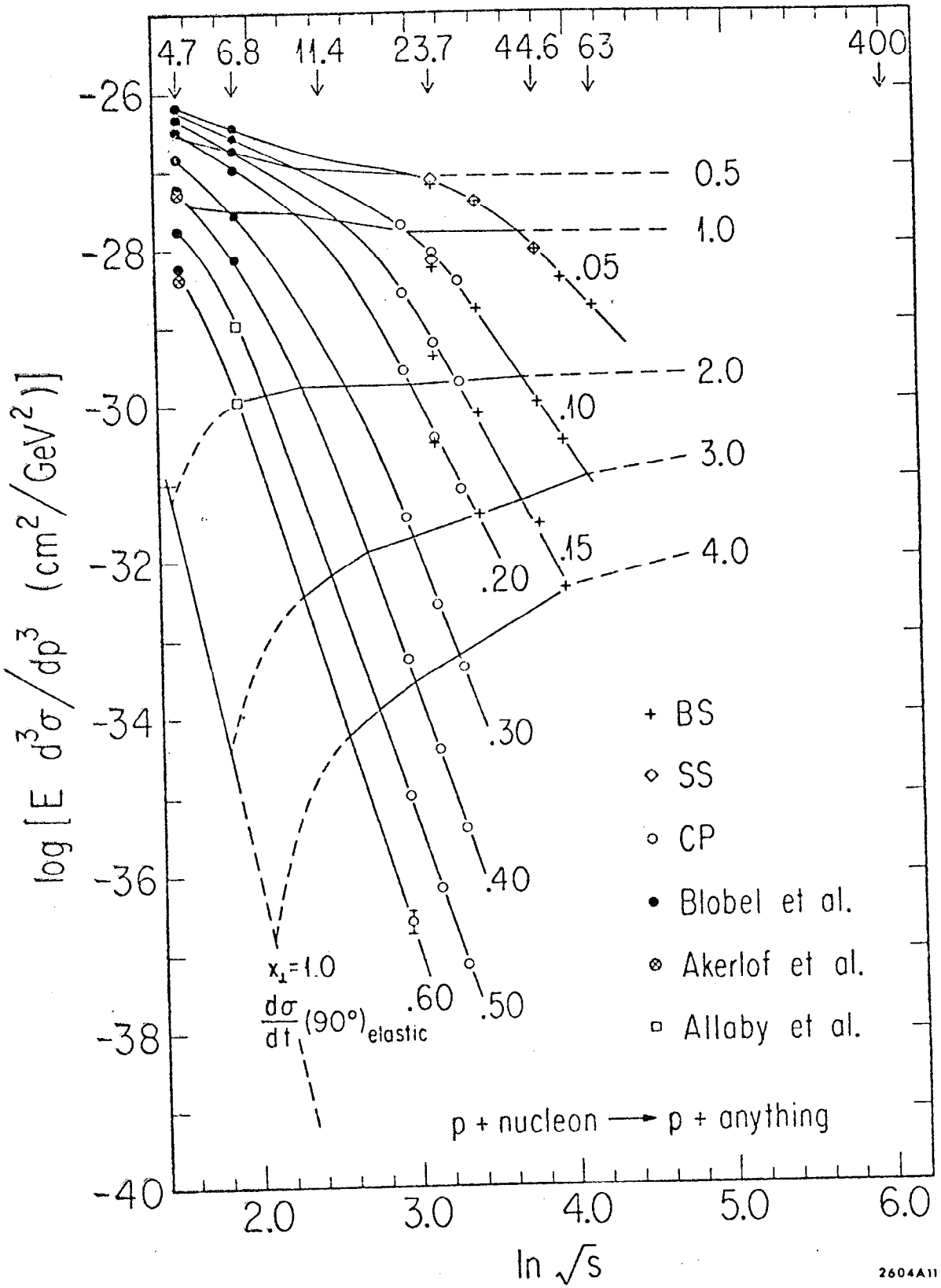
4.7
6.8
11.4
23.7
44.6
63
400
-26
-28
-30
-32
-34
-36
-38
-40
0.5
1.0
2.0
3.0
4.0
.05
.10
.15
.20
.30
.40
.50
.60
$x_\perp = 1.0$
$\frac{d\sigma}{dt}(90°)_{elastic}$
+ BS
◇ SS
○ CP
• Blobel et al.
⊗ Akerlof et al.
□ Allaby et al.
p + nucleon → p + anything
$\log [E\, d^3\sigma/dp^3 \ (cm^2/GeV^2)]$
2.0
3.0
4.0
5.0
6.0
$\ln \sqrt{s}$
2604A11

FIG. IIB.8

C. Data on Correlations and Associated Multiplicities

The most decisive tests of models based on specific dynamical mechanisms involve the complete phase space structure of individual events containing a large p_T particle. Until such data are available we can construct partial tests using available data on two-body correlations and associated multiplicities. Since the experiments which measure these quantities are much more difficult than single-particle inclusive measurements, we can only make a beginning at answering those questions which enable us to discriminate between different models.

In order to understand the issues involved, recall that hard scattering models assume the existence of a quasi-two-body subprocess which leads to large transverse momentum in a single step. This substructure can be used to define the jet hypothesis. Event-by-event, the population of secondary hadrons is confined to the usual low p_T region and to two approximately coplanar regions along the direction of the high p_T particles. These jet axes approximately coincide with the direction of the underlying constituents after scattering. The jet hypothesis is illustrated in Fig. I.6 taken from Savit (1973).

When we detect a large transverse momentum hadron, say with a finite value of $x_T = 2p_T/\sqrt{s}$, we know that its momentum must be balanced by the other particles in the event. It is a dynamical question how this balancing takes place. If it is balanced only by particles with small transverse momentum, one obviously needs a large number of these associated particles, at least

$$\langle n_A \rangle \simeq \frac{x_T}{2} \frac{\sqrt{s}}{\langle p_T \rangle} \cong \frac{p_T}{\langle p_T \rangle} \qquad \text{(IIC. 1)}$$

If, on the other hand, there is an underlying hard interaction the momentum can be balanced by one particle with equal and opposite transverse momentum. Most models choose intermediate behaviors for associated multiplicity, often logarithmic. A more detailed discussion of the model predictions can be found in the review of Bjorken (1973c).

One type of experiment which is extremely valuable is that done by a Brookhaven-Purdue-Virginia Polytechnic collaboration (Anderson et al., 1974). Using a multiparticle spectrometer system (ARGO) they measured the mean charged multiplicity associated with a high transverse-momentum proton or pion. The data on $\langle n_c(p_T, \mathcal{M})\rangle$ for the reaction

$$pp \rightarrow p + X$$

at $p_{LAB} = 28.5$ GeV/c are shown in Fig. IIC.1b as a function of the transverse momentum of the proton for different values of missing mass. A striking feature of the data is a rise of $\Delta\langle n_c\rangle$ charged particles over an interval of approximately 0.3 GeV/c in p_T. The location of the structure moves to smaller p_T as the missing mass increases. The position of the structure is found to be approximately fixed in angle at around $\theta_{CM} = 33^o$ ($\tan \theta_{CM} = 0.66$). The structure is seen in all pronged cross sections. Outside the region of the rise $\langle n_c(p_T, \mathcal{M})\rangle$ is approximately independent of transverse momentum except for possible kinematic effects. This type of sudden structure was not predicted by any model. Possible explanations such as a change over from one fireball to two fireballs or a damping of bremsstrahlung in a hard scattering model do not seem to work in detail. However, Alonso and Wright (1975), find the sharp transition in multiplicity can be accommodated in a two component model consisting of a hard scattering term plus a normal hadronic background. There is a definite need for more theoretical work in

this area as well as more experiments of this type at both higher and lower energies.

The same group has also presented data on $<n_c^{\pi}(p_T, \mathcal{M})>$ in the reaction

$$pp \rightarrow \pi^+ + \text{anything}$$

which is plotted in Fig.IIC.1a. These data also show a jump structure. An interesting fact is that the difference $\Delta = <n_c^p(p_T, \mathcal{M})> - <n_c^{\pi}(p_T, \mathcal{M})>$ is almost independent of both p_T and $\mathcal{M}$ over the entire kinematic region. A plot of this quantity is shown in Fig.IIC.2.

As interesting as the Brookhaven-Purdue-Virginia Polytechnic data are, we cannot be sure that we are at high enough energy to be sensitive to the same dynamics that dominate FNAL and ISR. Its real importance for our present purposes is that it provides a basis of comparison for higher energy data to come. We therefore turn to data from three ISR experiments which have reported results on multiplicities associated with a large transverse momentum particle. None of these experiments measure the momentum of the associated particles and none have acceptance over the full solid angle.

The Pisa-Stony Brook experiment (see Del Prete, 1974 ; Finocchiaro et al., 1974) on charged multiplicities associated with a large transverse momentum γ has a detection system covering around 80% of the full solid angle. Data in Fig.IIC.3 demonstrate the rise in multiplicity as a function of p_T of a γ emitted near $\theta_{CM} = 90^o$. The data are normalized to the multiplicities at each energy with a low p_T trigger.

In the absence of any measurements of the momentum of the associated particles, the experimenters made a parametrization

$$<n_A(\sqrt{s}, p_T)> = <n^{low}(\sqrt{s} - 2p_T)> + <n^{jet}(\sqrt{s}, p_T)> \qquad \text{(IIC.2)}$$

where $<n^{low}(\sqrt{s} - 2p_T)>$ is the value of the average multiplicity of low transverse momentum events evaluated at the "reduced" energy $\sqrt{s} - 2p_T$. With this crude correction for phase-space effects the value of $<n_{jet}(\sqrt{s}, p_T)>$ is found to be roughly independent of energy

$$<n^{jet}(\sqrt{s}, p_T)> \simeq 0.5\ p_T \qquad \text{(IIC. 3)}$$

See Fig.IIC.4. Comparison with Eq. (IIC. 1) shows a contradiction unless $<p_T> \cong 2$ for the balancing particles.

When we ask where the extra particles associated with a large p_T γ appear in phase space, we see from Fig.IIC.5 that they are concentrated in the opposite hemisphere from the trigger in a large neighborhood around zero rapidity. Momenta are not measured so the data are plotted as a function of $\eta = \log \tan \eta = \log \tan (\theta_{CM}/2)$. Since the data are normalized to low p_T triggers the usual two particle correlation effect is divided out or, depending on your point of view, folded in. The basic behavior of associated multiplicities with energy and p_T is confirmed by the other experiments.

The azimuthal dependence of the multiplicity in a region around $\eta = 0$ is shown in Fig.IIC.6. Again the data is renormalized to a small p_T trigger. The multiplicity does peak in the direction opposite the detected γ as suggested by simple ideas concerning the conservation of momentum. The width of the distribution in the azimuthal angle ϕ is quite broad, corresponding to $\Delta\phi \approx 100^{\circ}$ FWHM. The data may also be consistent with a simple form of the jet hypothesis if, in addition to a large transverse momentum jet in the opposite hemisphere there are also many low transverse momentum particles. Momentum measurements of the associated particles would prove very interesting. Data from the CCR group on azimuthal correlations between π^{o}'s has been

parametrized

$$C(\phi) = \exp\left[-B \sin \Delta\phi\right] \qquad \text{(IIC.5)}$$

where $\Delta\phi$ is the deviation in azimuthal angle from 180°. When both π_0's are restricted to be larger than 2 GeV/c they find $B = 1.5 \pm 0.2$. This translates into an average component of momentum normal to the hypothetical scattering plane of

$$\langle p_N \rangle \cong 1.3 \text{ GeV/c}$$

This is considerably broader than is expected from simple ideas concerning jets where the spread around the hypothetical jet axis is expected to be about the same as the average momentum spread around the beam direction in "soft" scattering events. One way of quantifying this lack of coplanarity (due to J. D. Bjorken) is to make the strong assumption of a random walk around the jet axis so that the normal component of momentum is expected to be

$$\langle p_N \rangle \cong \frac{\langle p_T \rangle}{\sqrt{2}} \sqrt{n} \qquad \text{(IIC.6)}$$

where $\langle p_T \rangle$ is the average transverse momentum in a typical hadronic process. In the parton model this equation might be expected to be approximately true with n=4 reflecting the $2 \rightarrow 2$ nature of the hard scattering process while $\langle p_T \rangle \cong 0.3 - 0.4$ GeV/c. If we do not introduce a new large mass scale into the large p_T processes we are left with the alternative of considering a large number of degrees of freedom,

$$n \cong 20 - 35 \qquad \text{(IIC.7)}$$

in (IIC.6). Since this number is not small compared to the average number of particles produced in a collision at the ISR, it suggests that most particles participate in the "balancing" of the transverse momentum.

The Pisa-Stony Brook collaboration have also triggered their apparatus at $E_{CM} = 53$ GeV on a large transverse momentum photon coming out at $\theta_{CM} = 17.5^{o} \pm 4^{o}$ ($\eta = 1.9 \pm 0.2$) instead of $\theta_{CM} = 90^{o}$. In the new setting a photon has nearly 3 times the CM energy of a photon with the same transverse momentum at $\theta_{CM} = 90^{o}$. The normalized total multiplicity, shown in Fig. IIC.7, still displays a rise with p_T but it is less rapid and begins at a larger value of p_T than in the 90° data. The angular distributions of the normalized multiplicity are compared with the 90° data in Fig. IIC.8. There is a substantial depletion in the number of particles at angles equal to or smaller than that of the photon. This effect may be due to energy and longitudinal momentum conservation. Remember that the data are normalized to low transverse momentum events where there is a positive correlation when two particles both have $\eta \cong 2$.

The direct comparison of the data at 90° and 17.5^{o} suggest that, roughly independent of the longitudinal momentum of the trigger particle, its transverse momentum is balanced by the emission of particles at approximately $\theta_{CM} = 90^{o}$ and spread over a wide range of azimuthal angle. The behavior is roughly consistent with a jet hypothesis but might conflict with the most naive forms of the parton model with narrow coplanarity.

In the studies of events associated with high p_T photons the Aachen-CERN-Heidelberg-Munich collaboration (Betev et al., 1974), triggered on a photon and then examined the correlation between two other particles. This important correlation function was positive over a range of $\eta \simeq 2$ and seemed to have no strong dependence on the transverse momentum of the trigger γ. This tends to say that the short-range-order hypothesis (i.e., that the

correlation distribution has a fixed range in rapidity) does not break down for those events containing large p_T particles.

The CERN-Columbia-Rockefeller collaboration (F. Busser et al., 1974) have measured the correlation function

$$R(p_1, p_2) = \frac{E_1 E_2 \, d\sigma/d^3p_1 \, d^3p_2}{E_1 \, d\sigma/d^3p_1 \; E_2 \, d\sigma/d^3p_2} \qquad \text{(IIC. 6)}$$

for two large p_T π^0's. The data for π_0's on opposite sides are shown in Fig. IIC. 9 and compared with curves calculated from the "uncorrelated jet model". The "uncorrelated jet model" consists of a factorizable matrix element and no dynamic correlations. To the extend the data agree with these curves we can conclude that the observed correlation is just a reflection of conservation of momentum. The correlation on the same side, Fig. IIC. 10, indicates a substantial probability for producing π_0's in clusters. Whether this is just the same clustering effect observed at small p_T is not known. The plot of the distribution in the invariant mass of the $2\pi^0$ system is displayed in Fig. IIC. 11.

The CERN-Columbia-Rockefeller-Saclay group have arranged lead glass behind a magnetic spectrometer on one side of the ISR storage rings and a magnetic spectrometer on the other side in order to study π^0-charged particle correlations. They trigger on a π^0 with $p_T > 3$ GeV/c and measure the associated probability of having a large p_T charged particle. The data at $\sqrt{s} = 52.7$ GeV is shown in Fig. IIC. 12. When the charged particle is opposite the π^0 we see an enhancement such as that which might be expected on the basis of momentum conservation. When the charged particle is on the same side as the π^0 we not only see some correlation such as might be

expected from clustering but the probability of having a large p_T charged particle is approximately equal to what it is on the other side. This feature does not seem to be natural in any simple model and it is important to find out whether it persists at other energies and other choices for the particles involved. The center-of-mass motion of the hard subprocess can effect the normalization of the opposite side correlation.

We will return to the theoretical interpretation of these data in Section V.

LIST OF FIGURES FOR SECTION IIC

from the detected photon. Detected photon at $\theta_{CM} = 90^{o}$; detected photon at $\theta_{CM} = 17.5^{o}$.

IIC. 9 Data from the CERN-Columbia-Rockefeller collaboration on the correlation function, e.g., IIC.6, for $pp \rightarrow \pi^{o}\pi^{o}X$, the curves represent calculations in the uncorrelated jet model (phase space).

IIC. 10 Correlation function for two large p_T π^{o}'s on the same side.

IIC. 11 Plot of the invariant mass of two π^{o}'s on the same side of the CCR experiment. The acceptance of the apparatus suppresses low mass pairs.

IIC. 12 Data from the CERN-Columbia-Rockefeller-Saclay experiment on the probability for detecting a charged particle with and without a trigger on a π^{o} with $p_T > 3$ GeV/c.

- ● All inelastic interactions.
- ○ Trigger on π_0, charged particles in same azimuthal direction of π_0.
- △ Trigger on π_0, charged particles in opposite hemisphere from π_0.

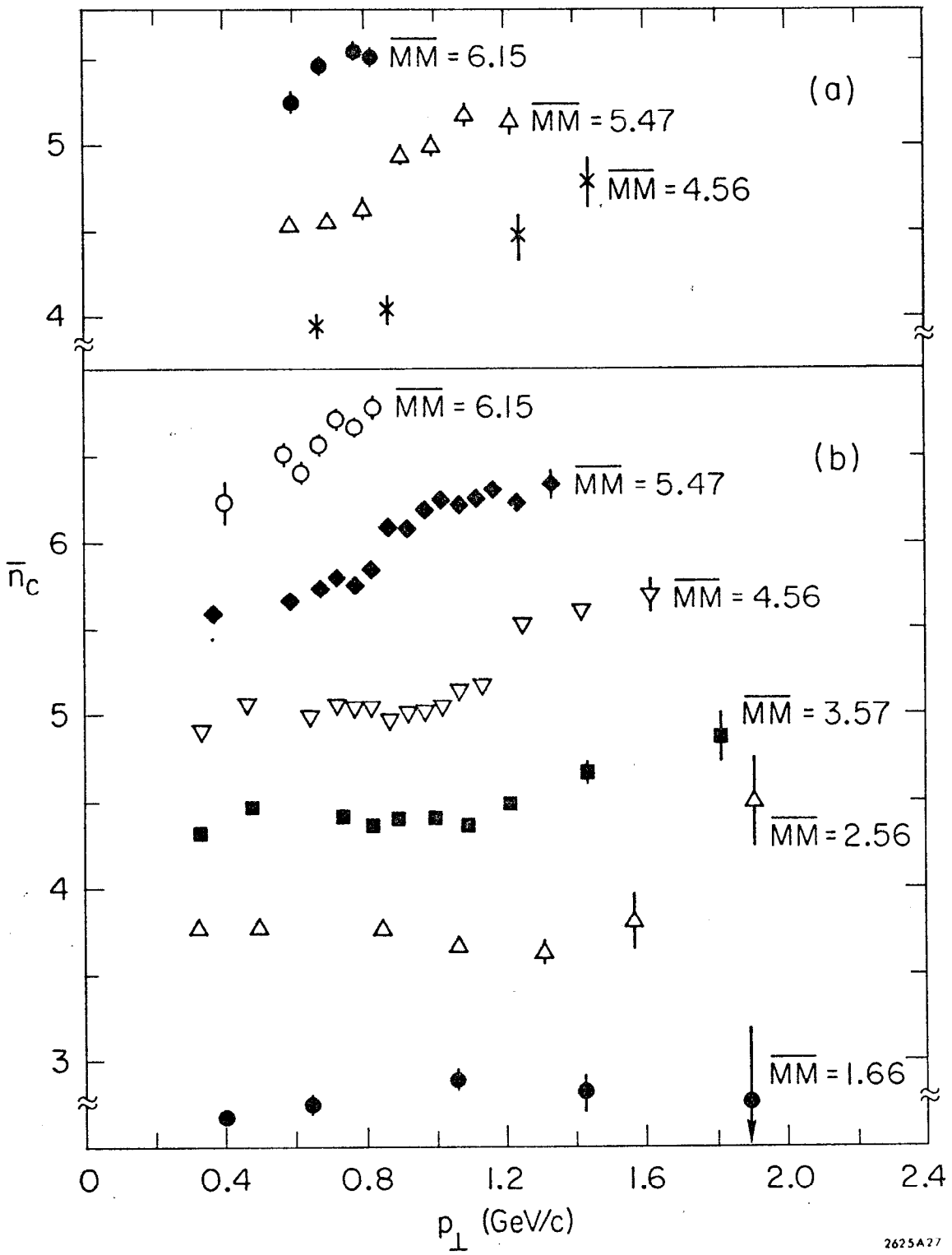
$\overline{MM}$ = 6.15
(a)
$\overline{MM}$ = 5.47
$\overline{MM}$ = 4.56
5
4
$\overline{MM}$ = 6.15
(b)
$\overline{MM}$ = 5.47
6
$\overline{n}_c$
$\overline{MM}$ = 4.56
5
$\overline{MM}$ = 3.57
$\overline{MM}$ = 2.56
4
3
$\overline{MM}$ = 1.66
0
0.4
0.8
1.2
1.6
2.0
2.4
$p_\perp$ (GeV/c)
2625A27

FIG. IIC. 1

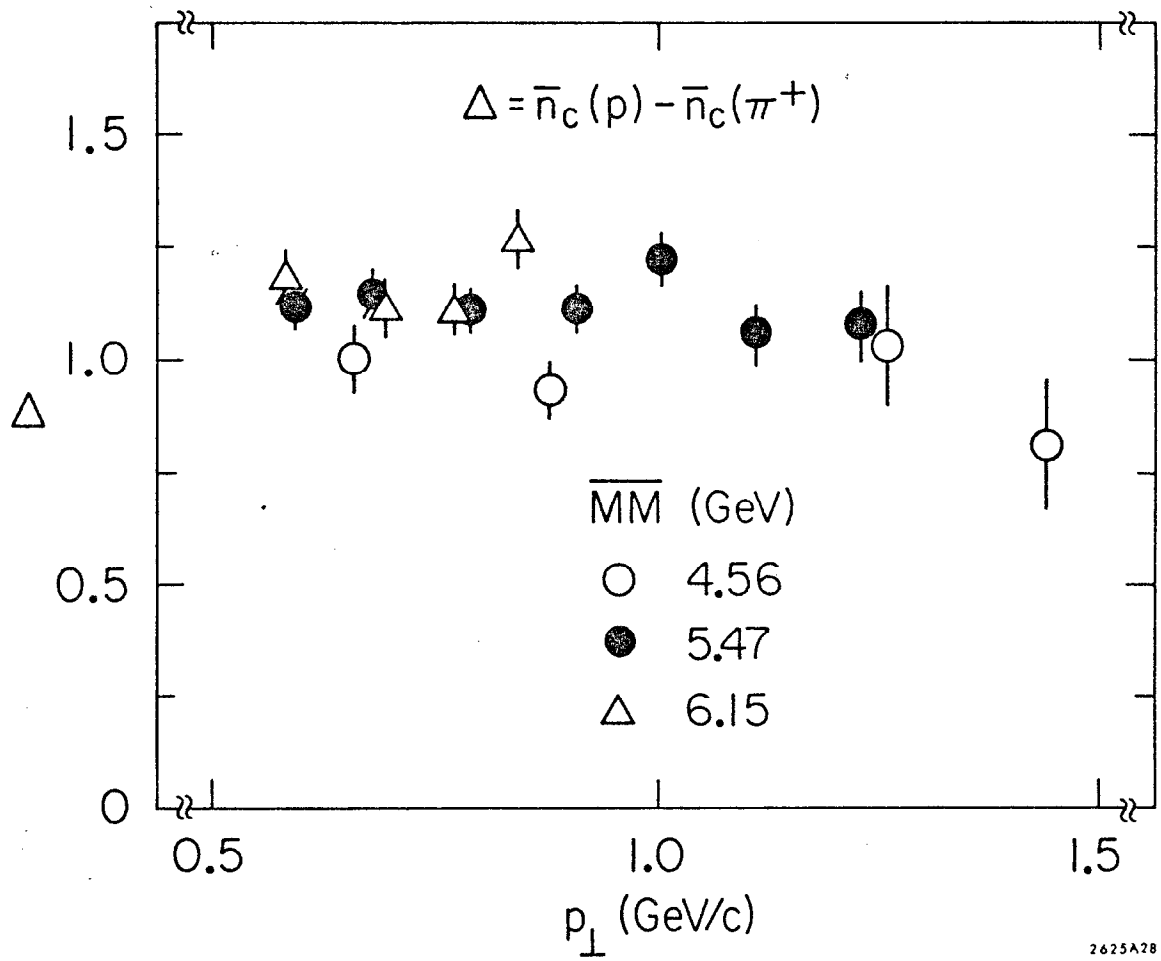
$\Delta = \bar{n}_c(p) - \bar{n}_c(\pi^+)$
1.5
1.0
0.5
0
Δ
$\overline{MM}$ (GeV)
4.56
5.47
6.15
0.5
1.0
1.5
$p_\perp$ (GeV/c)
2625A28

FIG. IIC. 2

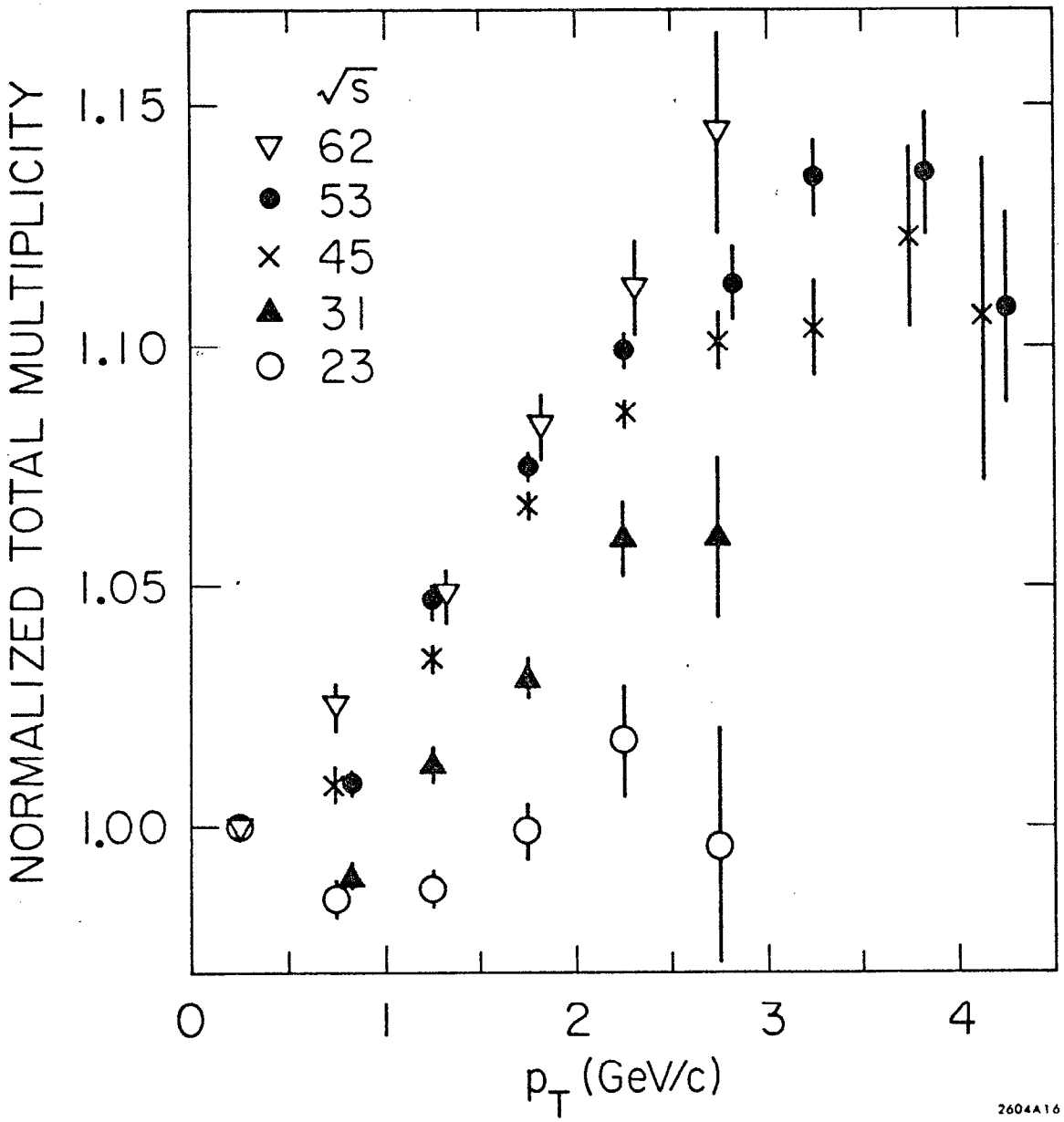
NORMALIZED TOTAL MULTIPLICITY
1.15
1.10
1.05
1.00
$\sqrt{s}$
62
53
45
31
23
0
1
2
3
4
p_T (GeV/c)
2604A16

FIG. IIC.3

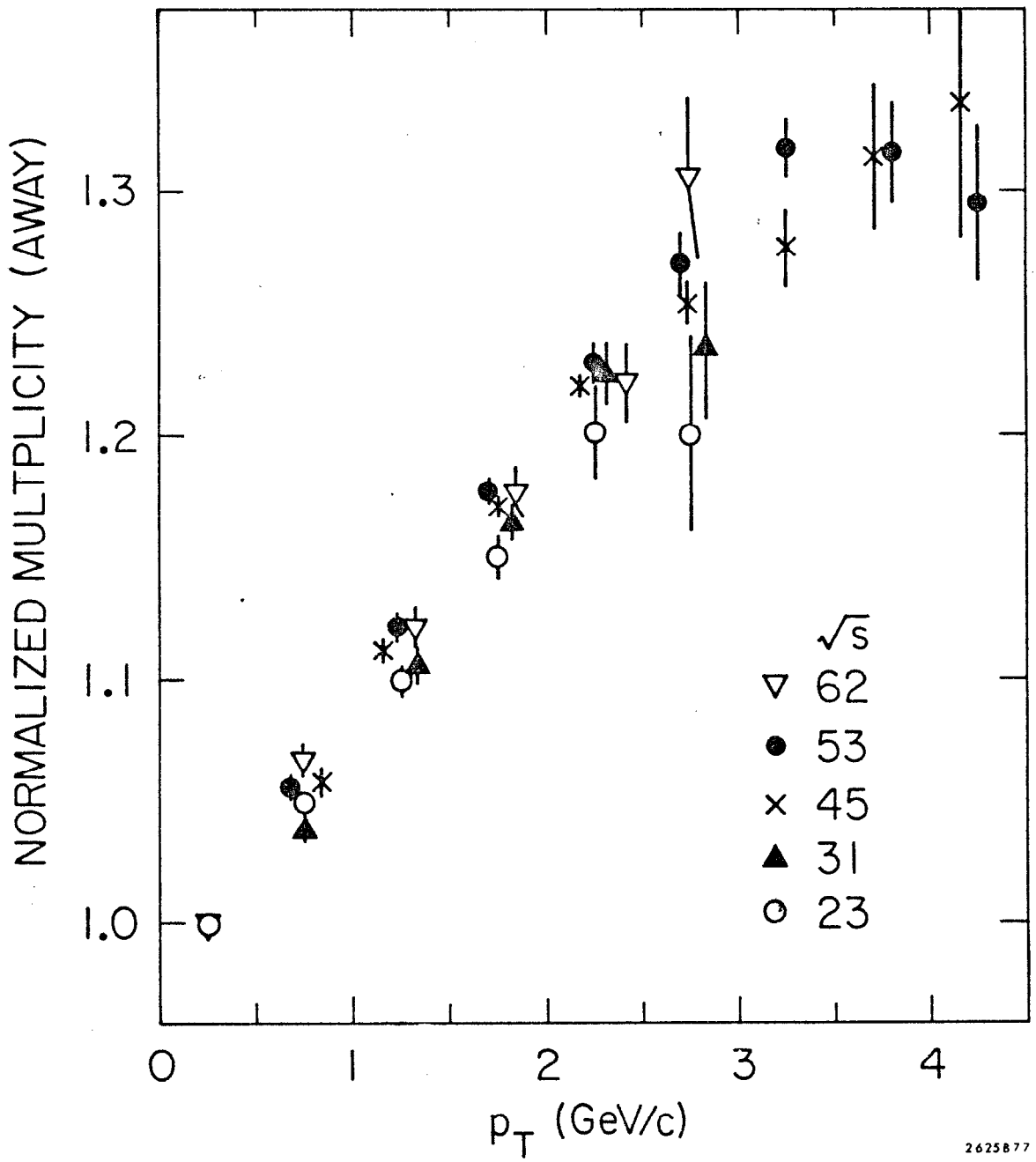
NORMALIZED MULTPLICITY (AWAY)
1.3
1.2
1.1
1.0
0
1
2
3
4
p_T (GeV/c)
$\sqrt{s}$
62
53
45
31
23
2625877

FIG. IIC.4

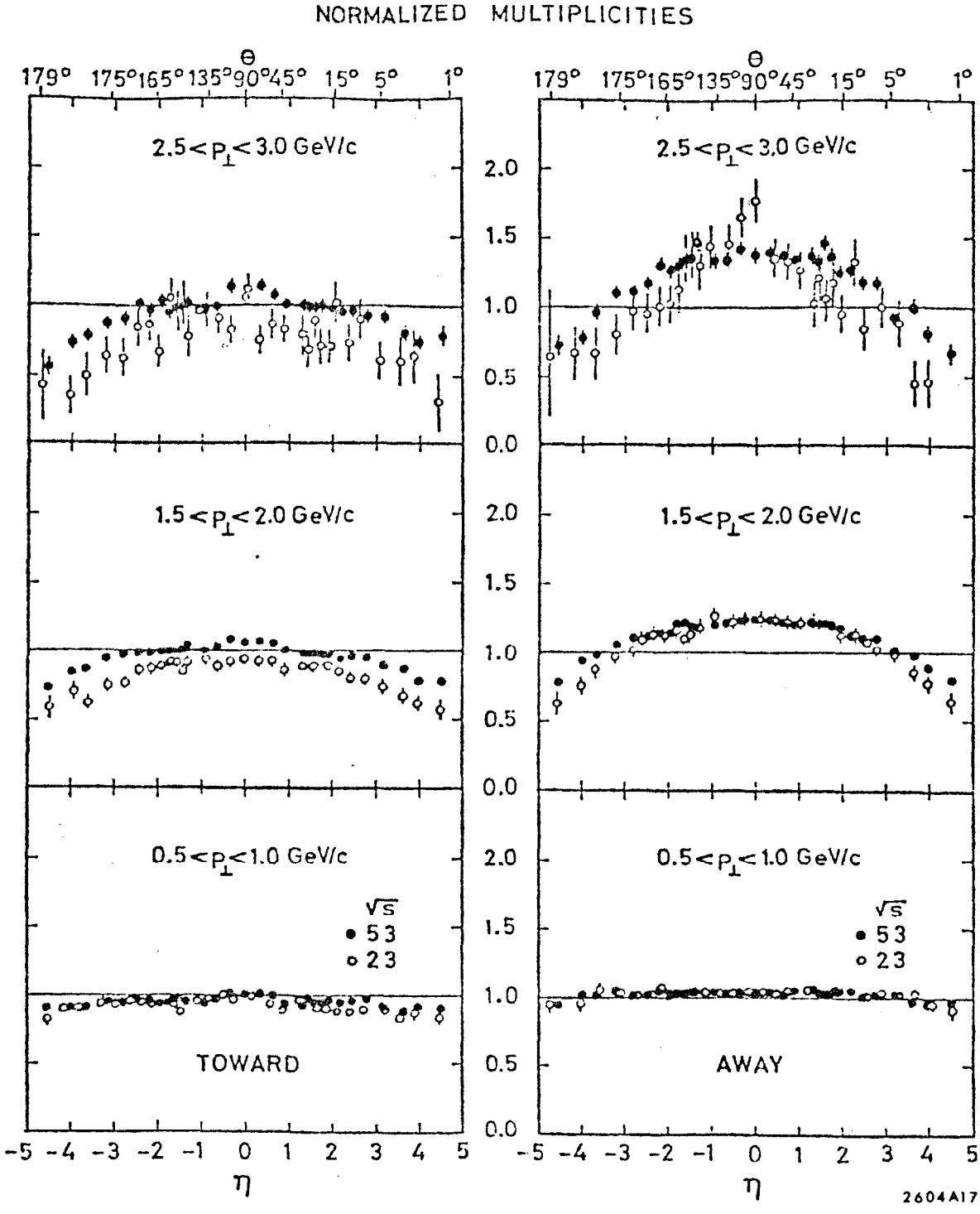
NORMALIZED MULTIPLICITIES
θ
179° 175° 165° 135° 90° 45° 15° 5° 1°
2.5<p⊥<3.0 GeV/c
1.5<p⊥<2.0 GeV/c
0.5<p⊥<1.0 GeV/c
√s
• 53
○ 23
TOWARD
AWAY
2.0
1.5
1.0
0.5
0.0
-5 -4 -3 -2 -1 0 1 2 3 4 5
η
2604A17

FIG. IIC.5

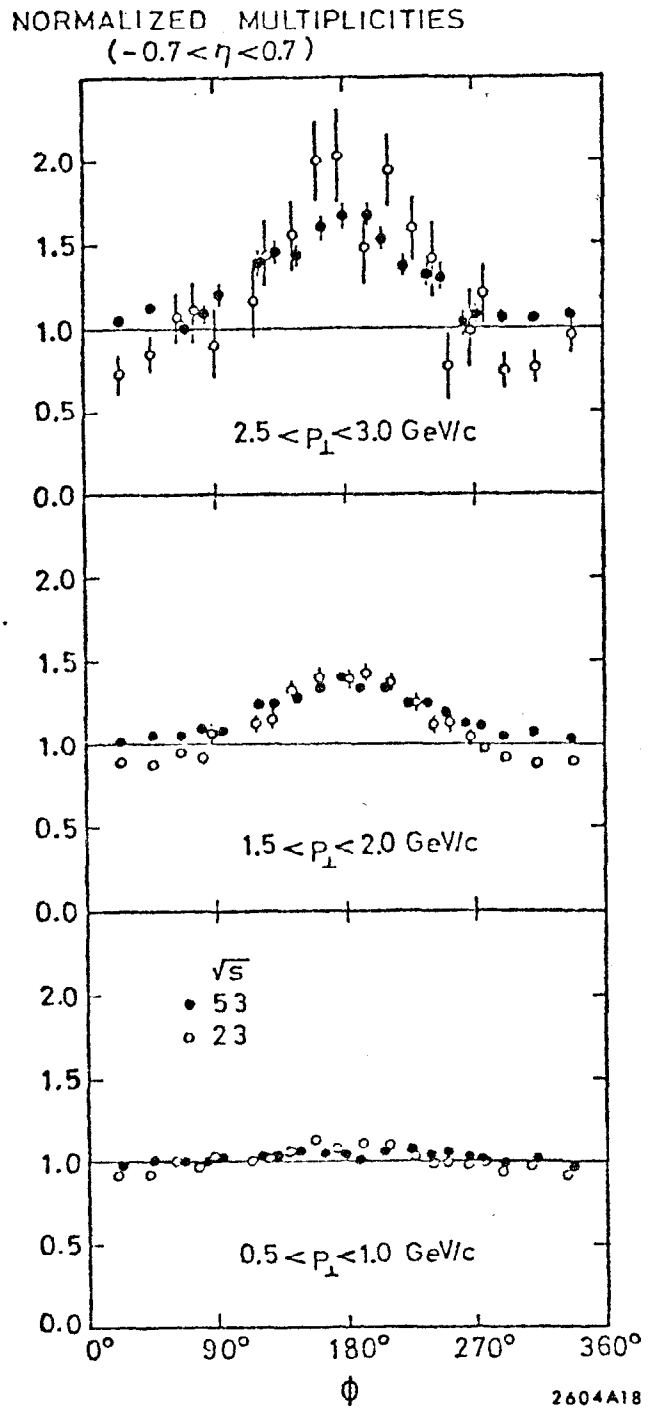
NORMALIZED MULTIPLICITIES
(-0.7 < η < 0.7)
2.0
1.5
1.0
0.5
0.0
2.5 < P⊥ < 3.0 GeV/c
1.5 < P⊥ < 2.0 GeV/c
√s
53
23
0.5 < P⊥ < 1.0 GeV/c
0°
90°
180°
270°
360°
φ
2604A18

FIG. IIC. 6

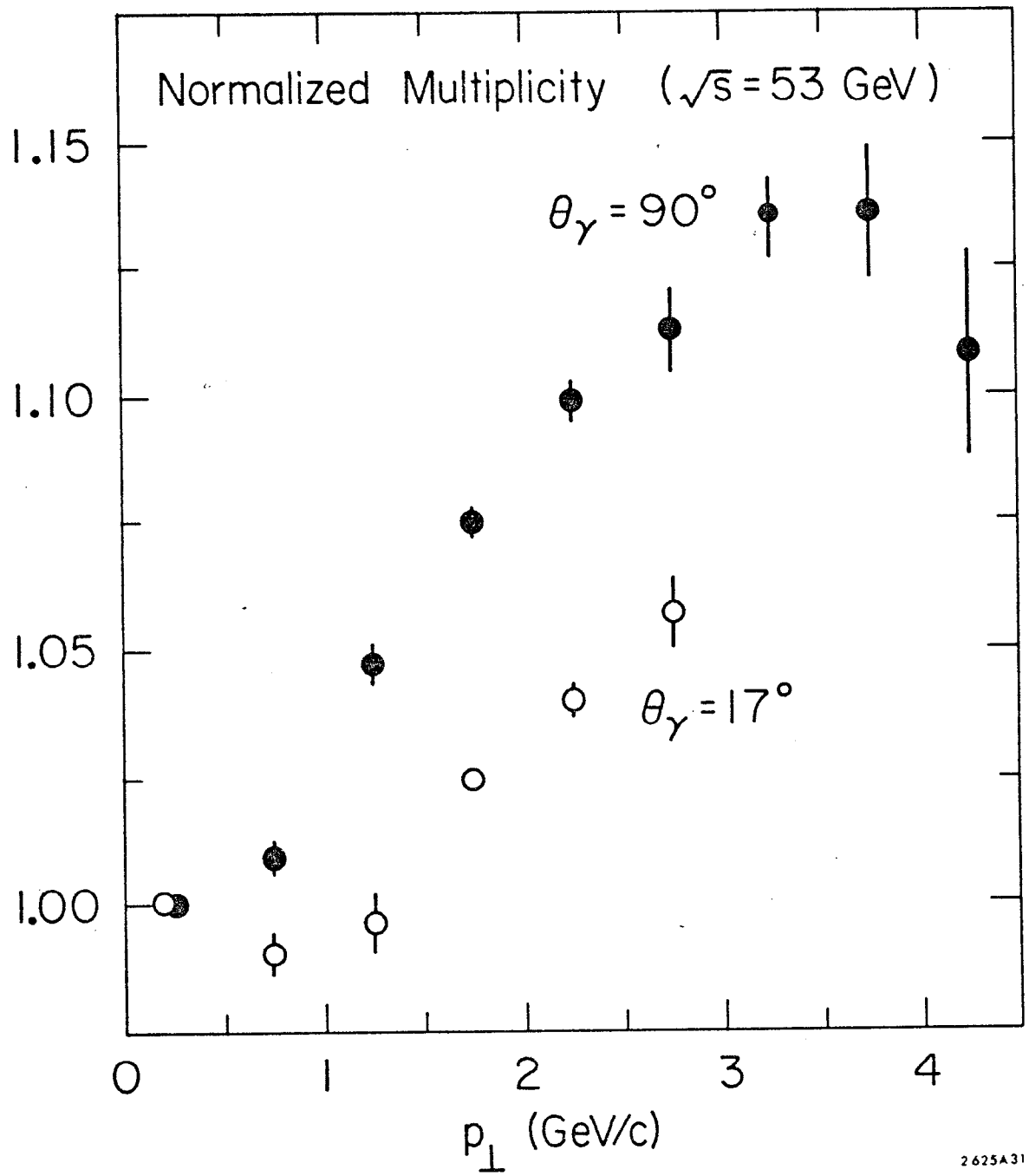
Normalized Multiplicity ($\sqrt{s}$ = 53 GeV)
θ_γ = 90°
θ_γ = 17°
1.15
1.10
1.05
1.00
0
1
2
3
4
$p_\perp$ (GeV/c)
2625A31

FIG. IIC.7

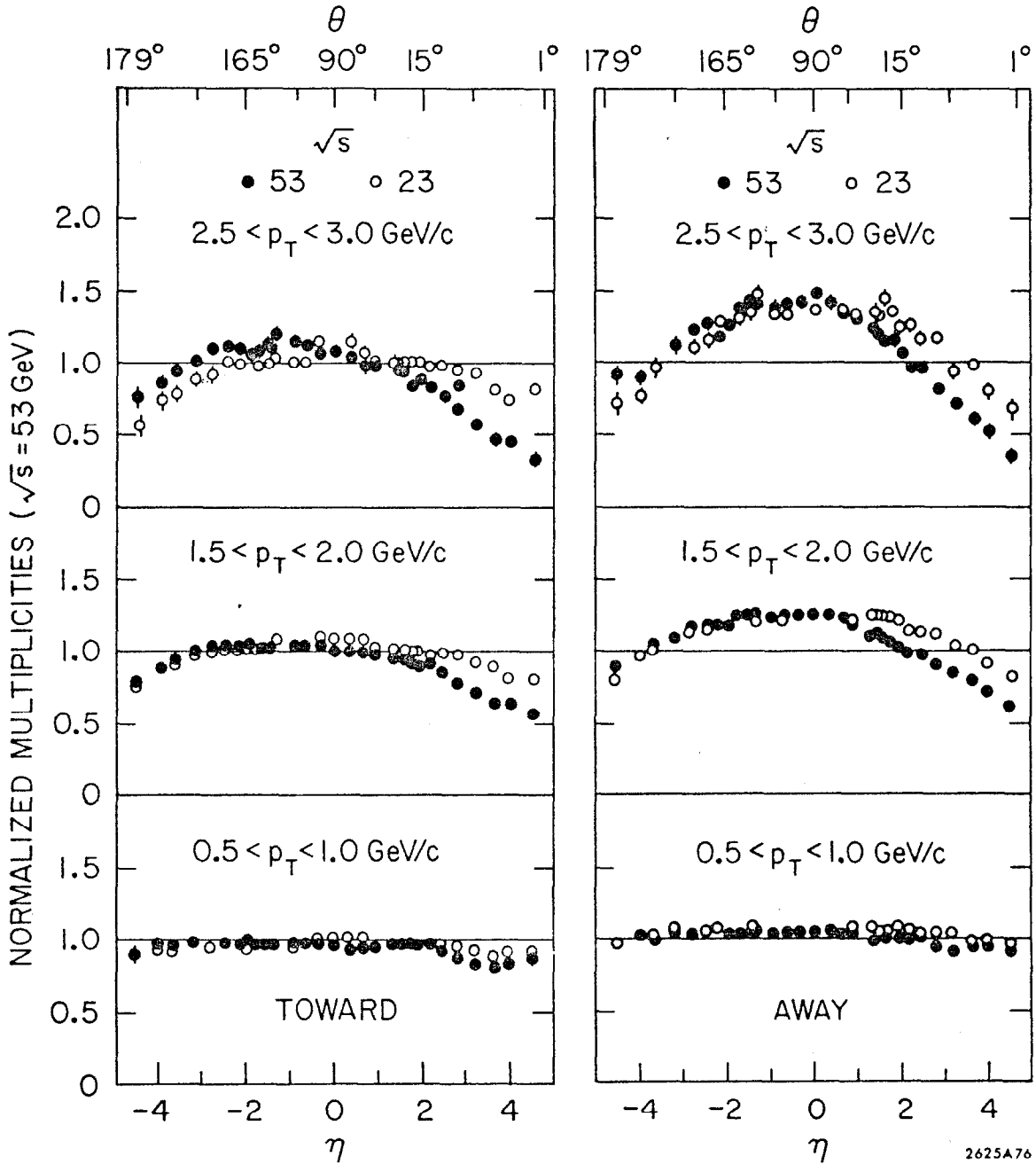
θ
179°
165°
90°
15°
1°
√s
● 53
○ 23
2.5 < p_T < 3.0 GeV/c
1.5 < p_T < 2.0 GeV/c
0.5 < p_T < 1.0 GeV/c
TOWARD
AWAY
NORMALIZED MULTIPLICITIES (√s = 53 GeV)
2.0
1.5
1.0
0.5
0
-4
-2
0
2
4
η
2625A76

FIG. IIC.8

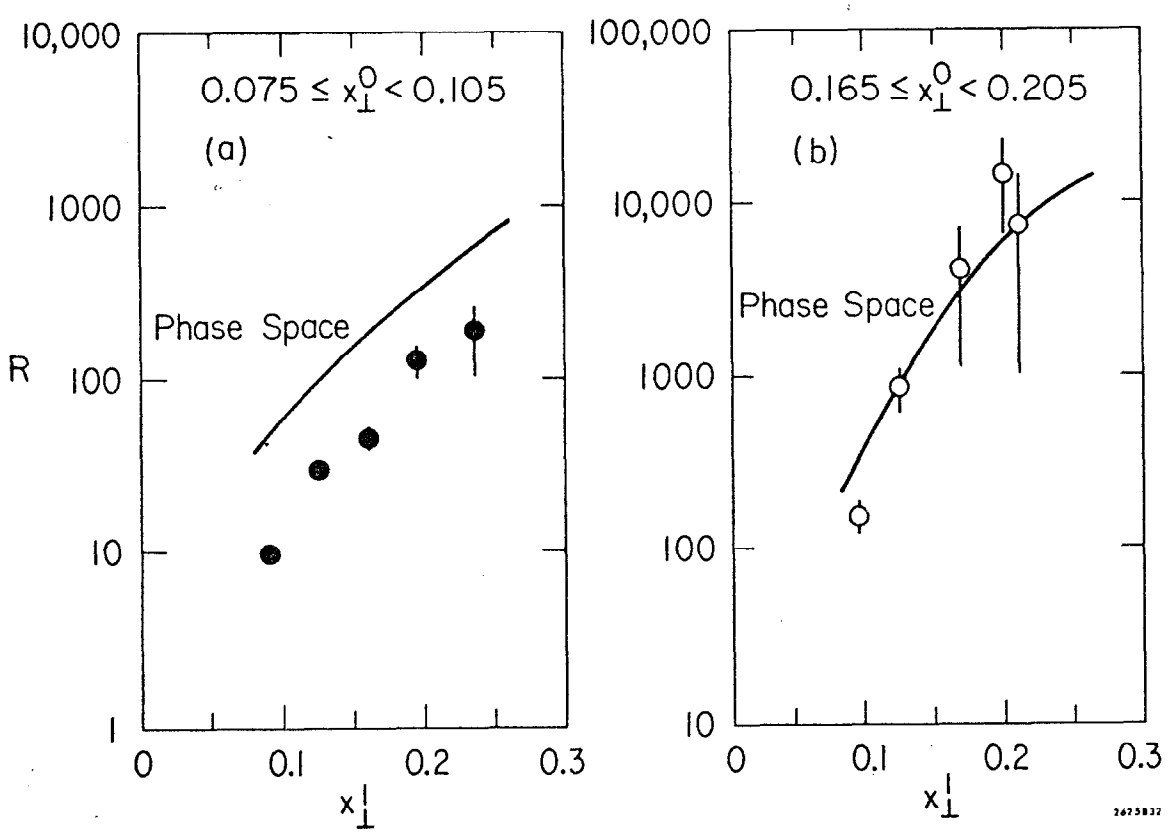
10,000
1000
100
10
1
R
0.075 ≤ x⊥0 < 0.105
(a)
Phase Space
0
0.1
0.2
0.3
x⊥
100,000
10,000
1000
100
10
0.165 ≤ x⊥0 < 0.205
(b)
Phase Space
0
0.1
0.2
0.3
x⊥

FIG. IIC. 9

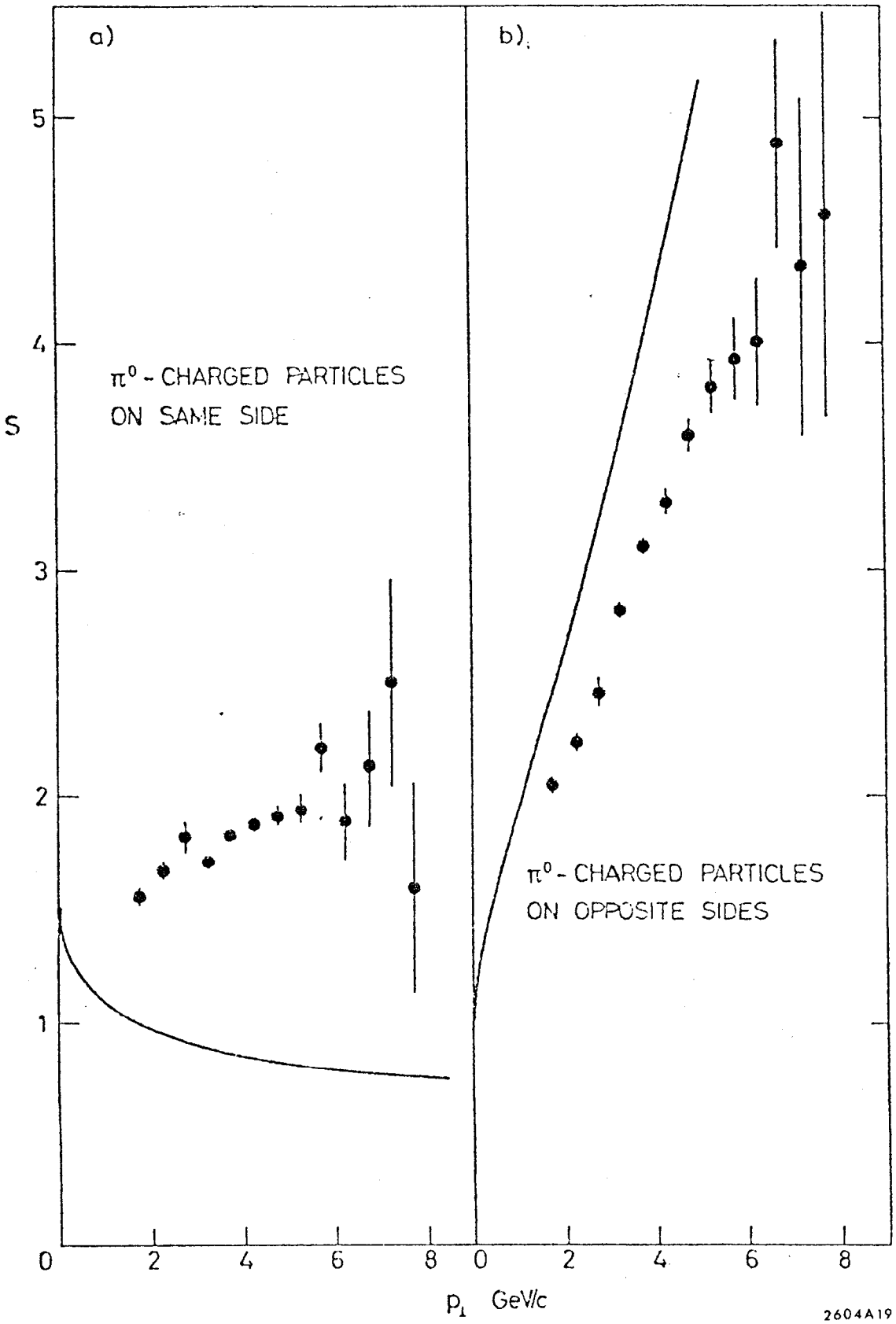
a)
b)
S
5
4
3
2
1
0
2
4
6
8
0
2
4
6
8
π^0 - CHARGED PARTICLES
ON SAME SIDE
π^0 - CHARGED PARTICLES
ON OPPOSITE SIDES
$p_\perp$ GeV/c
2604A19

FIG. IIC. 10

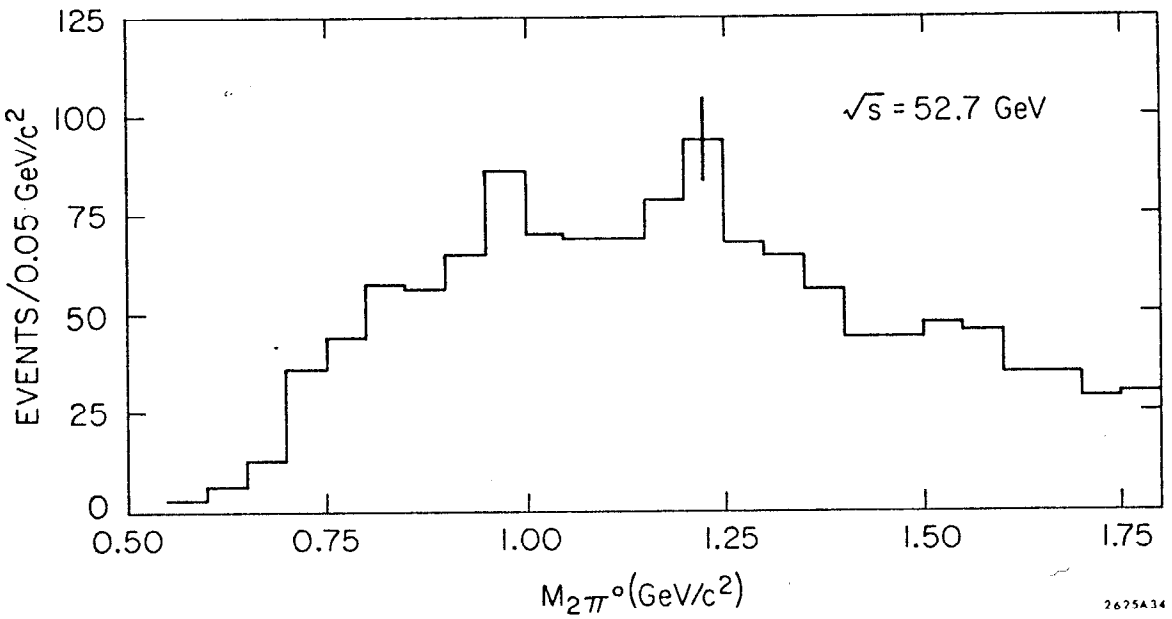
125
100
75
50
25
0
EVENTS/0.05 GeV/c²
√s = 52.7 GeV
0.50
0.75
1.00
1.25
1.50
1.75
M2π°(GeV/c²)
2675A34

FIG. IIC. 11

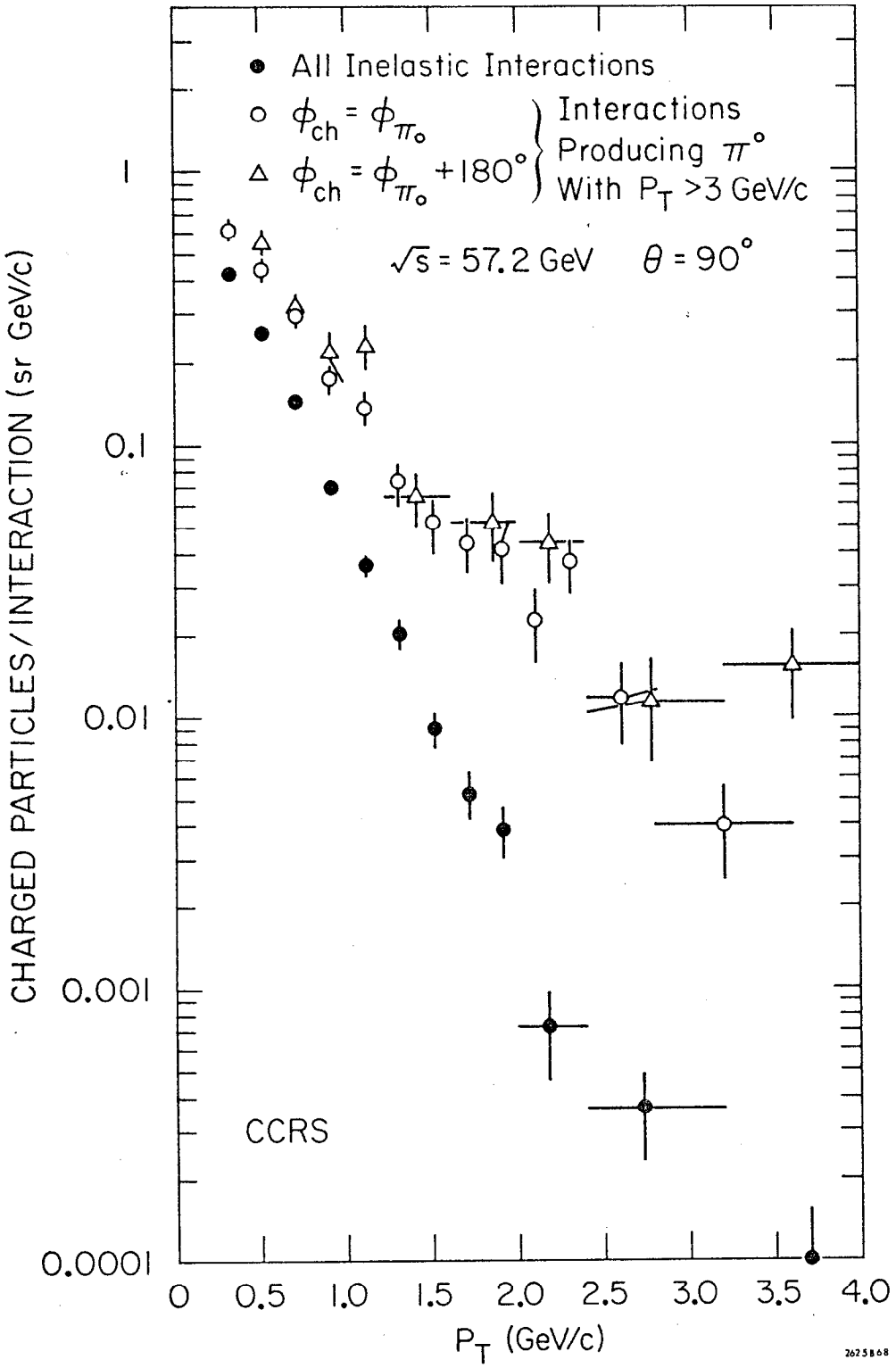
All Inelastic Interactions
$\phi_{ch} = \phi_{\pi_o}$
$\phi_{ch} = \phi_{\pi_o} + 180°$
Interactions Producing π^o With P_T >3 GeV/c
$\sqrt{s}$ = 57.2 GeV θ = 90°
CCRS
CHARGED PARTICLES/INTERACTION (sr GeV/c)
1
0.1
0.01
0.001
0.0001
0
0.5
1.0
1.5
2.0
2.5
3.0
3.5
4.0
P_T (GeV/c)
2625868

FIG. IIC. 12

D. The Direct Production of Leptons

Another process which has attracted considerable theoretical and experimental attention involves the production of a single lepton pair. In most of the hard scattering models we discuss here, this process is related dynamically to the production of large transverse momentum hadrons and we therefore feel justified in including in this section a brief digression from our main topic. In addition, the recent observation of a heavy, narrow enhancement with mass 3.105 GeV in the reaction $pp \to \ell^+\ell^-$ + anything (Aubert et al., 1974) has intensified interest in understanding the process away from the resonant peak. In this section we review the data on the hadronic production of lepton pairs and the inclusive cross sections for single leptons and discuss briefly their implications for models.

Figure IID.1 shows the data of Christenson et al. (1970, 1973) on the cross section for the inclusive production of lepton muon pairs. The shoulder in these data is now associated with the production of the sharp enhancement observed by Aubert et al. (1974) smeared by the resolution of the spectrometer. The smooth curve is the experimentalists estimate of the "background" process $pp \to \gamma$ + anything $\to \ell^+\ell^-$ + anything. The continuum is parametrized at 29.5 GeV/c by

$$\frac{d\sigma}{d\mathcal{M}} = 2 \times 10^{-32}\ (\mathrm{cm}^2)\frac{(1-\tau^4)}{\mathcal{M}^{5.8}} \qquad \text{(IID. 1)}$$

where $\tau = \mathcal{M}/(s^{1/2} - 2m_p)$.

The most popular theoretical model for the production of a massive time-like photon is the Drell-Yan mechanism (Drell and Yan, 1971) in which the virtual photon is creased as a result of a quark from one initial hadron annihilating with an antiquark from the other. This contribution can be written in

the form

$$\frac{d\sigma}{d\mathcal{M}} = \left(\frac{4\pi\alpha^2}{3}\right) \frac{2}{\mathcal{M}^3} \left\{\tau^2 \int_0^1 dx\, dy \left[\Sigma\ e_i^2\left(F_i(x)\ \bar{F}_i(y) + \bar{F}_i(x)\ F_i(y)\right)\right] \times \delta(xy - \tau^2)\right\} \qquad \text{(IID. 2)}$$

where the $F_i(x)$ are the quark distribution functions. Perhaps the closest analogy with large p_T hadronic processes involves the subprocess quark-antiquark annihilation into two high p_T mesons as described by Landshoff and Polkinghorne (1973).

Since the quark distribution functions are in principle separately determined from data on electroproduction and neutrino interactions, the formula (IID. 2) involves no undetermined coefficients. There is an uncertainty of a factor of 3 depending on whether or not quarks carry SU(3) color. This contribution alone does not seem able to describe the data. Note particularly that the $\mathcal{M}$-behavior at fixed τ does not agree with (IID. 1).

A different model has been suggested by Berman, Levy and Neff (1969) in where there is the production of a virtual charged particle which bremsstrahlungs a massive photon. This model is not absolutely normalized since we need to make some assumptions about the production of off-mass-shell particles. Using something like inverse vector dominance logic we can argue that any of the mechanisms we have discussed, CIM, fireball models, etc., which can create vector mesons can be used to make massive photons. These extra mechanisms may perhaps make up the difference between the data and the contribution from quark-antiquark annihilation.

Recently a number of experiments have reported data on the inclusive reaction (Jain et al., 1974; Boymond et al., 1974; Appel et al., 1974b)

$$p + \text{nucleon} \rightarrow (\text{lepton})^{\pm} + \text{anything} \qquad \text{(IID. 3)}$$

(where the "direct" leptons are those not attributable to π or K decays) for $\sqrt{s}$ between 11 and 53 GeV. As demonstrated in Figs. IID. 2 and IID. 3 experiments are in agreement with the observation that the ratio

$$\mu/\pi \cong 10^{-4} \qquad \text{(IID. 4)}$$

is approximately independent of p_T. The Drell-Yan mechanism and the other methods of producing massive lepton pairs can contribute but are to be small. Since the ratio is roughly constant, this employs a power p_T^{-8} at fixed $\mathcal{M}^2/s$ approximately the same as hadronic production, which is quite difficult from the p_T^{-4} prediction of the Drell-Yan mechanism. Of course, we expected contributions from the decays of ρ^o, ω^o, and ϕ^o. Since these are expected to have the correct p_T dependence, let us see how the ratio (IID. 4) can be attained. In the spirit of cluster models (see the review of G. Ranft, 1974), let us consider the most extreme case and assume that a significant fraction of all π's observed come from the decay of the known vector mesons. With equal production of

$$\rho^+, \rho^-, \rho^o, \omega^o \rightarrow 3\pi^+ + 3\pi^- + 3\pi^o + (0.67 + 0.76) \times 10^{-4}\, \mu^+\mu^-$$

we could expect a ratio

$$\frac{\mu^+}{\pi^+} = \frac{1.43}{3} \times 10^{-4} = 0.48 \times 10^{-4}$$

Now if there are substantial ϕ's produced a reasonable contribution from their leptonic decays can be expected. If we assume $\sigma(\rho^o) = \sigma(\rho^\pm) = \sigma(\omega)$ and put in the fact that the production of ϕ's from proton-proton collisions should be suppressed dynamically $\sigma(\phi_0) = \epsilon\sigma(\rho^o)$ we get a ratio

$$\frac{\mu^+}{\pi^+} = \frac{1.43 + 2.5\epsilon}{3 + 0.15\epsilon} \times 10^{-4}$$

which can be made roughly consistent with the experimental ratio if ϵ is fairly large. The experimental data on ϕ production (Busser et al., 1974) yields

$$\frac{\sigma(\phi_0)}{\sigma(\pi_-)} \leq \frac{\sigma(\phi_0)}{3\sigma(\rho_0)} = \frac{\epsilon}{3} \leq 0.2$$

but from other sources (for example, $d\sigma/dt\ (\pi^- p \rightarrow \phi n)/d\sigma/dt\ (\pi^- p \rightarrow \omega n) \lesssim 1/280$), we might expect ϵ to be much smaller.

If we neglect ϕ production as a source of μ's we are left with a large cross section to explain, for example, the production of charmed particles or of ψ, ψ'.

Now because of the large branching fraction of the $\psi(3105)$ into lepton pairs (J. Augustin et al., 1974) we can use the single lepton cross section to put an upper bound on the production of ψ's in high energy pp collisions. Using the above assumption we get

$$\frac{\sigma(\psi)}{\sigma(\rho_0)} < 2.8 \times 10^{-3}$$

$$\frac{\sigma(\psi)}{\sigma(\pi^{\pm})} < 9.3 \times 10^{-4}$$

This is considerably larger than the observed ratio of cross sections at BNL or FNAL so that unless the amount of ψ production grows significantly with energy the new particles do not give a major contribution to the single lepton rate.

LIST OF FIGURES FOR SECTION IID

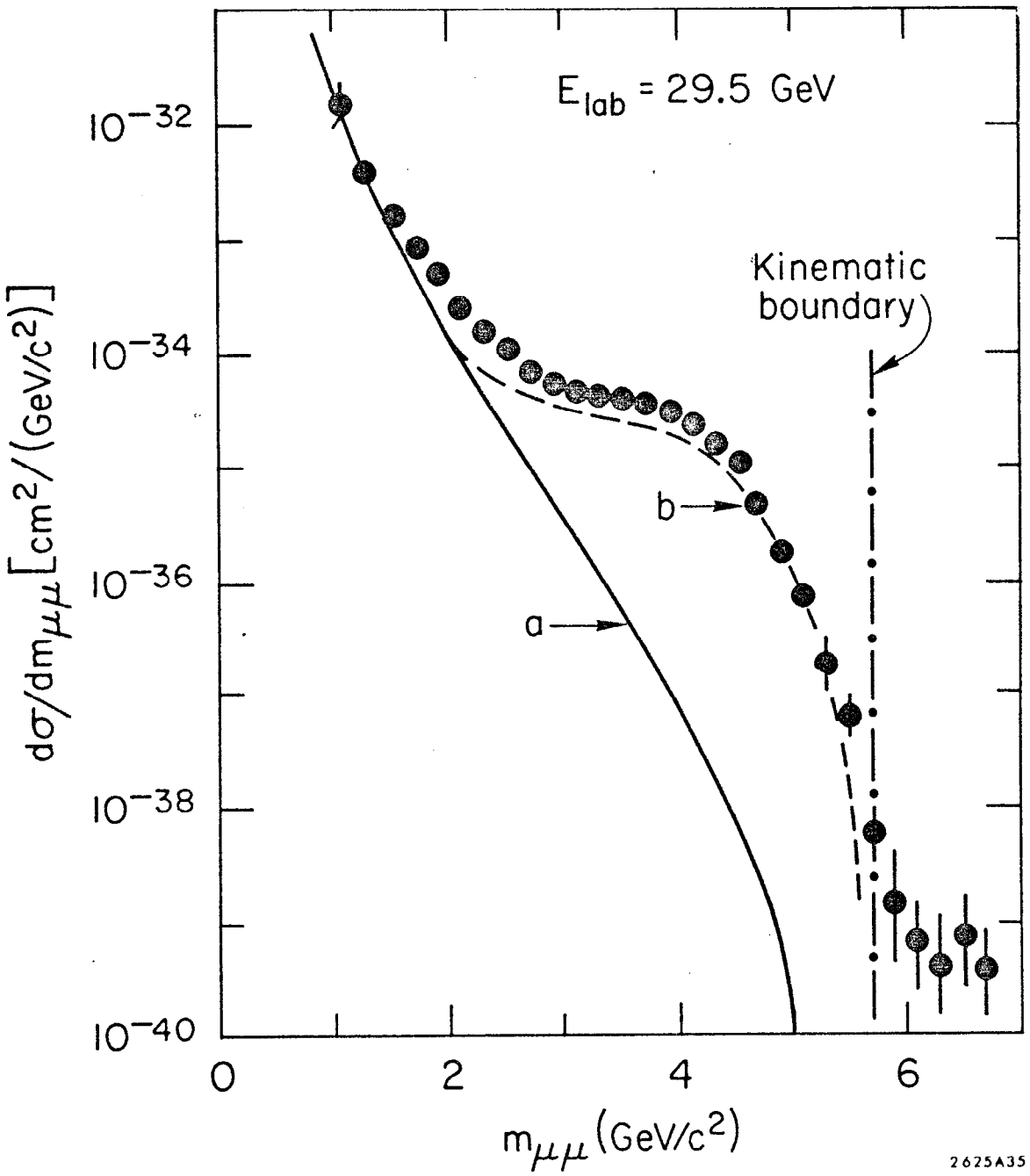
E_{lab} = 29.5 GeV
Kinematic boundary
b
a
10^{-32}
10^{-34}
10^{-36}
10^{-38}
10^{-40}
$d\sigma/dm_{\mu\mu}$ [cm^2/(GeV/c^2)]
0
2
4
6
$m_{\mu\mu}$ (GeV/c^2)
2625A35

FIG. IID.1

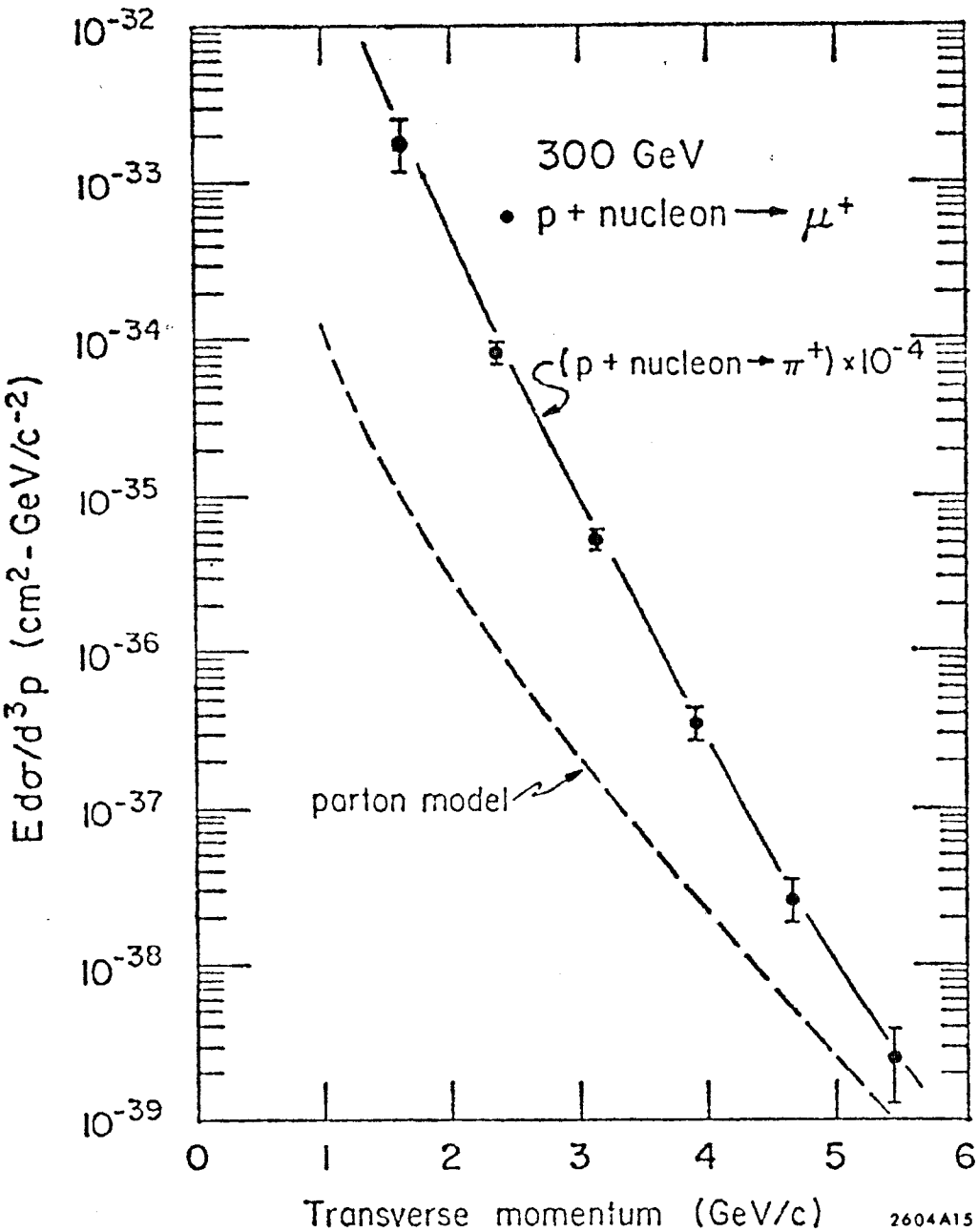
300 GeV
• p + nucleon → μ+
(p + nucleon → π+) × 10-4
parton model
Edσ/d3p (cm2 - GeV/c-2)
Transverse momentum (GeV/c)
2604A15

FIG. IID.2

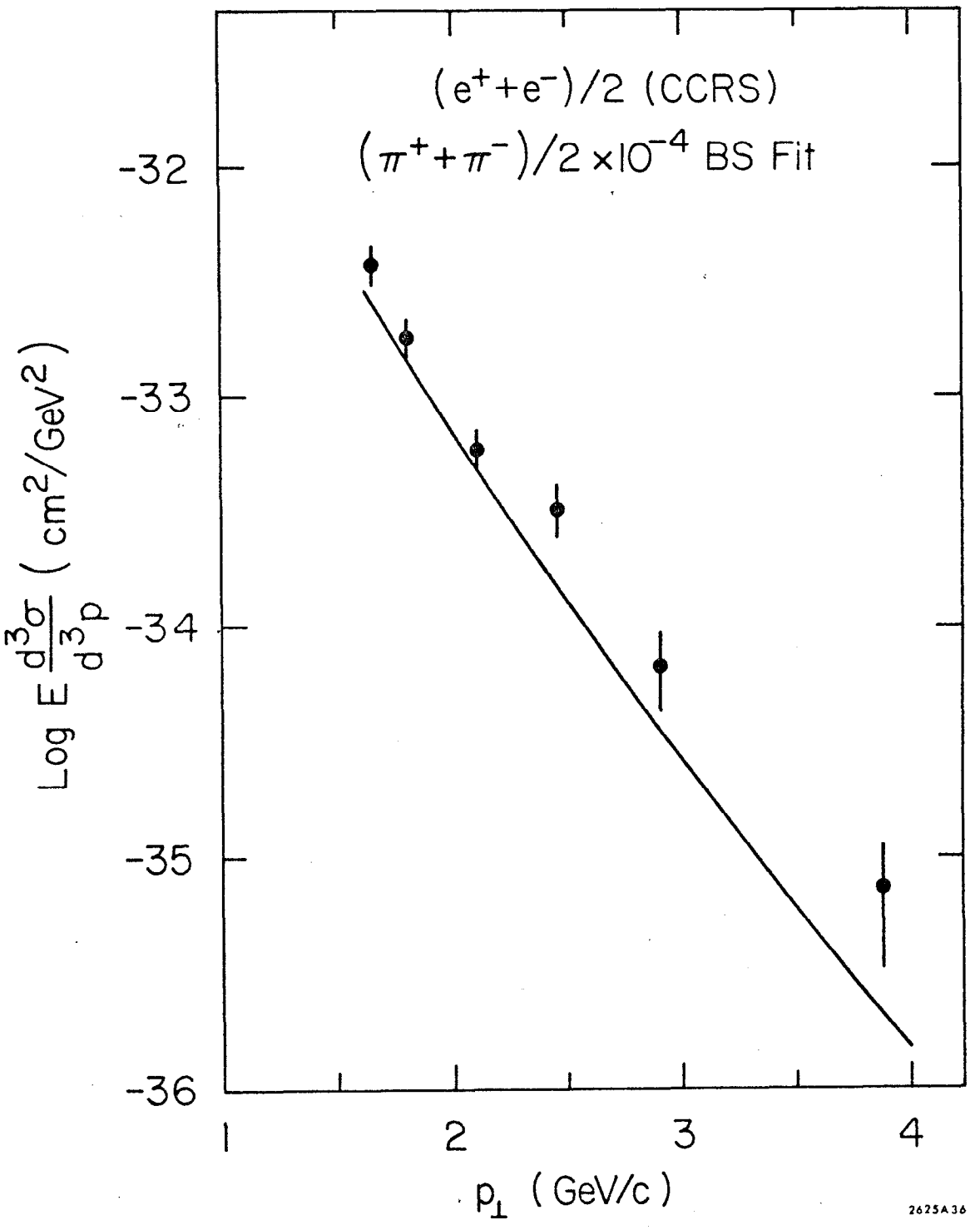
(e⁺+e⁻)/2 (CCRS)
(π⁺+π⁻)/2 ×10⁻⁴ BS Fit
-32
-33
-34
-35
-36
Log E d³σ/d³p (cm²/GeV²)
1
2
3
4
p⊥ (GeV/c)
2625A36

FIG. IID. 3

III. MODELS WITHOUT POINTLIKE CONSTITUENTS

It is an interesting exercise to see how we would go about describing the large-transverse momentum behavior of hadronic models without pointlike constituents. Since the quarks within hadrons are well hidden, it is possible that, at some level, we do not need to invoke quarks as essential degrees of freedom to describe the dynamics of hadronic collisions. It seems evident, for example, that the diffractive scattering of high energy hadrons has very little to do with the interactions of individual quarks. On the other hand, deep inelastic lepton scattering data display strong evidence for quarklike constituents in the proton. Without careful discrimination, it is not immediately clear whether large-transverse-momentum hadronic processes will be sensitive to quark structure.

We shall see here that nonparton approaches to large-angle scattering processes have been relatively successful. For present data, their predictions are at least as successful as those of constituent models. To describe inclusive data, however, models without partons must apparently find a new framework or new dynamical mechanisms in order to be competitive.

A. Nonparton Models for Fixed-Angle Scattering

Models for the scattering of two hadrons through a large angle at high energy are divided naturally into two classes according to whether the underlying interactions is governed by a distance scale or whether it is pointlike. Dual models (Krzywicki, 1971a,b), geometrical models (Chu and Hendry, 1972, 1973; Schrempp and Schrempp, 1973, 1975), statistical models (Frautschi, 1972; Eilam et al., 1973) belong to the former class while the second group relies on ideas based on pointlike constituents tested in electroproduction. The parton model (Abarbanel, Drell and Gilman, 1969; Horn and Moshe, 1973), constituent interchange model (Blankenbecler et al., 1972), the massive quark model (Preparata, 1974b), and the constituent counting rules of Brodsky and Farrar (1973) and Matveev et al. (1973) based on study of Feynman diagrams are examples of models without a distance scale. More details can be found in the article by Sivers (1975a).

Historically, one of the first formal discussions of high energy fixed angle amplitudes was in the form of a lower bound developed by Cerulus and Martin (1964). This work was very important in that it first showed how an amplitude at fixed angle is constrained by analyticity postulates.

The bound of Cerulus and Martin occurs if we assume:

1. The amplitude, $A(s,z)$, has the usual Mandelstam analyticity. That is, it is analytic in the z plane cut from $-\infty$ to $-(1+c/s)$ and from $(1+c/s)$ to $+\infty$ where c is some constant;
2. There is a finite domain in the z-plane in which the amplitude is bounded by s^N.

Through the use of a clever conformal mapping and the application of Hadamard's three circle theorem, Cerulus and Martin showed that these

assumptions imply the fixed angle lower bound,

$$|A(s,z)| \geq d \exp\left[-c(z)\, s^{1/2} \ln s\right] \qquad \text{(IIIA. 1)}$$

where c(z) is some positive function of $z = \cos\theta$.

Aside from being a triumph in the application of complex variable techniques to high energy physics, the bound (IIIA. 1) has turned out to have phenomenological impact. Motivated, in part, by an empirical fit to the differential cross section of pp scattering by Orear (1964).

$$\left(\frac{d\sigma}{d\Omega}\right) \cong A \exp(-q_T/q_0) = A \exp(-q \sin\theta/q_0) \qquad \text{(IIIA. 2)}$$

where A = 34 mb/sr and $q_0 = 0.151$ GeV/c, Kinoshita (1964) proposed that the bound (IIIA. 1) may be saturated by physical amplitudes for angles outside of the peripheral peaks. He formulated the principle of a "minimal interaction" which implies that fixed angle scattering amplitudes should assume the smallest value consistent with the general requirement of analyticity and unitarity. This hypothesis implies the absence of any really "hard" component in hadronic scattering so that instead of observing frequent collisions in which hadrons scatter through large angles we find instead the production of new hadrons at high energy.

Using the uncertainty relation, Kinoshita's conjecture can be given a simple geometrical interpretation. Let us, for example, assume that there is an absence of find structure so that the uncertainty relation can be interpreted as an approximate equality for some $\Delta L(s)$, the range in angular momentum in which the scattering amplitude is significant,

$$\frac{A(s,\theta)}{A(s,0)} \cong \exp\left\{-\Delta L(s)\,\theta\right\} \qquad \theta \leq \pi/2 \qquad \text{(IIIA. 3)}$$

For pp scattering we can ask whether (IIIA. 3) can be valid with $\Delta L(s)$ determined by the diffractive channel alone,

$$\Delta L(s) \cong \frac{b_0}{2} s^{1/2} \tag{IIIA. 4}$$

with $b_0 \cong 1$ fm (5.1 GeV^{-1}). For the 90° ($\theta = \pi/2$) differential cross section this predicts

$$\begin{aligned} s^2 \frac{d\sigma}{dt}(s, \theta = \pi/2) &\propto \exp\left\{- 5.1 \frac{\pi}{2} \sqrt{s}\right\} \\ &\propto \exp\left\{- 8.0\ s^{1/2}\right\} \end{aligned} \tag{IIIA. 5}$$

which is much more rapid than the experimental falloff. We conclude that diffraction is negligible at 90° and that a geometrical model for pp scattering must contain a peripheral component as well as a diffractive one.

In Fig. IIIA. 1 we compare data on 90° pp scattering with a form

$$s^2 \frac{d\sigma}{dt}(s, \theta = \pi/2) \sim \text{const} \exp\left\{-(\Delta b) \frac{\pi}{2} s^{1/2}\right\} \tag{IIIA. 6}$$

where Δb can be interpreted as the width of a peripheral band of partial waves. The value

$$\Delta b \cong 0.48 \text{ fm} \tag{IIIA. 7}$$

is suggested by a study of the impact parameter in K p scattering (Schmid, 1971). On the same graph the constituent counting prediction

$$\frac{d\sigma}{dt}(s, \theta = \pi/2) \sim \text{const } s^{-10} \tag{IIIA. 8}$$

is compared with the data. In view of the fact that the corrections to the asymptotic form expected from each model are not known, the agreement of the data with the two alternatives is comparable.

As emphasized by Hendry (1974) one advantage of the geometrical approach is the possibility of a simple and direct understanding of the structure in the

cross section in terms of fixed-t dips associated with Bessel function (or Legendre function) zeros. The approximate double-zero structure of the large-angle pp polarization data, Fig. IIA.9, is fairly direct evidence for a central plus peripheral decomposition of the pp scattering amplitudes (Hendry and Abshire, 1974).

Another reason for studying geometrical models is to test the region of validity of field theory approach. The asymptotic constituent counting rules should be strictly valid in a regime where all spin amplitudes are proportional so there is no polarization and where the amplitudes are smooth and featureless. The present data may be in a transition region where both approaches are approximately valid due to some sort of duality which makes the application of simple asymptotic estimates valid right down to small energies. Kane (1974) has shown how the introduction of absorption effects into hard scattering models leads to an oscillating factor of t modifying the asymptotic fixed angle power-law behavior predictions.

An alternate approach to fixed angle scattering assumes the existence of a large number of direct channel resonances such as in dual models. While dual models in their simplest form violate the Cerulus-Martin bound they can be interpreted in the spirit of statistical bootstrap models (Frautschi, 1972). If we consider the process $ab \rightarrow cd$, neglecting spin and assume that in the region of interest $|A|^2$ can be approximated by the incoherent sum of resonances

$$|A(s,z)|^2_{\theta \cong 90^o} \cong \sum_{i,\ell} \frac{(2\ell+1)^2 \, P^2_\ell(\cos\theta)\left(\gamma^{i\ell}_{ab}\right)^2\left(\gamma^{i\ell}_{cd}\right)^2}{\left(\sqrt{s} - m_{i,\ell}\right)^2 + 1/4\,\Gamma^2_{i,\ell}} \qquad \text{(IIIA.9)}$$

The sum in ℓ extends over the range $\ell \in (0, qR)$, where R is a typical hadronic radius. If we neglect the dependence of the residues over this range we can

factor out the θ dependence

$$\xi(s,\theta) = \frac{\sum_{0}^{qR} (2\ell+1)^2 P_\ell^2(\cos\theta)}{\sum_{0}^{qR} (2\ell+1)} \tag{IIIA. 10}$$

and deal with the appropriate average quantities in the form

$$|A(s,z)|^2 \cong \frac{(2\pi)\left(\gamma_{ab}(\sqrt{s})\right)^2\left(\gamma_{cd}(\sqrt{s})\right)^2 \rho(\sqrt{s})\ \xi(s,\ )}{\Gamma(\sqrt{s})} \tag{IIIA. 11}$$

Now the further statistical assumption of equal partition of probability among channels

$$\frac{\left(\gamma_{ab}(\sqrt{s})\right)^2}{\Gamma(\sqrt{s})} \cong \frac{\left(\gamma_{cd}(\sqrt{s})\right)^2}{\Gamma(\sqrt{s})} \cong \frac{1}{\rho(\sqrt{s})} \tag{IIIA. 12}$$

allows us to simplify further

$$\left.\frac{d\sigma}{d\Omega}\right|_{\theta\cong 90^o} \cong \frac{1}{64\pi^2 s}\ \frac{\Gamma(\sqrt{s})}{\rho(\sqrt{s})}\ \xi(s,\theta) \tag{IIIA. 13}$$

By simple space-time arguments we know that a resonance cannot decay before a signal can pass across a typical hadronic radius and that

$$\Gamma(\sqrt{s}) = 0(\sqrt{s}) \tag{IIIA. 14}$$

The statistical bootstrap model gives, of course, a specific prediction for both $\Gamma(\sqrt{s})$, and $\rho(\sqrt{s})$ and has been compared to data by Eilam et al. (1973). The only parameters are an overall normalization factor in the expression for the density of states and a small ambiguity concerning the value of kT_0. Fits to πp and $\bar{p}p$ elastic scattering at 90° are shown in Fig. IIIA. 2 and compared to the power behavior of constituent models. The agreement with the data is good.

A major flaw in the statistical approach is that no predictions are made for the behavior of fixed angle cross sections in exotic channels. One possible way

around this is to extend the observed spectrum to exotic channels and just state that the density of states in exotic channels is small. This would then imply, for example

$$\left.\frac{d\sigma/d\Omega\,(pp \to pp)}{d\sigma/d\Omega\,(\bar{p}p \to pp)}\right|_{\theta \cong 90^{o}} >> 1 \qquad \text{(IIIA. 15)}$$

$$\left.\frac{d\sigma/d\Omega\,(K^{+}p \to K^{+}p)}{d\sigma/d\Omega\,(K^{-}p \to K^{-}p)}\right|_{\theta \cong 90^{o}} >> 1 \qquad \text{(IIIA. 16)}$$

which is in agreement with present observations. It would also seem that the naive approach would imply large fluctuations about the mean in such exotic channels. This is not observed. Presumably, the correct answer for exotic channels involves getting the spectrum in nonexotic channels right and then implementing crossing.

There exists one solid piece of support for the existence of high mass resonance states of the type necessary for the statistical approach discussed here. This consists of the rapid fluctuations with energy of the large t differential cross section for $\pi^{\pm}p$ elastic scattering observed by F. Schmidt et al. (1973) and illustrated in Fig. IIA. 10 . The existence of these rapid fluctuations was predicted on the basis of a statistical treatment of overlapping resonances by Ericson (1963). Their importance in terms of the statistical bootstrap program has been emphasized by Frautschi (1972). Basically we expect a large number of overlapping resonances which, on the average, have random phases to be partially coherent in local regions of energy. The period of the fluctuations produced should give a measure of the average resonance width and the relative size of the fluctuations should vary inversely with the density.

It is impossible to learn on the basis of the single observation of fluctuations reported by Schmidt et al. whether they correspond in period or size with those

predicted by the statistical model. Many more measurements of this type are needed but it does seem most natural to attribute these data to some sort of high-mass resonance phenomena.

One of the most crucial distinctions between finitely-composite hadrons and infinitely-composite hadrons involves the asymptotic form of Regge trajectories. There has been a considerable effort to extend the constituent interchange model from the fixed-angle region into the fixed-t region. This effort has resulted in predictions for the large-t behavior of Regge trajectories. Let us consider here the status of the predictions

$$\begin{aligned} \lim_{t \to \infty} \alpha_{\pi p}(t) &= -1 \\ \lim_{t \to \infty} \alpha_{pp}(t) &= -2 \end{aligned} \qquad \text{(IIIA. 19)}$$

This prediction can be tested by measuring the effective trajectory in $\pi^- p \to \pi^0 n$ and pp elastic scattering. In contrast, dual or geometrical ideas would require infinitely falling trajectories.

Barger, Halzen and Luthe (1972) have calculated an effective trajectory in pp scattering using

$$\ln \frac{d\sigma}{dt}(pp \to pp) = \left(2\alpha_{eff}(t) - 2\right) \ln s + \ln \beta(t) \qquad \text{(IIIA. 20)}$$

This is shown in Fig. IIIA. 3. Blankenbecler et al. (1974) have calculated the effective trajectory in Fig. IIIA. 4a using

$$\ln \frac{d\sigma}{dt}(pp \to pp) = \left(2\alpha_{eff}(t) - 2\right) \ln(-u) + \ln \beta(t) \qquad \text{(IIIA. 21)}$$

which they claim is more consistent with the duality properties of the pp elastic amplitude. The difference in the t-dependences of these two trajectory functions is primarily due to

$$\ln(-u) = \ln(s + t - 4m^2) = \ln(s) + \ln\left(1 + \frac{t-4m^2}{s}\right) \qquad \text{(IIIA. 22)}$$

and so the fact that the trajectory of Barger et al. falls below -2 should therefore not necessarily rule out (IIIA. 19).

The ρ-trajectory extracted from charge exchange data of Brockett et al. (1974) seems to fall below the expected value of -1. However, elastic $\pi^- p$ analyzed by Blankenbecler et al. (1974) as shown in Fig. IIIA. 4b supports (IIIA. 19).

Possibly more significant evidence concerning the large-t behavior of Regge trajectories is the study using finite energy sum rules of the amplitude structure of $\pi^- p \rightarrow \pi^0 n$. Elvekjar et al. (1973) report that the large t region the amplitudes are very similar to what is expected from a simple ρ-Regge pole with a linear trajectory. In particular they point out the right-signature zero at $t = -1.6$ and a second wrong-signature zero at $t \cong -2.4 - 2.5$ consistent with the places where a linear trajectory would pass through -1 and -2 respectively. Their results are shown in Fig. IIIA. 5. There is some feedback through the "optimized convergence" finite energy sum rule of the form assumed for the trajectory function and the structure in the amplitude. However, if this structure is confirmed independently, for example, by amplitude analysis at large t then it would argue quite strongly for the existence of indefinitely falling trajectories.

LIST OF FIGURES FOR SECTION IIIA

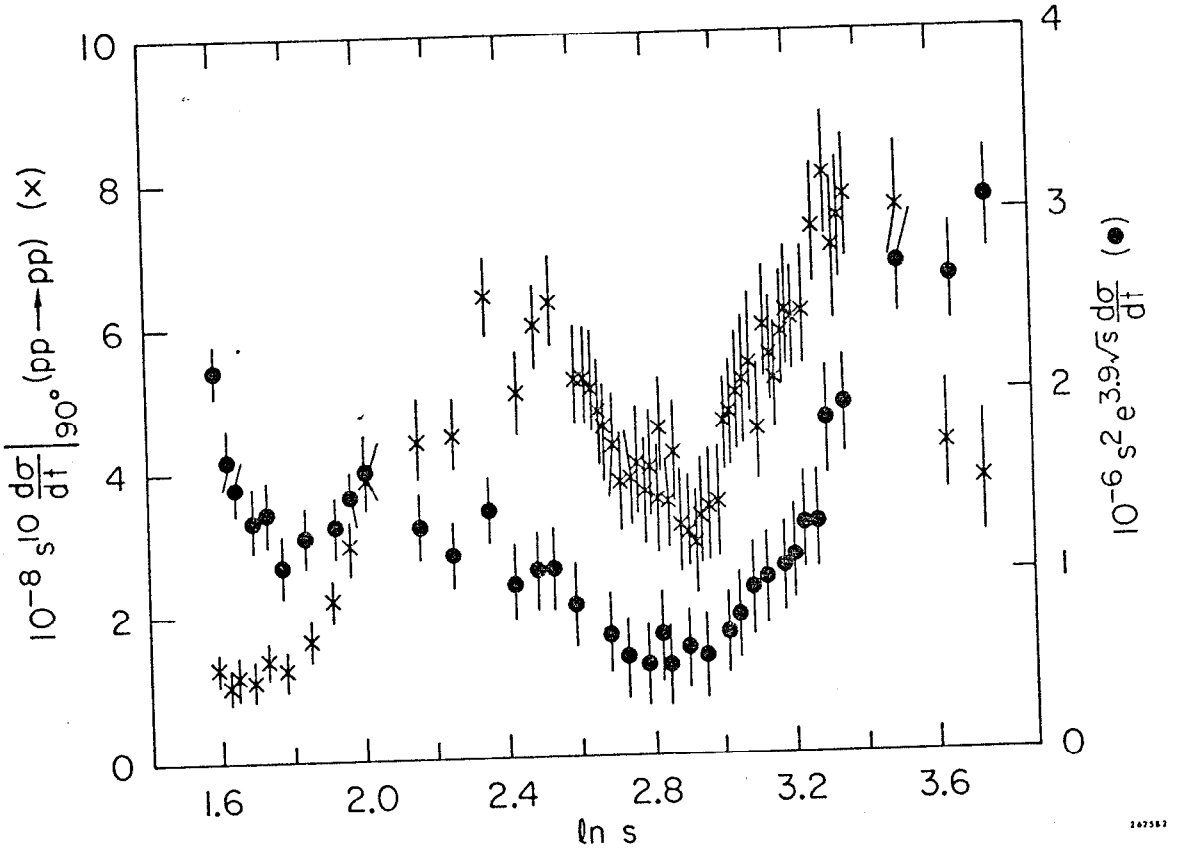
10
8
6
4
2
0
4
3
2
1
0
1.6
2.0
2.4
2.8
3.2
3.6
ln s
$10^{-8}\, s^{10} \frac{d\sigma}{dt}\Big|_{90°} (pp \to pp)$ (x)
$10^{-6}\, s^{2}\, e^{3.9\sqrt{s}} \frac{d\sigma}{dt}$ (●)

FIG. IIIA. 1

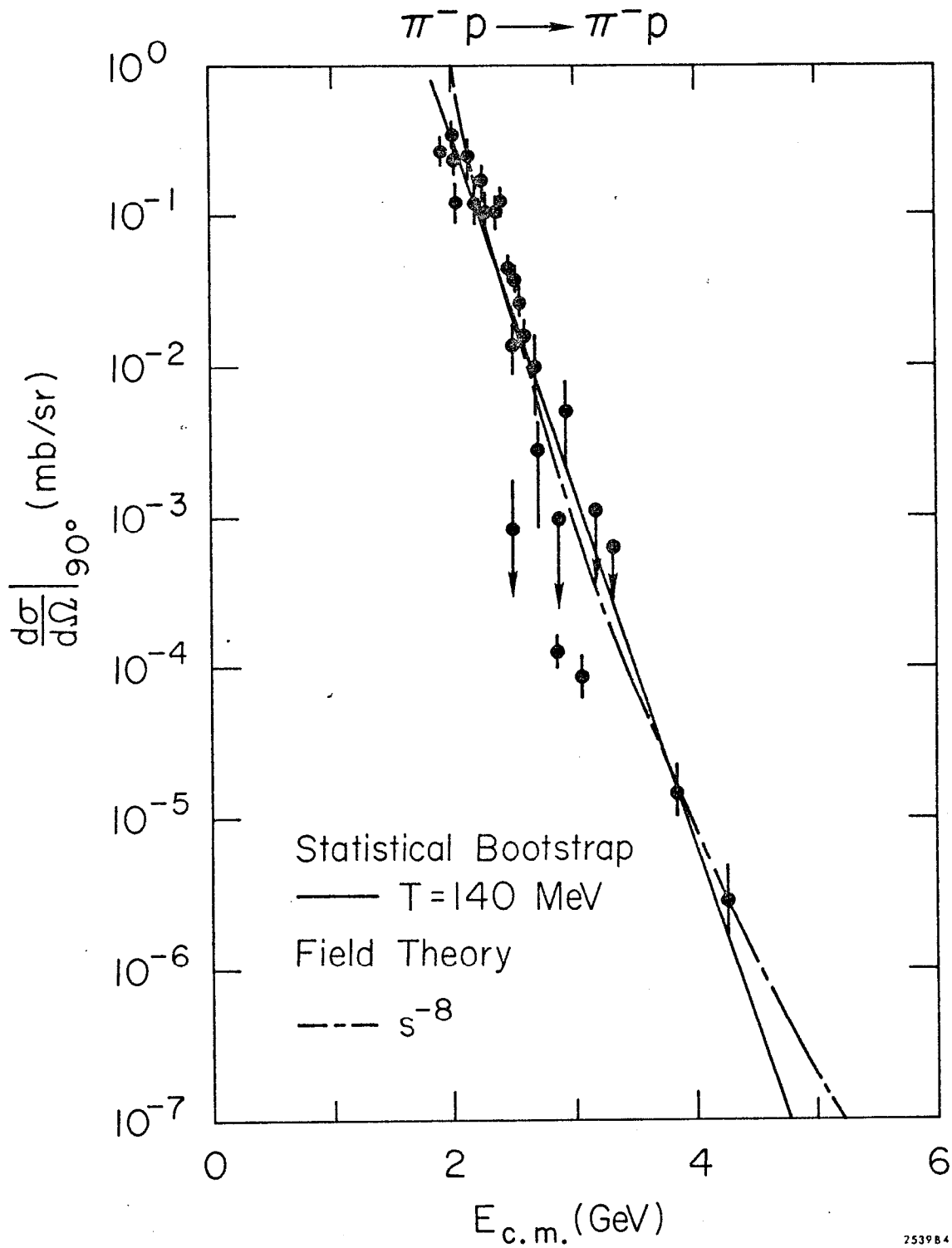
$\pi^- p \longrightarrow \pi^- p$
10^0
10^{-1}
10^{-2}
10^{-3}
10^{-4}
10^{-5}
10^{-6}
10^{-7}
$\left.\frac{d\sigma}{d\Omega}\right|_{90°}$ (mb/sr)
Statistical Bootstrap
T = 140 MeV
Field Theory
s^{-8}
0
2
4
6
$E_{c.m.}$ (GeV)
2539B4

FIG. IIIA. 2a

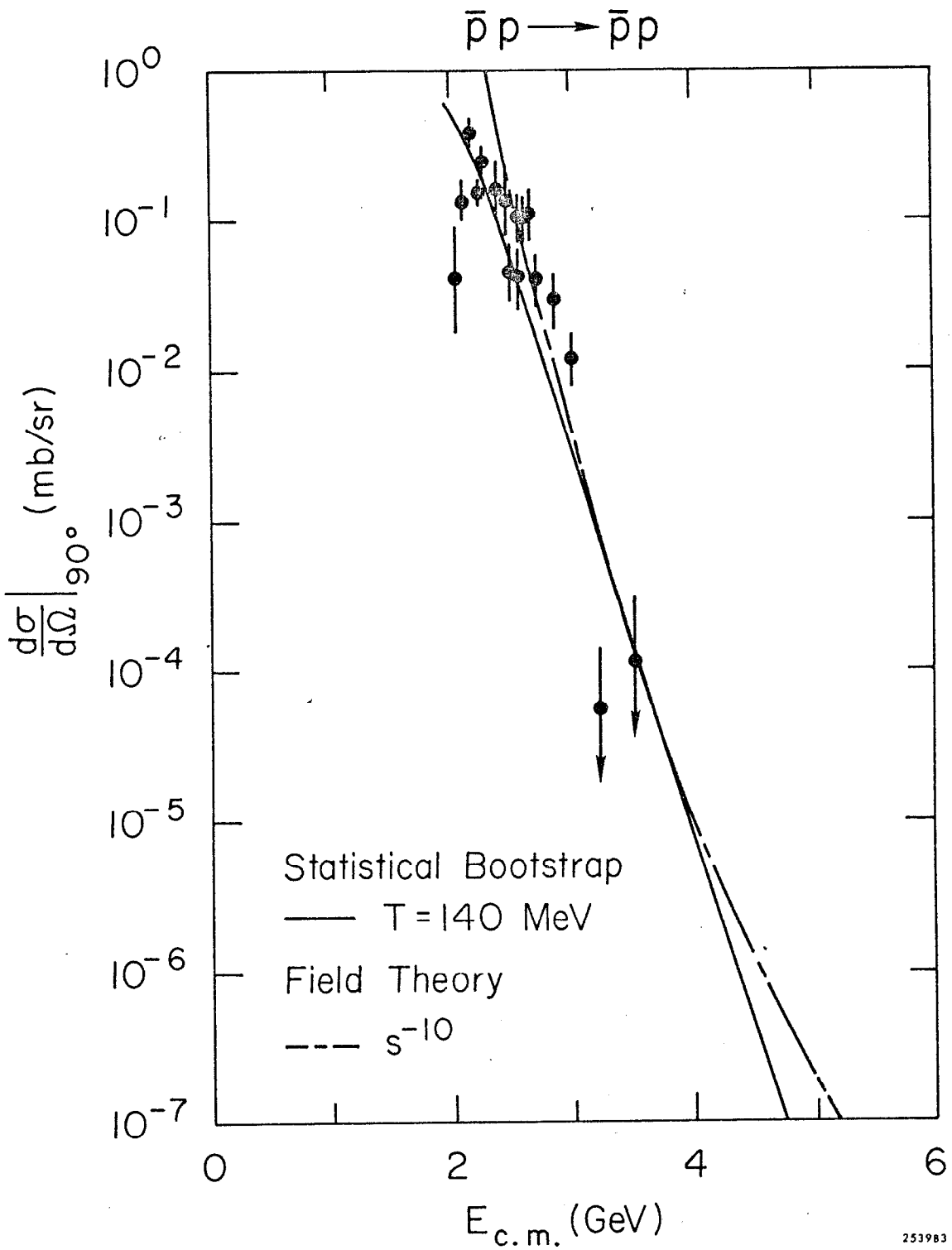
$\bar{p}p \longrightarrow \bar{p}p$
10^0
10^{-1}
10^{-2}
10^{-3}
10^{-4}
10^{-5}
10^{-6}
10^{-7}
$\left.\frac{d\sigma}{d\Omega}\right|_{90°}$ (mb/sr)
Statistical Bootstrap
T = 140 MeV
Field Theory
s^{-10}
0
2
4
6
$E_{c.m.}$ (GeV)
253983

FIG. IIIA.2b

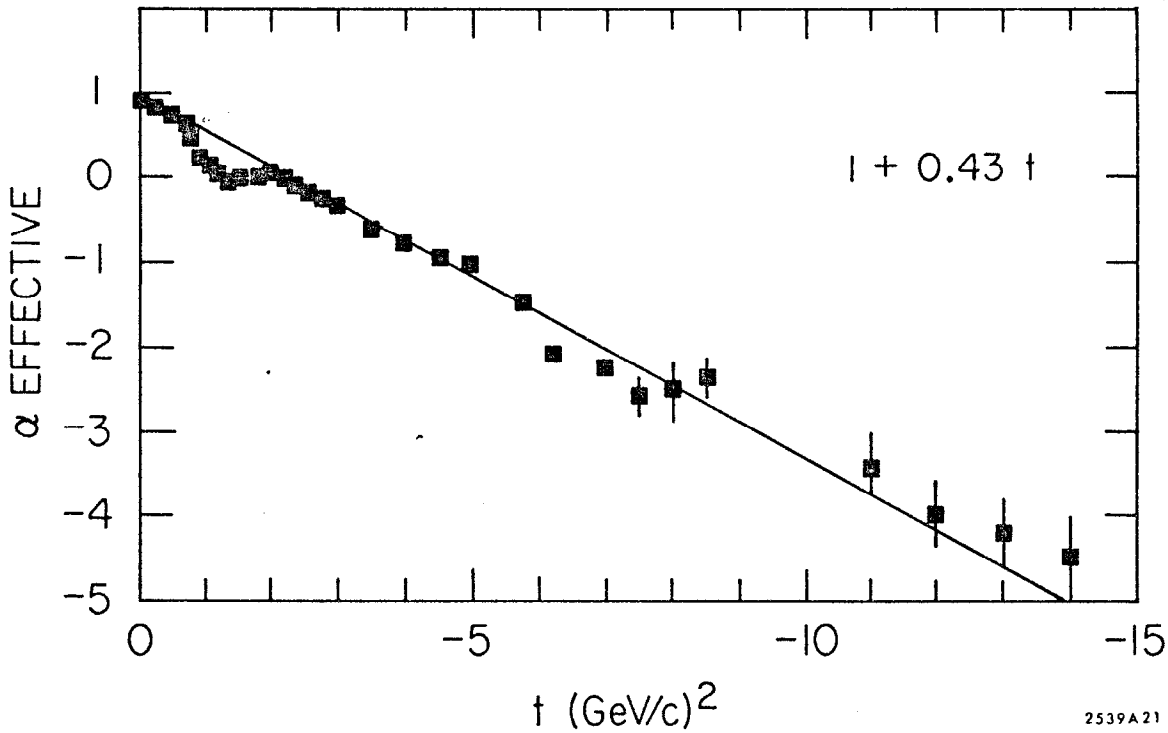

FIG. IIIA.3

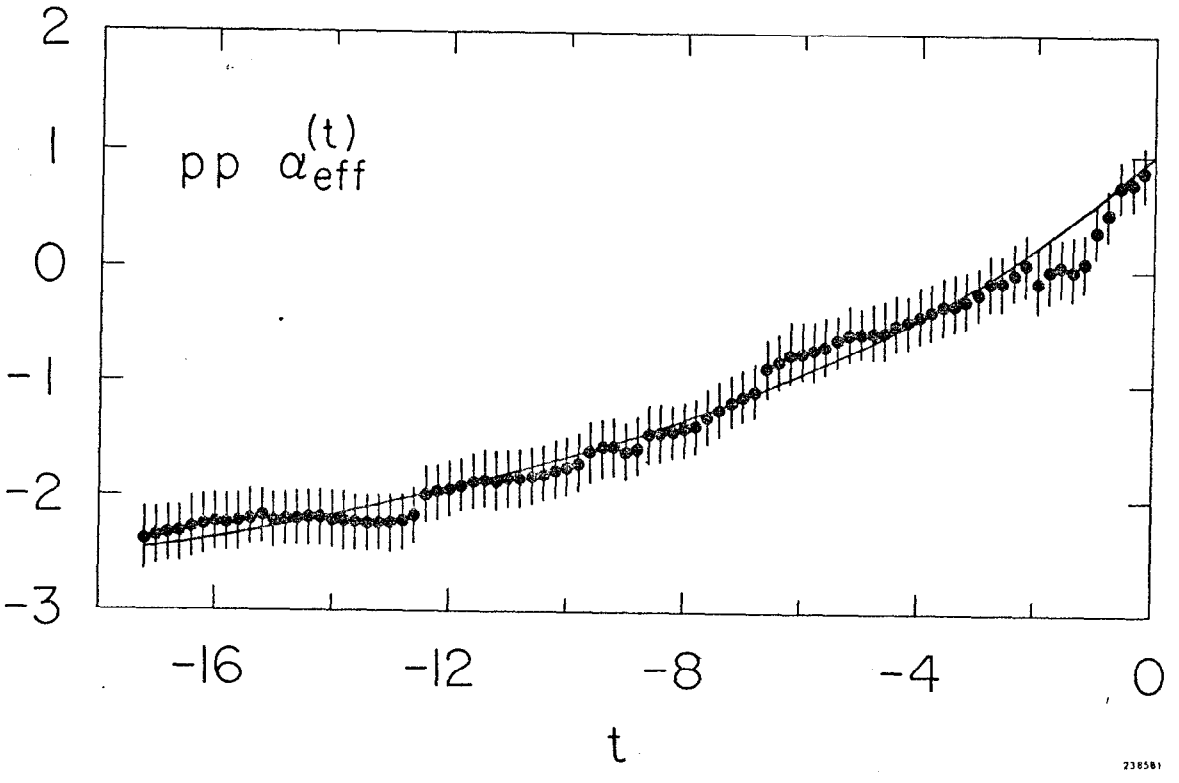

FIG. IIIA.4a

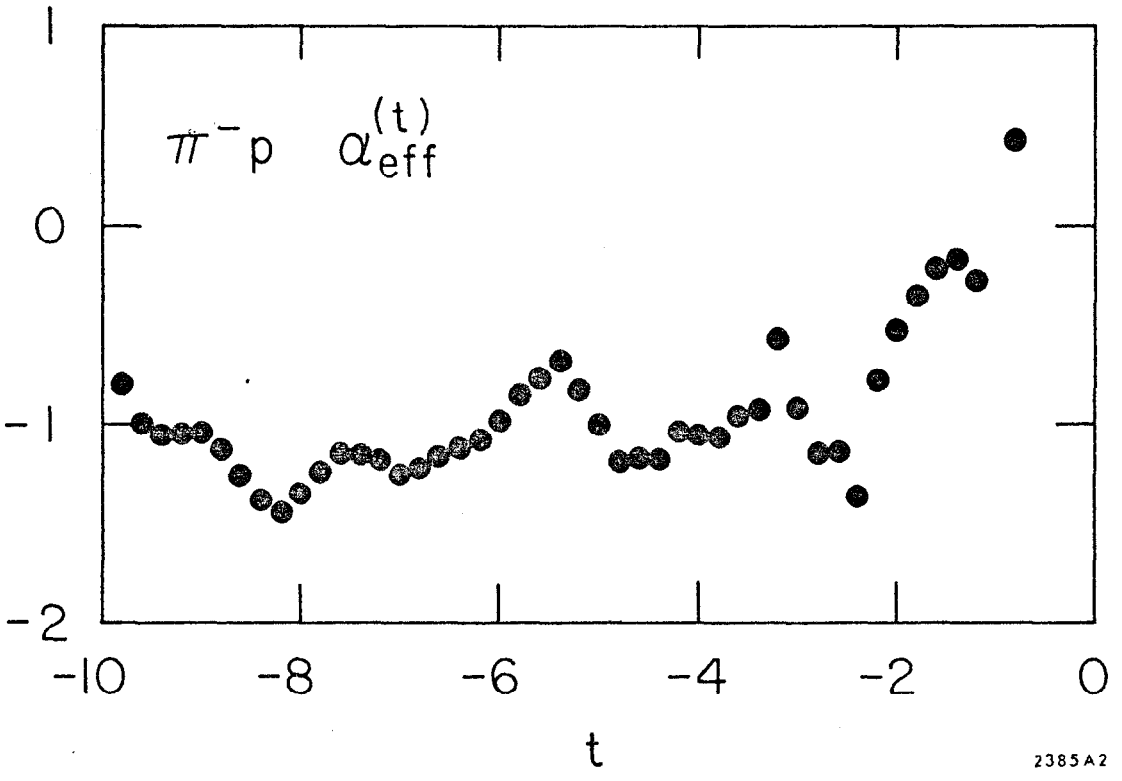

FIG. IIIA.4b

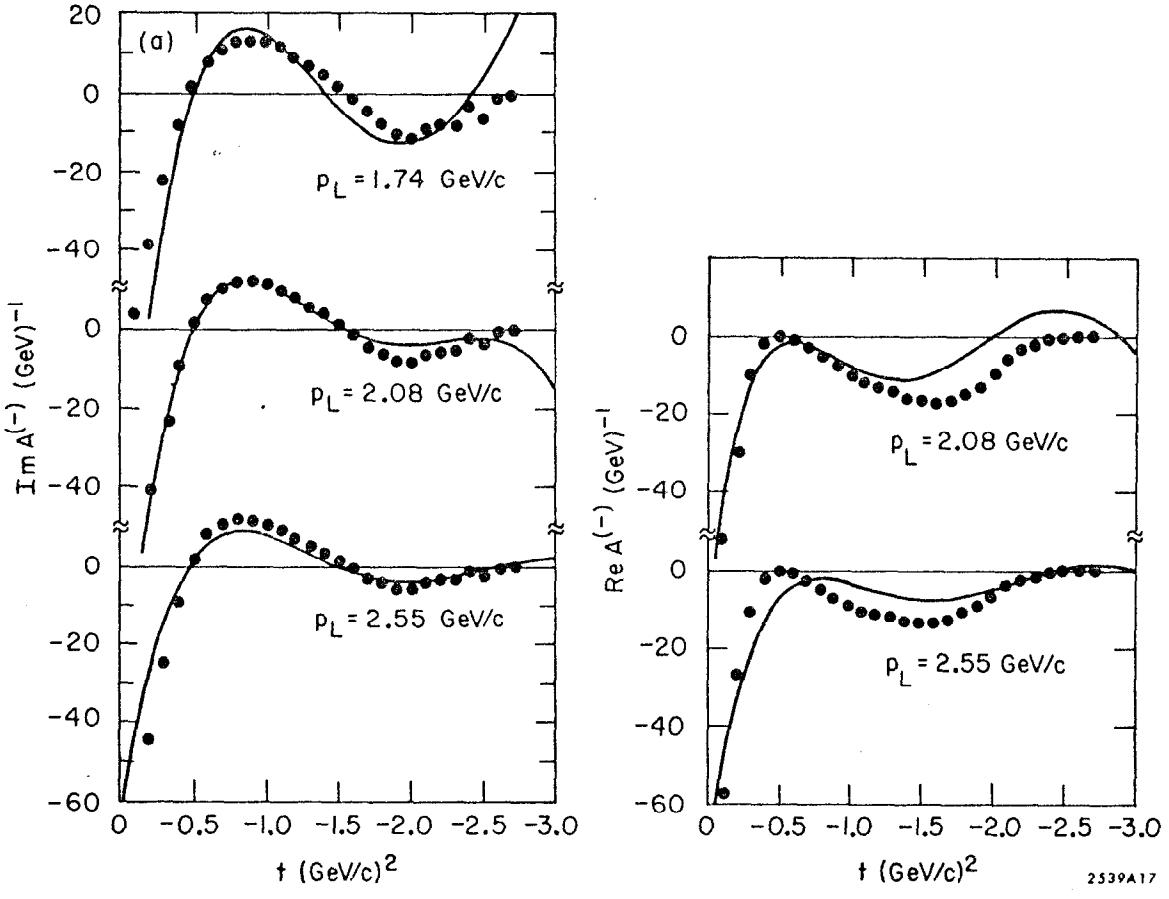
(a)
p_L = 1.74 GeV/c
p_L = 2.08 GeV/c
p_L = 2.55 GeV/c
Im $A^{(-)}$ (GeV)$^{-1}$
Re $A^{(-)}$ (GeV)$^{-1}$
t (GeV/c)^2
2539A17

FIG. IIIA.5

B. Hadronic Fireball Approaches to Large p_T Inclusives

In this section we turn our attention to models which attempt to explain high p_T phenomena without invoking quark-like structureless constituents. These hadronic models instead relate the production of large transverse momentum particles to ideas which have proved useful in understanding low p_T data.

The first, and one of the most important, thing to keep in mind is that based on purely hadronic ideas there is no reason to expect large p_T inclusive cross sections anywhere near as large as they have been observed to be. We can be more explicit about this. Two reasonably complete and self-consistent models have made predictions for the p_T distributions of inclusive hadronic processes. The dual resonance model (DeTar et al., 1971) predicts

$$Ed^3\sigma/d^3p\Big|_{p_L \cong 0} \propto e^{-4\alpha' p_T^2} \qquad \text{(IIIB. 1)}$$

(which conflicts with a simple extension of the Cerulus-Martin bound to inclusive process). The statistical bootstrap model (Hagedorn and Ranft, 1968; Hagedorn, 1968) gets

$$Ed^3\sigma/d^3p\Big|_{p_L \cong 0} \propto e^{-p_T/m_\pi} \qquad \text{(IIIB. 2)}$$

Within the context of these models there is no apparent need for large p_T events from some sort of violent subprocess. The observation of large cross sections characterized by Eq. (IB. 3) or Fig. I. 1 then indicates that these models are wrong or, at best, incomplete and that they need to be modified. The hadronic models we discuss here make modifications of a somewhat ad hoc nature, invoking new mechanisms or new, unsuspected mass scales but we will temporarily overlook the lack of internal theoretical motivation. The unexpected,

large cross sections are motivation enough. As is evident in the rest of this review the hard scattering models in which large cross sections are expected are not without their own shortcomings. One main purpose in considering non-parton models is to gain further insight into the problem of just how important it is that we consider quarks to be an essential dynamical degree of freedom in large p_T hadronic interactions.

Before we go on to consider the ad hoc models which attempt to describe the current data, let us try to get the flavor of the two models which predict exponentially falling cross sections at large p_T. The dual resonance model prediction is based on a Mueller-Regge analysis of the dual 6-point function. Consider, for example, the term with the ordering of particles shown in Fig. IIIB.1. The dual model amplitude with this ordering has the discontinuity

$$\begin{aligned}
\mathrm{disc}_{\mathcal{M}^2} B_6 \sim \frac{a\pi i}{\Gamma(\alpha_{a\bar{a}}+1)} (\alpha)^{\alpha_{a\bar{a}}} \left(\frac{-\alpha_{ac}}{\alpha}\right)^{\alpha_{bc}} \left(\frac{-\alpha_{\bar{a}\bar{c}}}{\alpha}\right)^{\alpha_{\bar{b}\bar{c}}} \\
\times \int_0^\infty \int_0^\infty dy_1\, dy_2\, \theta(1-y_1-y_2)\, y_1^{-\alpha_{b\bar{c}}-1}\, y_2^{-\alpha_{\bar{b}\bar{c}}-1} \left(1-\frac{\alpha}{\alpha_{ac}} y_1\right)^{\alpha_{bc}+\alpha_{b\bar{b}}-\alpha_{a\bar{a}\bar{c}}} \\
\left(1-\frac{\alpha}{\alpha_{\bar{a}\bar{c}}} y_2\right)^{\alpha_{\bar{b}\bar{c}}+\alpha_{b\bar{b}}-\alpha_{\bar{a}ac}} \left(1-\frac{\alpha}{\alpha_{ac}} y_1 - \frac{\alpha}{\alpha_{\bar{a}\bar{c}}} y_2\right)^{-\alpha_{a\bar{a}}-\alpha_{b\bar{b}}+\alpha_{a\bar{a}c}+\alpha_{\bar{a}ac}} \\
(1-y_1-y_2)^{\alpha_{a\bar{a}}} \qquad \text{(IIIB.3)}
\end{aligned}$$

where $\alpha_{a\bar{a}} = \alpha\left((p_a+p_{\bar{a}})^2\right)$, $\alpha = \alpha\left((p_a+p_b+p_c)^2\right) = \alpha(\mathcal{M}^2)$, etc., are the linear trajectory functions. At fixed x_L and large p_T we have

$$\alpha_{bc} \cong \alpha_{\bar{b}\bar{c}} \cong -\alpha' p_T^2/x_L \qquad \text{(IIIB.4)}$$

and we get a contribution from the integrand near $y_1 = y_2 = 1/2$ proportional to (Virasoro, 1971)

$$\exp\left[-2\alpha' p_T^2 \left(\frac{1}{x_L} \ln\left(\frac{1+x_L}{1-x_L}\right)\right)\right] \qquad \text{(IIIB.5)}$$

In the central region, $x_L = 0$, this continues into the form (IIIB.1).

The exponential falloff in p_T^2 in the inclusive distribution of the dual model is related quite closely to the fixed-angle behavior of the dual 4-point function. The absence of Regge cuts or multiplicative fixed poles in the J-plane allows the exchange of a linear Regge trajectory to dominate at large momentum transfers. It is important to keep in mind the fact that the dual model does not implement unitarity and that the simple predictions (IIIB.1) and (IIIB.5) are probably not stable under the unitarization of the model. There have been some attempts to generalize such results (Ellis and Freund, 1970; Sivers, 1975) but these remain very speculative. The predictions (IIIB.1) and (IIIB.5) are, of course, in drastic conflict with the data. This fact along with the inability of dual models to define reasonable current amplitudes and form factors must now be considered a major challenge to the continued application of the dual approach.

Hagedorn's statistical bootstrap (Hagedorn, 1968) constitutes another fundamental model which does not invoke structureless quarks in order to make a definite prediction for the transverse momentum distribution. The basic postulate of the statistical bootstrap model (Frautschi, 1971) is that there exists a spectrum of high mass hadrons and that the energy of interaction in hadron-hadron collisions goes predominantly into the production of these massive fireballs. Consistency arguments based on the unitarity equation then require

that the density of hadronic levels is given by

$$\rho(\mathcal{M}) = C\mathcal{M}^a \exp(\mathcal{M}/T_0) \qquad \text{(IIIB.6)}$$

where T_0 is a temperature and $a \leq 5/2$. This hadronic density seems to be approximately realized in nature by the observed low mass states as demonstrated by Fig. IIIB.2. From this we deduce $T_0 \cong 160$ MeV.

The distribution in transverse momentum of the secondary decay products in the statistical bootstrap model then follows from the fact that the dominant decay mode of the high-mass fireballs is the so-called cascade decay $M^* \rightarrow M^{*\prime} + m_c$. To the extent that we can neglect recoil momentum we expect this distribution in the fireball rest frame to be given by a Boltzmann factor

$$\exp\left[-\left(p_L^2 + p_T^2 + m_c^2\right)^{\frac{1}{2}}/T\right] \qquad \text{(IIIB.7)}$$

where the temperature, T, is closely related to the temperature in the density of states, (IIIB.6),

$$T \lesssim T_0 \quad . \qquad \text{(IIIB.8)}$$

In high energy collisions, the superposition of fireballs with different longitudinal velocities smears out the Boltzmann factor in the longitudinal direction but, since most fireballs are produced with small transverse momentum, the dependence in the transverse direction remains almost unchanged.

The fact that for a reasonable range of intermediate momenta the experimentally observed transverse momentum behavior

$$Ed^3\sigma/d^3p \simeq c(p_L)\, e^{-6p_T} \qquad (0.1 \leq p_T \leq 1.0 \text{ GeV/c}) \qquad \text{(IIIB.9)}$$

agrees quite well with (IIIB.7) where the value of T is given by T_0 in the density of states, (IIIB.6), was originally considered an outstanding success of the model. Now that we have to deal with new observations indicating that the data

at high transverse momentum be several orders of magnitude above (IIIB.9) we are faced with a problem. Do we believe that the agreement of low p_T data with (IIIB.9) fortuitous or do we recognize the model as having limited range of validity? If we take the latter viewpoint we can imagine that relaxing some of the assumptions of the model will enable us to extend our understanding out to larger p_T.

Most of the models we discuss here, whether or not they follow precisely the spirit of the statistical bootstrap model, retain the concept of the fireball and therefore share many conceptual features. The idea of a fireball or cluster of hadrons has, of course, been a valuable aid in understanding the correlations in low p_T data. The review of Ranft (1974) is particularly instructive in outlining the importance of this concept.

One simple approach to large transverse momentum discussed by Jabs (1974) is to introduce a new class of fireballs. A high energy collision is assumed to proceed via two distinct mechanisms, fragmentation and pionization. The pionization component coincides roughly with the usual statistical bootstrap ideas but fragmentation is handled separately. Specifically, Jabs assumes that the fireballs carrying the quantum numbers of the leading particles have quite different properties than those produced in the pionization region.

The contributions of the fragmentation fireballs to the inclusive cross section in this model is

$$\left.\frac{E d^3\sigma}{d^3p}\right|_{FRAG} \propto M_F^* \, p_T \int_1^{\gamma_F^{max}} \gamma_F \, w(\gamma_F) \, d\gamma_F \, \exp\left[-\frac{p_T}{kT_F}\gamma_F\right] \qquad \text{(IIIB.10)}$$

where γ_F is the Lorentz factor given approximately by

$$\gamma_F = \left(\frac{\sqrt{s} - E_\pi}{M_F^*}\right) \qquad \text{(IIIB.11)}$$

where E_π is the amount of C.M. energy going into pionization and $w(\gamma_F)$ is a normalized distribution of fireballs. By allowing these fireballs to occasionally be very massive and slow in the C.M. system and assuming they decay statistically with a temperature $T_F \cong 2T_0$, the single particle inclusive data can be roughly understood.

While there can be no fundamental objection to the ad hoc introduction of a new temperature or mass scale it is not inherently satisfying. A simplifying assumption used by Jabs is that the fireballs are produced strictly along the collision axis; without further clarification of how reasonable this assumption is, the understanding of the production is incomplete.

Pokorski and van Hove (1974a) have a similar view of the origin of high p_T particles. They point out that if the leading fireball is assumed to be produced diffractively in the spirit of the diffractive dissociation model (Hwa and Lam, 1971) or the nova model (Jacob and Slansky, 1972), then the low masses of diffractive fireballs and the competition of different channels combine to keep transverse momenta of decay products low. At NAL or ISR, however, the production of heavy fireballs can lead to large transverse momenta.

In a separate paper Pokorski and van Hove (1974b) also make an interesting connection between fireball models and quark parton models. They note that the average fraction of C.M. energy carried off by protons in proton-proton inelastic collisions is near one-half. Also, the average fraction of the proton's momentum carried by quarks as deduced from analysis of lepton-proton inelastic scattering is close to a half. This suggests that the fragmentation fireball can be considered to carry the quantum numbers and approximately the same C.M. energy as the initial quarks. The assignment of a large mass to this fireball can then be considered roughly equivalent to giving the valence

quarks a large relative momentum and the "decay" of a large mass fireball to produce high transverse momentum hadrons can have the same underlying dynamics as the quark-parton model. In the synthesis of Pokorski and van Hove, it is unspecified at what level the underlying fundamental constituents become the important dynamical entities instead of the fireball. More explicit calculations are needed. One thing which is clear is that it is over-simplifying things to consider only fireballs which themselves have no transverse momentum.

An interesting calculation in the context of statistical models has been performed by Bouquet, Letessier and Tounsi (1974). The heavy clusters which are formed are assumed to decay in a sequential cascade mechanism. This would lead to the Boltzmann distribution Eq. (IIIB.7) for the transverse momentum of the decay products if the recoil momentum of the heavy cluster is neglected. They then observe that the buildup of successive recoils to produce a large momentum is statistically unlikely but not so unlikely as to be unable to produce the observed yield of high transverse momentum hadrons. Detailed numerical calculations described in their paper yield the curve shown in Fig. IIIB.3. The calculations are complicated enough that it is difficult to abstract any features of the data which will conclusively support their contention. It remains an interesting piece of work which shows that it can be dangerous to use statistical arguments when the number of particles in the decay mode is still relatively small.

One modification of the statistical model which has not received much attention is the possibility that high mass fireballs have a small "fission" decay mode where they decay into two approximately equal mass objects as well as the usual cascade decay mode. A reasonable branching fraction into a fission mode can result in substantial large p_T inclusive cross sections. Of course, this decay mode could also give jet-like structure to the population of hadrons in the

final state. Detailed calculations on this approach have not been made although the formalism is available (Barnett and Silverman, 1974).

A distinct version of the fireball model is advocated by Berger and Branson (1973). In their approach low mass fireballs are produced at large θ through a hard scattering mediated by the current-current interaction of Berman and Jacob (1971). The invariant cross section for the production of these baryonic clusters in Fig. IIIB.4 is given by

$$\frac{E_c d\sigma_c}{d\mathcal{M}_c^2 d^3p_c} = \frac{c}{\pi s} F_2(\omega_1) F_2(\omega_2) \left(\frac{s^2}{t^2 \omega_1 \omega_2} + \frac{s}{t} + \frac{\omega_1 \omega_2}{2} \right)$$
$$+ [\cos\theta \longleftrightarrow -\cos\theta] \qquad \text{(IIIB. 12)}$$

where F_2 is the usual dimensionless scaling function νW_2 and

$$\omega_1 = \frac{1}{t}\left[s^{1/2}\left(m_1^2 + p^2\right)^{1/2} - 2m_p^2 - (s - 4m_p^2)^{1/2} p\cos\theta\right]$$
$$\omega_2 = \frac{-1}{t}\left[s - s^{1/2}\left(m_2^2 + p^2\right)^{1/2} - 2m_p^2 - (s - 4m_p^2)^{1/2} p\cos\theta\right] \qquad \text{(IIIB. 13)}$$

The cross section (IIIB. 12) when integrated over all finite region of phase gives a contribution to the total inelastic cross section which rises linearly with s. Because of the magnitude of the large p_T cross section this rise is not a problem at current energies but there must be some sort of mechanism, possibly a natural cutoff, which removes this linear divergence.

Because the fireballs in Berger and Branson's calculation have baryon number one and a small mass, they predict the proton/pion ratio to be quite large. A value of 5 for this ratio is cited in their paper but the actual value is sensitive to the input mass spectrum for the fireballs. However, the observed value $p/\pi \simeq 1$ at $p_T = 3$ GeV/c (see Figs. IIB.5 and IIB.6) is uncomfortably small for a model with light baryonic fireballs.

An approach related to fireball models which attempts to incorporate an idea of the space-time structure of a collision is the "hydrodynamical" model originally proposed by Landau (1953). The picture is that some portion of the hadronic matter goes to form a massive fireball localized in some volume characteristic of the incident energy. One idea of the time evolution of this fireball is that it expands adiabatically for some period during which the behavior of the hadronic matter is governed by the classical dynamics of a perfect fluid. The expansion continues as the system "cools" until a temperature of order m_π is achieved and the system condenses into pions and other hadrons.

In a detailed study of the hydrodynamic equations done by Carruthers and Duong-Van (1973), approximate solutions for the particle distribution due to condensation suggests a gaussian dependence on rapidity. In the longitudinal rapidity $y_L = 1/2\ \ell n\,(E+p_L/E-p_L)$

$$\frac{E\,d^3\sigma}{d^3p} \propto e^{-y_L^2/R_L^2} \qquad \text{(IIIB. 14)}$$

the width, R_L, is approximately related to the Lorentz contraction

$$R_L \cong 1/2\ \ell n\,(s/s_0) \qquad \text{(IIIB. 15)}$$

From symmetry arguments, Carruthers and Duong-Van suggest that the 90° inclusive cross section should also be given by a gaussian in transverse rapidity, $y_T = 1/2\ \ell n\ (E+p_T/E-p_T)$

$$\left.\frac{E\,d^3\sigma}{d^3p}\right|_{y_L\cong 0} \propto e^{-y_T^2/R_T^2} \qquad \text{(IIIB. 16)}$$

where the width is now approximately independent of incident energy. The data is roughly consistent with this gaussian form over many orders of magnitude

although it is hard to understand the s-dependence of the high p_T cross section unless correction terms derived from beam fragmentation are important. One interesting suggestion is to take the hydrodynamical model for the dependence of the hadron irreducible interaction in a hard scattering picture for the interaction like Fig. I.5.

A suggestion due to Dumont and Heiko (1974) and Heiko (1974) is that although the bulk of particles can appear only at the condensation stage, some particles may escape from the hadronic matter at any time and will have a momentum reflecting the "temperature" at that time. They divide, rather arbitrarily, the progression of the fireball into the formulation or initial stage, the expansion stage and the condensation stage. For particles escaping from the initial fireball they expect a distribution in p_T approximately given by

$$\left.\frac{Ed^3\sigma}{d^3p}\right|_{init} = Ax_T\, e^{-Bp_T/s^{1/4}} \qquad \text{(IIIB. 17)}$$

which can be understood in terms of the original Fermi statistical model where (Fermi, 1951) where the highest temperature achieved is proportional to $s^{1/4}$. For particles escaping during the expansion stage they propose an empirical form

$$\left.\frac{Ed^3\sigma}{d^3p}\right|_{exp} = C\, p_T\, e^{-p_T/\left(D+Es^{1/4}\right)} \qquad \text{(IIIB. 18)}$$

so that the effective temperature interpolates the initial temperature and the breakup temperature $T \cong m_\pi$. The small p_T data is then fit by the usual Hagedorn spectrum (IIIB. 7).

With the fair number of parameters displayed in the model they can achieve a reasonable fit to the inclusive cross section. A typical fit and the values of

the parameters are shown in Fig. IIIB.5. The global display of the data given by Cronin, Fig. IIB.7, does not favor such an arbitrary division but the essence of the idea is that there is a continuum of temperatures between $T = Bs^{1/4}$ and $T = m_\pi$ which are important, and this would not argue for the existence of breaks. Meng Ta-Chung (1974) has proposed an alternate form where the temperature is proportional to $s^{1/8}$.

An alternate hadronic model which should stand separately from fireball models is the so-called asymptotic bootstrap model of Harte (1969, 1972). This model assumes that hadrons are infinitely composite in the sense that there are no poles in the irreducible kernel of a Bethe-Salpeter-type integral equation which represents unitarity. Self-consistency arguments are then used to derive the asymptotic behavior of vertex functions when one or more momentum transfers is large.

The model has predictions for electroproduction not too dissimilar from present data. In contrast, it predicts that the cross section $\sigma_{e^+e^- \to h}$ falls <u>faster</u> than $1/Q^2$. The predictions we want to mention here start with the predicted behavior of electromagnetic form factors

$$F(t) \sim e^{-af(m^2, m^2)(-t)^{1/4}} \qquad \text{(IIIB.19)}$$

(See also Stack, 1967.) This is in good agreement with the data. The fixed angle behavior of exclusive cross sections in this model is also expected to fall exponentially with $(-t)^{1/4}$. The inclusive production of hadrons at large p_T in this model come from graphs such as that shown in Fig. IIIB.6 where the heavy line is a $p^2=0$ propagator. In diagram a of this figure the maximum contribution comes from t near t_{min} and leads to an inclusive cross section

behaving asymptotically as

$$\frac{E\, d^3\sigma}{d^3p}\bigg|_{90^o} \sim f(s, x_T)\, e^{-c\, p_T^{1/2}} \qquad \text{(IIIB.20)}$$

where c is a universal constant and f is slowly varying. A comparison of this single contribution with data on $pp \to \pi^o$ from the CCR group is shown in Fig. IIIB.7. The other diagrams have not been computed.

None of the models discussed here can be considered completely successful in the sense that the large inclusive cross sections for high p_T hadrons are a natural expectation. Several models cannot be ruled out with existing data but these cannot be considered attractive because they contain ad hoc features. One important constraint is that the models make interesting nontrivial predictions for two-body inclusives, multiplicity correlations, etc. which can be compared to new data. An important consequence of the work of Pokorski and van Hove is that it may be possible to make a synthesis of fireball and quark-parton models which allows all kinematic ranges to be dealt with on a uniform basis. This exciting possibility deserves careful exploration.

LIST OF FIGURES FOR SECTION IIIB

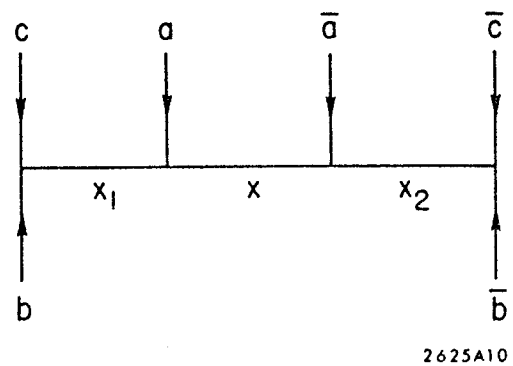

FIG. IIIB.1

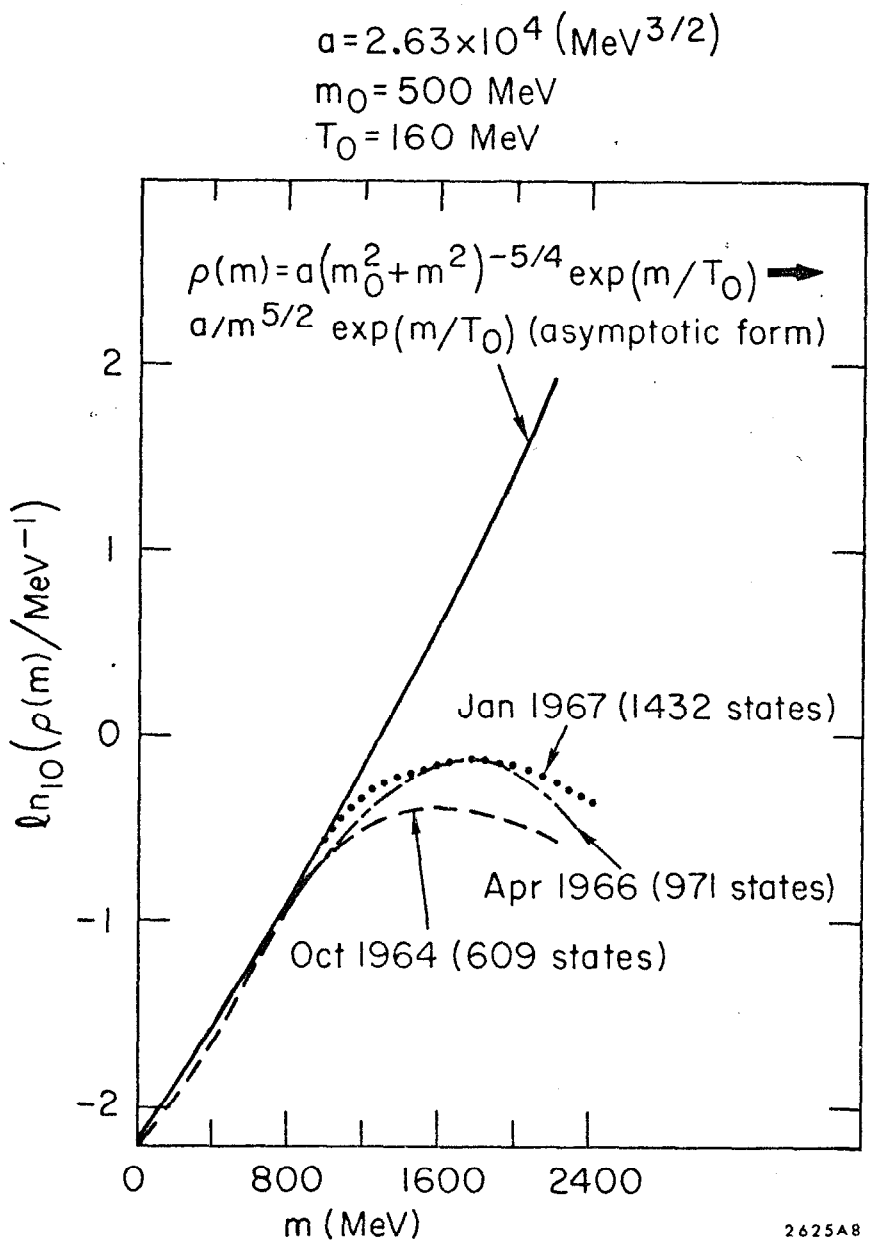
a = 2.63×10^4 (MeV^3/2)
m0 = 500 MeV
T0 = 160 MeV
ρ(m) = a(m0^2 + m^2)^-5/4 exp(m/T0)
a/m^5/2 exp(m/T0) (asymptotic form)
Jan 1967 (1432 states)
Apr 1966 (971 states)
Oct 1964 (609 states)
ln10(ρ(m)/MeV^-1)
2
1
0
-1
-2
0
800
1600
2400
m (MeV)
2625A8

FIG. IIIB.2

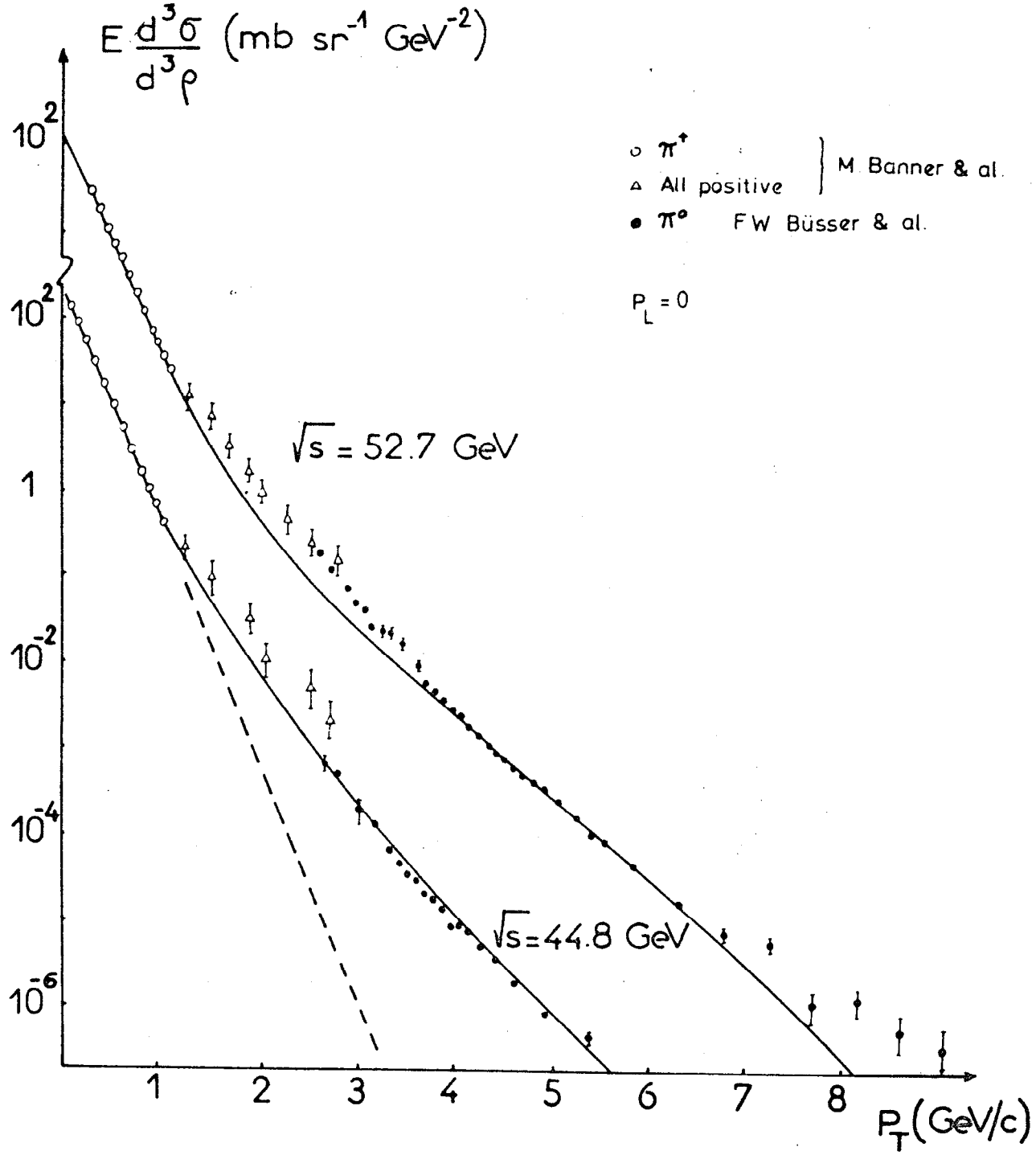
$E\frac{d^3\sigma}{d^3p}$ (mb sr^{-1} GeV^{-2})
10^2
10^2
1
10^{-2}
10^{-4}
10^{-6}
○ π^+
△ All positive
M. Banner & al.
● π^0 FW Büsser & al.
$P_L = 0$
$\sqrt{s}$ = 52.7 GeV
$\sqrt{s}$=44.8 GeV
1
2
3
4
5
6
7
8
P_T(GeV/c)

FIG. IIIB.3

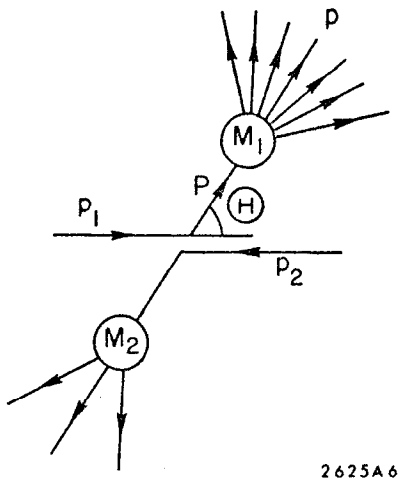

FIG. IIIB.4

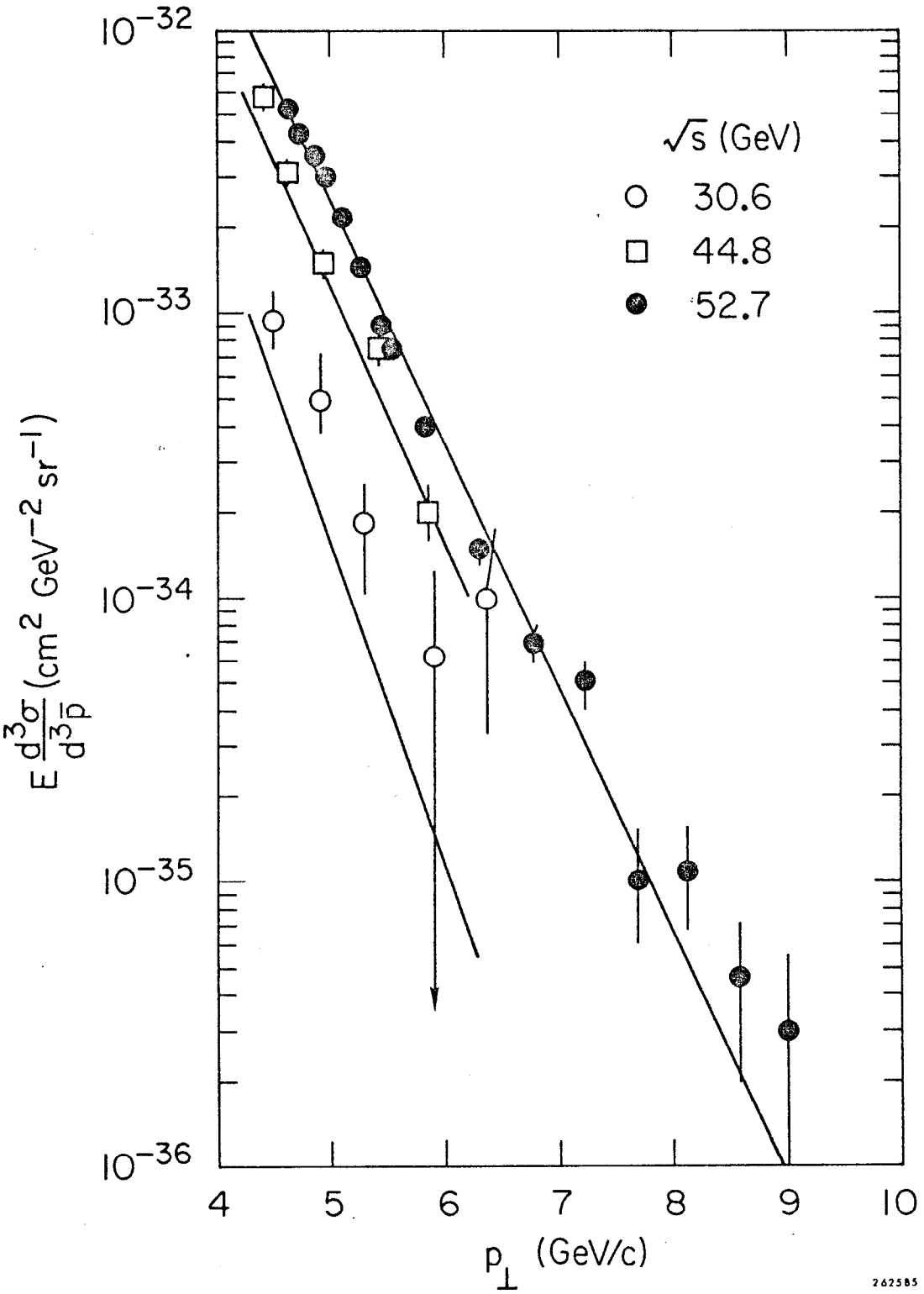
10^{-32}
10^{-33}
10^{-34}
10^{-35}
10^{-36}
$E\frac{d^3\sigma}{d^3\bar{p}}$ (cm^2 GeV^{-2} sr^{-1})
$\sqrt{s}$ (GeV)
30.6
44.8
52.7
4
5
6
7
8
9
10
$p_\perp$ (GeV/c)
262585

FIG. IIIB.5

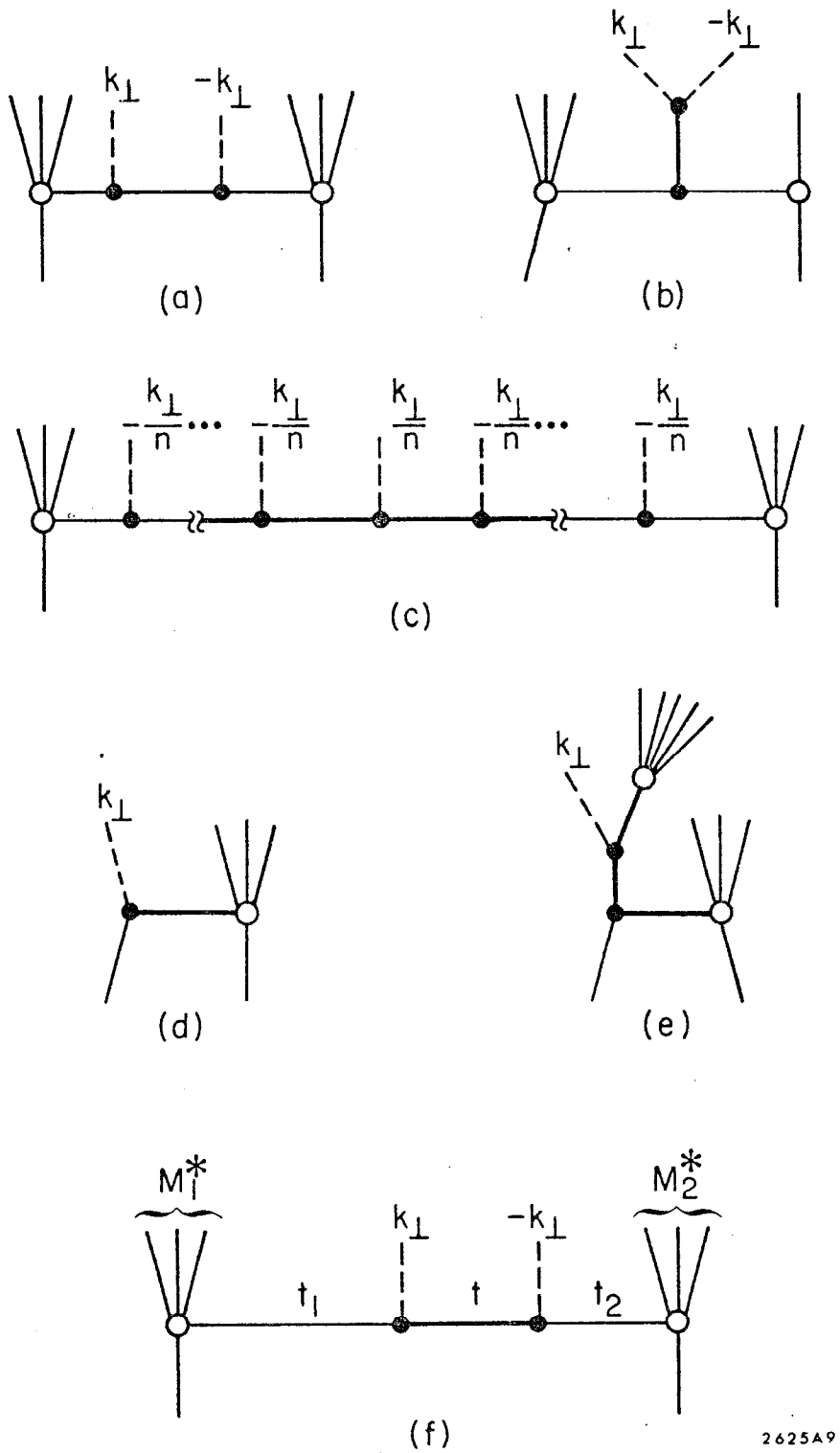

FIG. IIIB.6

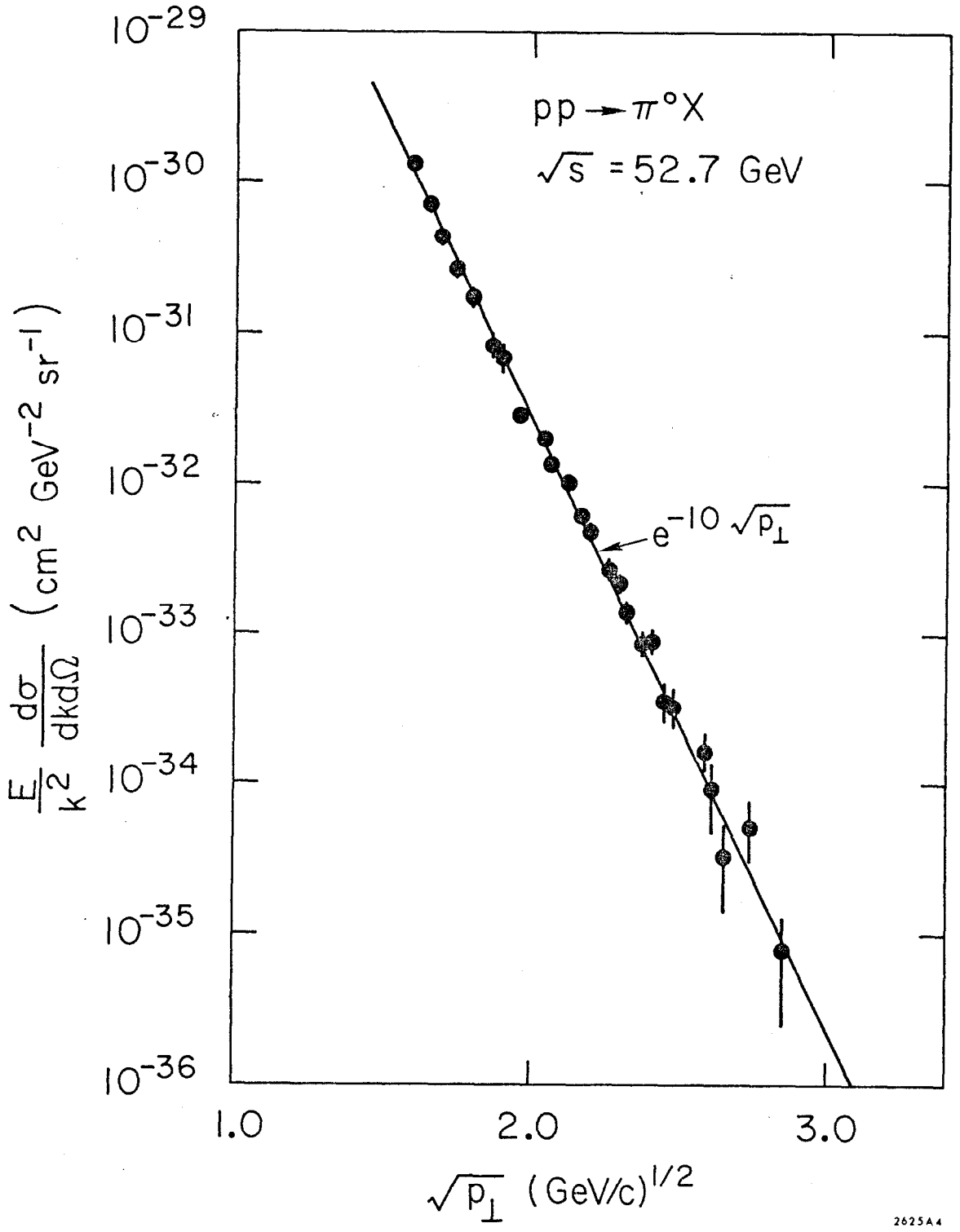
10^{-29}
10^{-30}
10^{-31}
10^{-32}
10^{-33}
10^{-34}
10^{-35}
10^{-36}
$\frac{E}{k^2}\frac{d\sigma}{dk d\Omega}$ $(cm^2\ GeV^{-2}\ sr^{-1})$
$pp \rightarrow \pi^\circ X$
$\sqrt{s} = 52.7$ GeV
$e^{-10\sqrt{p_\perp}}$
1.0
2.0
3.0
$\sqrt{p_\perp}$ $(GeV/c)^{1/2}$
2625A4

FIG. IIIB.7

IV. HARD SCATTERING MODELS

A. Introduction

Hadronic reactions involving the production of particles at large transverse momentum possess the exciting possibility of directly reflecting the underlying structure of hadrons and the interaction of their possible constituents at very short distances. Although the underlying dynamics are certainly more complex than the simple parton model description of deep-inelastic lepton-hadron scattering, an important first question is whether one can adequately describe the behavior of large p_T reactions in terms of a few simple but general constituent scattering mechanisms, and whether the quark model does in fact determine the essential degrees of freedom of hadronic matter at short distances.

In the following, we shall attempt to describe the simplest approaches to this objective in the class of hard scattering models. The rules of dimensional counting will be discussed and then applied to a more definite constituent model of the hadrons to discuss exclusive and inclusive reactions. A similar type of theory using the eikonalization properties of softened vector meson theories will be discussed also, and the possible connection with constituent theories will be elaborated upon.

B. Counting Laws for Large p_T Reactions

As we have emphasized, the inclusive cross section for $A+B \to C+X$ in any hard scattering model is given simply by the sum of cross sections for each contributing subprocess $a+b \to c+d$ at large p_T weighted by the fractional momentum fragmentation probabilities $G_{a/A}$, $G_{b/B}$, and $\tilde{G}_{C/c}$. Since the fragmentation probabilities are scale-invariant, the large p_T scaling behavior of $Ed\sigma/d^3p\,(A+B \to C+X)$ reflects the scaling behavior of the subprocess cross

section $d\sigma/dt'$ $(a+b \rightarrow c+d)$. Depending on the model, the interacting particles a, b, c, d can each be hadrons, quarks, or diquarks. In order to compute the contribution of each type of subprocess we can use the dimensional counting rules which are based on an underlying scale-invariant theory. The counting rules for elastic scattering and form factors were derived independently by Brodsky and Farrar (1973) using renormalizable field theory methods and by Matveev, Muradyan and Tavkhelidze (1973) using the ansatz of scale-invariance or "automodality" of the quark scattering amplitudes. Some applications to the p_T power of inclusive reactions were also discussed by Brodsky and Farrar (1973). A complete discussion of the generalized structure functions and the threshold behavior of inclusive reactions was given by Blankenbecler and Brodsky (1974). Some of these results were obtained by different methods by Gunion (1974a). The rules are as follows: First, one counts the minimum number of "active" elementary fields participating in the large p_T process

$$n_{active} = n_a + n_b + n_c + n_d \qquad \text{(IVB. 1)}$$

and the minimum number of spectators (noninteracting fragments) or "passive" fields in A, B, and C:

$$n_{passive} = n(\bar{a}A) + n(\bar{b}B) + n(\bar{C}c) \qquad \text{(IVB. 2)}$$

Then following the guide of simple Born graphs in renormalizable field theories one can derive the following result for each contributing subprocess:

$$\frac{Ed\sigma}{d^3p}(AB \rightarrow CX)\Big|_{\substack{s,u,t\\ \text{large}}} \propto \frac{1}{\left(p_T^2\right)^N} f(\theta_{CM}, \epsilon) \underset{\epsilon \rightarrow 0}{\sim} \frac{1}{\left(p_T^2\right)^N} f(\theta_{CM})\, \epsilon^F \qquad \text{(IVB. 3)}$$

for $\epsilon = \mathcal{M}^2/s$ fixed, where

$$N = n_{active} - 2 \tag{IVB.4}$$

and

$$F = 2n_{passive} - 1 \quad . \tag{IVB.5}$$

It is physically clear that N should increase as the number of fields forced to change direction increases, and that F (the degree of "forbiddenness") should increase as increasing numbers of spectators take away the available phase space. The reader can readily check that the usual scale-invariant parton predictions for deep inelastic lepton scattering or Compton scattering are included as special cases of the above rules. For $ep \to eX$, $n_{active} = 4$ (for $eq \to eq$) and $n^{hadronic}_{passive} = 2$ giving $\nu W_2(x) \sim (1-x)^3$ for $x \to 1$. For scattering on antiquarks (or strange or charmed quarks) in the proton, $n_{passive} = 4$ and $\nu W_{2(\bar{q})} \sim (1-x)^7$. This last result has been used by Gunion (1974a) and Farrar (1974) as a simple parametrization of the nucleon's antiquark distribution. Notice for $pp \to \mu X$, the Drell-Yan mechanism ($q\bar{q} \to \mu^+\mu^-$) predicts $N=2$, and $F=11$ (for 6 spectators).

More generally, the spectator rule gives for $x \to 1$

$$G_{a/A}(x) \sim (1-x)^{2n-1} \qquad n = n(\bar{a}A) \tag{IVB.6}$$

for the fractional longitudinal momentum distribution of (off-shell) hadron A in hadron B. Some examples are $G_{\bar{q}/\pi} \sim (1-x)$, $G_{\pi/p} \sim (1-x)^5$, $G_{\bar{p}/p} \sim (1-x)^{11}$, etc. One can also use this result to predict decay distributions (see Section VE) and the diffractive dissociation contributions to inclusive reactions $A+B \to C+X$ in the triple Regge region. Writing

$$\frac{E d\sigma}{d^3p} \sim (1-x)^{1-2\alpha_{eff}(0)} \tag{IVB.7}$$

one obtains $\alpha_{eff} = 1 - n(\bar{a}A)$. Generally, there are contributions from two step processes which give

$$\alpha_{eff}(0) = \tilde{\alpha}(0) - n(\bar{C}B) \quad ,$$

where $\tilde{\alpha}(0)$ is the trajectory for the process $a+B \rightarrow C+$anything. For the case of electromagnetic couplings, e.g., leptons or quarks to a photon, there are corresponding equivalent photon or equivalent lepton distributions as discussed by Chen and Zerwas (1974). For these processes the spectator rule (IVB.5) is generalized to (Blankenbecler et al., 1975)

$$F = 2n^{hadronic}_{passive} + n^{e.m.}_{passive} - 1 \qquad \text{(IVB.8)}$$

where $n^{e.m.}_{passive}$ is the number of spectator quarks or leptons coupling to a photon. Note that photons are <u>not</u> counted in the spectator rule, although extra factors of log s arise.

<u>Exclusive Processes</u>

The general result (IVB.3) can also be applied to exclusive two body processes, $n_{passive} = 0$, to yield

$$\frac{d\sigma}{dt}(AB \rightarrow CD) \sim \frac{1}{s^{n_a+n_b+n_c+n_d-2}} f(\theta_{CM}) \qquad \text{(IVB.9)}$$

which, for $eh \rightarrow eh$ gives the result

$$F_h(t) \sim t^{1-n_h} \qquad \text{(IVB.10)}$$

for the asymptotic behavior of spin-averaged form factors. For multiparticle exclusive processes the prediction is

$$\Delta\sigma \sim s^{-1-N_M-2N_B} \qquad \text{(IVB.11)}$$

where $\Delta\sigma$ is the cross section integrated over some fixed region of many body invariant phase space such that all two-particle invariants are large. In (IVB.11)

N_M is the number of meson ($q\bar{q}$) states and N_B the number of baryons (qqq). For example, this result makes predictions for specific exclusive channels in $\bar{p}p$ or e^+e^- annihilation. The region of phase space considered must be chosen to be outside of possible prominent resonance contributions.

The prediction (IVB.9) is compared with pp elastic scattering data in Fig. IVB.1 and with πp and Kp in Fig. IVB.2. The predictions for form factors are discussed in Section IVC. Other comparisons, including photoproduction, are discussed by Brodsky and Farrar (1973, 1975).

The dimensional counting rules are derived assuming that the composite systems have zero internal orbital angular momentum. Brodsky and Farrar (1975) present arguments which indicate higher orbital states can be dealt with by assuming that they contain extra elementary vector fields. It is also possible that there exist suppressions of various contributions from a more careful treatment of quantum numbers than is possible from just counting constituents. For example, the p-Δ electromagnetic transition may be suppressed due to the isotopic spin structure of the wave functions. This possibility is discussed in more detail by Scott (1973) and Gunion (1974a, b, c). Although not conclusive, the predictions using quark counting are sufficiently consistent with experiment that it becomes an important question to understand the theoretical conditions for their validity. This is done in some detail for the form factors in the following section, where it is found that up to finite powers of log t the result (IVB.9) is the canonical expectation for general classes of scale-invariant theories, and can be proved rigorously in certain field theories. The validity of the rules for hard processes in field theories of composite hadrons is also discussed there.

Application to Inclusive Processes

If we apply the dimensional counting rules for inclusive hadronic interactions, then the quark model predicts a sum of terms in Eq. (IVB.3) with $n_{active} = 4, 6, 8 \ldots$ as more and more constituents participate in the large p_T subprocess. The fact that a scale invariant term, p_T^{-4}, is not observed could be due to any number of possible reason:

(a) The gluon coupling strength could be very weak—at least at short distances. Of course, at order α^2, electromagnetic and/or weak contributions to quark-quark scattering are expected, but such contributions should not be important until $p_T > 25$ GeV (Berman, Bjorken and Kogut, 1971).

(b) The p_T^{-4} term could be suppressed via the quasi-exclusive nature of $pp \to \pi X$, but still be present in the measurement of "jet" production $pp \to J + X$, where the jet is defined as a group of hadrons with $p_T^{jet} = \Sigma_i p_T^i$ the total transverse momentum measured on one side (Ellis, 1974a). Accordingly, calorimeter-type measurements will be very interesting. The idea that the cross section is suppressed if a large fraction of the momentum of a scattered parton needs to be transferred to a single hadron is in apparent conflict with the simple Drell-Yan scaling predictions for semi-inclusive deep inelastic scattering processes $ep \to ehX$. However, in the case of asymptotic freedom theories at very large momentum transfers, the predicted deviation from scaling and suppression of the three structure functions $G_{q/A}$, $G_{q/B}$, $\tilde{G}_{C/q}$ (each required with $x \gtrsim 1/2$) could be sufficient to diminish the importance of the $qq \to qq$ term (Cahalan et al., 1974). Measurements of $ep \to \pi X$ and $\mu p \to \pi X$ might help to clarify the situation. The conventional parton prediction has a scale-invariant contribution from $\ell q \to \ell q$ (if the lepton balances the pion momentum) and a contribution $p_T^{-6}\left(\log\left(s/m_e^2\right)\right)$,

from $\gamma q \to \pi q$ (if a hadron balances the pion momentum). If $G_{q/\pi} \sim (1-x)$, then the p_T^{-4} coefficient should have ϵ^5 behavior for small ϵ.

(c) The process $q+q \to q+q$ may be suppressed when the quarks are effectively near their mass shells due to exponentiation of infrared factors; in the Fried and Gaisser (1973) model p_T^{-4} behavior is expected only for very small x_T (see Section II). As pointed out by Polkinghorne (1974), and by Appelquist and Poggio (1974), one could still retain scale-invariance of the $qq \to qq$ interaction in the "light cone" region where all quark legs are off-shell, and thus preserve the dimensional counting rules for exclusive processes.

(d) In the massive quark model of Preparata (1974), scale-invariance only occurs in the case of double-fireball production $\bar{q}q \to F\bar{F}$. This is suppressed by the $\bar{q}$ distribution in the nucleon, $G_{\bar{q}/p} \sim (1-x)^7$, as well as by a possible large mass scale. Similarly $qq \to qq$ may be suppressed relative to $q\bar{q} \to q\bar{q}$ if one uses duality as a guide. The latter gives a contribution of order $p_T^{-4}\ \epsilon^{13}$ for $pp \to \pi X$, since $n_{passive} = 7$. Such a term could well be hidden by the CIM contributions at NAL and ISR energies. Furthermore, the Landshoff (1974b) contributions to exclusive scattering are absent, except for $p\bar{p}$ scattering.

(e) Another possibility, suggested by Gunion (1974), is that the coherent sum of <u>all</u> gluon exchange contributions generates the Pomeron contribution to $qq \to qq$. Single gluon exchange would thus be suppressed at high p_T.

In the constituent interchange model, an explicit quark-quark interaction is never introduced. This idea was originally motivated by the fact that the observed angular dependence $f_{A+B \to C+D}(\theta_{CM})$ for exclusive processes can be rather simply explained in terms of quark-exchange diagrams. Quark-interchange is analogous to rearrangement collisions in atomic and molecular physics. This also seems to be a natural way for hadrons to scatter in the "bag" models. In

any event, the quark-hadron amplitude must exist just by the existence of the hadronic wave function. A review of the applications of the CIM to effective trajectories and θ_{CM} dependence in the interchange model may be found in Section V.

The leading processes for $pp \to \pi X^-$ in the CIM derive from quark-hadron interactions. The minimum ($n_{active} = 6$) terms correspond to $q+M \to q+M$ and $q+q \to B+\bar{q}$ or their crossing variants. An excellent fit to the CCR-ISR data for $pp \to \pi^0 X^-$ (but not the NAL data) can be obtained from Eq. (IVB. with $G_{q/\pi} \sim (1-x)^5$, $G_{q/p} \sim (1-x)^3$ giving $E\,d\sigma/d^3p \sim \left(p_T^2+M^2\right)^{-4} \epsilon^9$ since $n_{passive} = 5$. Similar fits have been given by Ellis (1974) and by Barnett and Silverman (1974). The relative importance of the two $n_{active} = 6$ contributions can be settled by measurements of quantum-number correlations.

However, for the Chicago-Princeton-NAL data, which involves $x_T > 0.4$, a $\sim p_T^{-11}$ scaling law is observed. This data, which is closer to the exclusive limit, indicates that other terms involving a larger number of active particles must be involved as ϵ becomes smaller. This is perhaps not unnatural: in general, as one approaches the exclusive limit, $\epsilon \to 0$, we can expect that more active quarks are required in order to produce a hadron with a sizable share of the available center-of-mass energy. In the CIM, the terms which contribute to $pp \to \pi X$ with $n_{active} = 8$ and minimal $n_{passive}$ (= 3) derive from the sub-processes $q+(qq) \to B^*+\pi$ or $p+q \to B^*+q$ ($\to q+\pi$) and give $p_T^{-12}\,\epsilon^5$. This suggests fits to the data of the form

$$\frac{E d\sigma}{d^3p} = \frac{A}{\left(p_T^2+m_8^2\right)^4}\epsilon^9 + \frac{B}{\left(p_T^2+m_{12}^2\right)^6}\epsilon^5 \qquad \text{(IVB. 12)}$$

The fits are quite good and even are consistent with data at BNL energies. For the ISR data the p_T^{-12} term is negligible; the p_T^{-8} and p_T^{-12} are of comparable

importance in the NAL-range, with the p_T^{-12} term dominant at large p_T due to its slower falloff in ϵ. Further details on these predictions and fits are discussed in Section V. It is interesting to note that p_T^{-12} contribution derives from subprocesses in which a baryonic system balances the large transverse momentum of the detected pion. For any subprocess, however, one expects resonance contributions (i.e., clusters) and a single particle in the recoil system is not likely. The effect of two contributions in $E\, d\sigma/d^3p$ implies that the effective power p_T^{-n} will vary from 8 to 12 as p_T increases across the NAL range, but remains close to 8 for the ISR data. However, at small $p_T < 2$ GeV the effective value of n will drop due to the mass terms and also the nonasymptotic behavior of the effective trajectory $\alpha(t)$. This last effect corresponds to the Reggeization due to the emission and absorption of hadronic bremsstrahlung softens the falloff of the subprocess in t.

Clearly there are a myriad number of contributions from subprocesses in which more and more constituents participate in the large p_T subprocesses. In order to make a simple classification, we can utilize the correspondence principle of Bjorken and Kogut (1973) which assures a smooth connection between the form of the inclusive cross section for $\epsilon = \mathcal{M}^2/s \to 0$ and a corresponding exclusive cross section. This is a generalization of Bloom-Gilman (1970) duality which has been proposed for deep inelastic lepton scattering. Thus if a contribution to the inclusive cross section for $A+B \to C+X$ at fixed θ_{CM} is to join smoothly for $\epsilon \to 0$ to an exclusive cross section for $A+B \to C+B$, we have

$$\int^{\overline{M}^2} d\mathcal{M}^2 \frac{d\sigma}{dt\, d\mathcal{M}^2}(A+B \to C+X) = \int^{\overline{M}^2} d\mathcal{M}^2 \frac{\pi}{s} \frac{1}{\left(p_T^2\right)^N} \epsilon^F f^{incl}(\theta_{CM})$$

$$= \frac{1}{{}_s p_{excl}} f_{A+B \to C+D}(\theta_{CM}) \qquad \text{(IVB. 13)}$$

We thus have

$$N+F+1 = N+2n_{passive}$$

$$= p_{excl} = n_A + n_B + n_C + n_D - 2 \qquad \text{(IVB. 14)}$$

and the identification

$$f^{incl}(\theta_{CM}) = f_{A+B \to C+D}(\theta_{CM}) \sin^2\left(\theta_{CM}\right)^N \qquad \text{(IVB. 15)}$$

Thus, generally speaking, for large p_T and small ϵ, one would expect contributions from those allowed subprocesses $(a+b \to c+d)$ which correspond to the minimum number of hadrons in the related exclusive channel to dominate. Note further that all of the contributions which yield the same p_{excl}, i.e., are dual to the same exclusive channel, may be summed in the form

$$\frac{d}{d^3p/E} \sim \frac{1}{p_T^{2\,N}} \epsilon^F \left[1 + 0\left(\frac{M^2}{p_T^2\,\epsilon}\right)^2 + \ldots + 0\left(\frac{M^2}{p_T^2\,\epsilon}\right)^{F+1}\right] f^{incl}(\theta_{CM}) \qquad \text{(IVB. 16)}$$

where the first term dominates for $p_T^2\,\epsilon >> M^2$, and where the subsequent terms correspond to allowing additional passive spectator quarks to become active participants in the large momentum transfer reaction. The last term gives the exclusive channel contribution. Note that the corrections to the leading term are of the same form as that obtained by expanding $\left(p_T^2\right)^N \epsilon^{-1} (\epsilon')^{F+1}$ where $\epsilon'^2 = \epsilon^2 + 0\left(M^4/p_T^4\right)$. This is analogous to the corrections to scaling introduced by the Bloom-Gilman variable $\omega = -(p\cdot q + M^2)/q^2$ in the analysis of deep inelastic scattering. Note that the ω' correction terms for $ep \to eX$ automatically includes the nonscaling contribution from the subprocess $e(qq) \to e(qq)$.

Thus the leading contributions in the CIM can be classified according to their dual exclusive channel (which determines N+F) and the distribution of active and passive quarks. To obtain the CIM candidates we only need to exclude

the basic subprocesses $qq \to qq$ and $q(qq) \to q(qq)$. A list of various contribution subprocesses for the inclusive processes involving meson and baryons, using meson and baryon or electromagnetic beams is discussed by Blankenbecler and Brodsky (1974) and Gunion (1974).

The scaling laws (IVB. 3) naturally take into account the underlying scale invariance at the constituent level, and correlate dynamical measurements with the degrees of freedom of the hadron in the simplest possible way. The rules also lead to simple asymptotic predictions for Regge trajectories and residue functions. These are reviewed in Section V. We also emphasize the importance of crossing behavior in models of large p_T reactions. The CIM combined with the rules (IVB. 3) give the simplest possible realization of a theory with correct crossing behavior, the exclusive-inclusive correction, and a natural continuity with the Regge region for exclusive and inclusive reactions. These results are developed and reviewed in Section VD.

LIST OF FIGURES FOR SECTION IVB

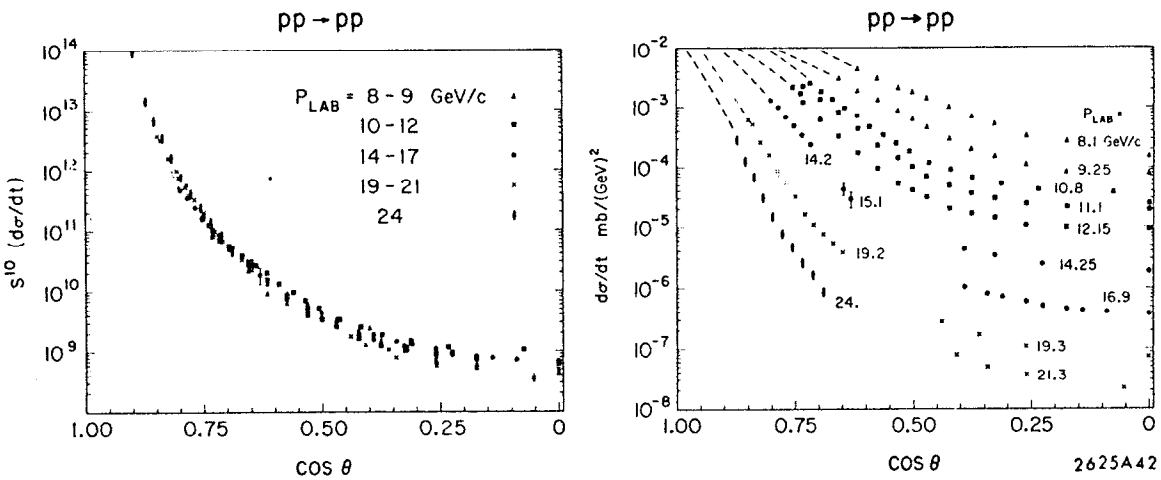
pp → pp
P_{LAB} = 8 - 9 GeV/c
10 - 12
14 - 17
19 - 21
24
s^{10} (dσ/dt)
cos θ
pp → pp
P_{LAB} =
8.1 GeV/c
9.25
10.8
11.1
12.15
14.25
16.9
19.3
21.3
14.2
15.1
19.2
24.
dσ/dt mb/(GeV)²
cos θ
2625A42

FIG. IVB.1

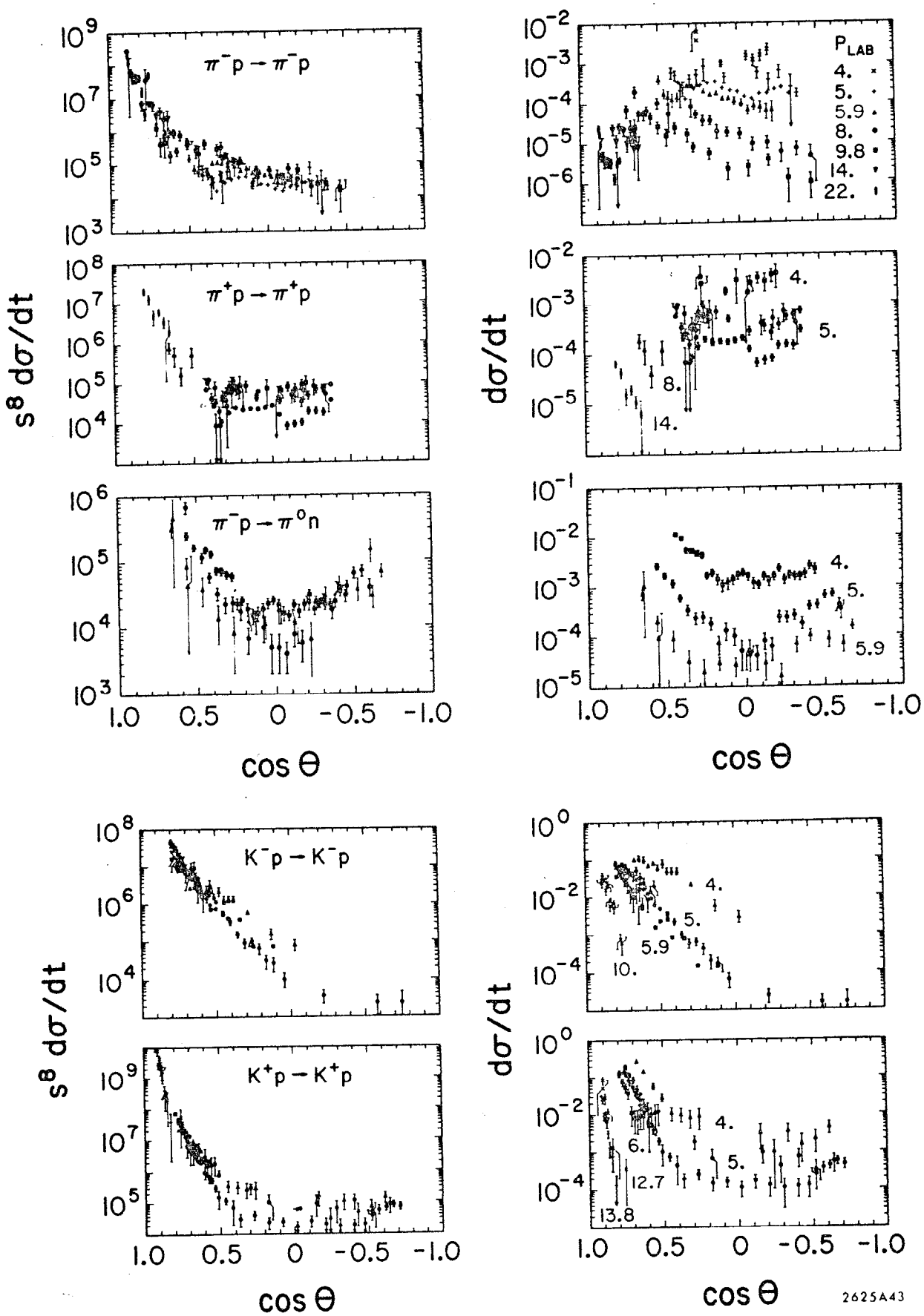
$\pi^- p \to \pi^- p$
$\pi^+ p \to \pi^+ p$
$\pi^- p \to \pi^0 n$
$K^- p \to K^- p$
$K^+ p \to K^+ p$
$s^8\, d\sigma/dt$
$d\sigma/dt$
P_{LAB}
4.
5.
5.9
8.
9.8
14.
22.
10.
6.
12.7
13.8
cos Θ
2625A43

FIG. IVB.2

C. Theories of the Elastic Form Factor

The asymptotic dependence of the elastic form factors of hadrons plays a critical role in theories of large-angle scattering. Physically, the elastic form factor is the probability amplitude for a hadron to remain a single hadron after the transfer of momentum. Thus, in the model of Wu and Yang (1965) (large t gluon exchange) or the CIM (large t quark interchange), the falloff of the exclusive scattering amplitude at large momentum transfer is controlled by the same physics that controls the falloff of the form factors. Many models, in fact, satisfy a relation conjectured by Theis (1972) for the spin-averaged amplitude

$$\mathcal{M}_{AB \to CD}(s,t) \sim s^{-1/2\,(p_A+p_B+p_C+p_D)}\, f(t/s) \qquad \text{(IVC. 1)}$$

for $s \to \infty$, fixed t/s, where $F_A(t) \sim t^{p_A}$, etc. for the spin-averaged form factor. This result has been recently proven by Creutz and Wang (1974) in elementary pseudoscalar field theory, and also holds in the CIM with dimensional counting (neglecting logarithmic modifications), the automodality model, and the eikonal model of Fried et al. (1971, 1972, 1973a,b).

It is well known that the proton form factors are quite adequately described by the dipole form $G_M(t) = \mu\left(1 - t/0.71\ \mathrm{GeV}^2\right)^{-2}$ and the scaling law $G_M(t) = \mu G_E(t)$. A graph of $t^2\, G_M^{exp}(t)$ (Fig. IVC. 1) shows that the asymptotic dependence of t^{-2} is consistent with the data. The pion form factor is less well known experimentally, but both spacelike (from $ep \to e\pi p$) and timelike data (from $e^+e^- \to \pi^+\pi^-$) are consistent with a falloff $F_\pi(t) \sim t^{-1}$ or slightly faster. A plot of $F_\pi(t)$ is shown in Fig. IVC. 2. A very important result, obtained by Bonneau et al. (1974) using a rigorous analysis of the data, shows that if the asymptotic falloff of $F_\pi(t) \sim t^{-n}$ on the average for $|t| > 2\ \mathrm{GeV}^2$, then $n < 1.2 \pm 0.3$. Thus the pion form factor cannot fall faster asymptotically on the average than $t^{-3/2}$. On the

other hand if asymptotia begins at much larger $|t|$, say $|t| > 9$ GeV^2, then the bound is much less restrictive (Pham and Wright, 1974).

The central theoretical question is thus the origin of the asymptotic behavior of the form factors. It is clear that one cannot give an a priori answer to this question without exact knowledge of the short distance structure of the hadrons. In the following we shall outline some of the main theoretical approaches to this question. An extensive Physics Report review has recently been given by Gourdin (1974). (For other reviews, see also Appelquist and Primack (1970) and Brodsky and Farrar (1974).)

There are three basic views of the short-distance structure of the hadrons which can be distinguished. (1) The constituent models—based typically on internal quark degrees of freedom; (2) models based on elementary field theories; and (3) infinitely composite systems—the hadronic bootstrap. In the following we will discuss in some detail the composite models and the connection to large transverse momentum phenomena.

Constituent Models and Dimensional Counting

The quark-constituent approach has the important virtue of connecting naturally with SU(3) or SU(6) spectroscopy, current algebra, and the quark-parton phenomenology of deep inelastic lepton scattering processes. We can make the following assumptions:

(a) The prominent mesons and baryons are $\ell=0$ Bethe-Salpeter bound states of two and three quark fields respectively. Thus in the limit of zero binding, the hadrons would become free quark states:

$$|B\rangle \rightarrow |qqq\rangle$$

$$|M\rangle \rightarrow |q\bar{q}\rangle$$

The higher particle number components can be shown to produce nonleading terms to the scaling law at large momentum transfer. Also, as we discuss below, we assume a simple physical limit on the high energy momentum components in the wave function which ensures the finiteness of the wave function in coordinate space.

(b) The interaction of the hadron constituents are asymptotically scale invariant, as implied by Bjorken scaling.

With these assumptions we can derive the dimensional counting and automodality prediction (modulo powers of log t)

$$F_H(t) \sim t^{1-n_H}, \qquad t \to \pm\infty \tag{IVC.2}$$

for the asymptotic dependence of the spin-averaged form factor of a hadron H containing n_H elementary fields. This constituent-counting rule thus predicts $F_{1p}(t) \sim t^{-2}$ and $F_\pi \sim -t^{-1}$ consistent with the data, and naturally accounts for the faster falloff of the baryon wavefunction relative to that of the mesons. Physically, the rule allows a factor of t^{-1} for each additional quark line which changes direction from along p to along p+q. The scale invariant assumption (b) requires the quark form factor itself to be pointlike—consistent with Bjorken scaling, and leads to dominance of spin nonflip amplitudes, i.e.: the dominance of the Dirac form factor $F_{2p}/F_{1p} \to 0$, and $G_E(t) \sim G_M(t)$.

A simple illustration of how the dimensional counting rule arises in the Bethe-Salpeter computation of the meson form factor is illustrated in Fig. IVC.3. If we assume a falloff of the Bethe-Salpeter wavefunction at large relative momentum, corresponding to a wavefunction which is finite at the origin in coordinate space, then the leading contribution to the asymptotic form comes from iterating the Bethe-Salpeter kernel wherever large relative momentum is

is required, as indicated in the diagram. Thus one obtains for large q^2

$$(2p+q)^\mu F_M(q^2) \sim \int \frac{id^4k}{(2\pi)^4} \int \frac{id^4\ell}{(2\pi)^4} \psi^\dagger_{p+q}(\ell)\, \mathcal{M}^\mu\, \psi_p(k) \qquad \text{(IVC. 3)}$$

where $\mathcal{M}^\mu$ is the connected amplitude for the photon coupling to the quark and antiquark with momenta k^μ and $(p-k)^\mu$ to ℓ^μ and $(p+q-\ell)^\mu$. The integrations are limited to the dominant region of each wavefunction: $k = xp + \kappa$, $\ell = y(p+q) + \kappa'$, with $\kappa \cdot p = \kappa' \cdot (p+q) = 0$, and $\kappa'^2 \sim \kappa^2 \sim O(m^2)$. Thus $\mathcal{M}^\mu$ represents the scattering of photon on the quark constituents, each of which has a finite fraction of the hadron momenta: $p_i \sim x_i p$, $\Sigma x_i = 1$. It is exactly the connected amplitude which occurs when hadronic binding is turned off adiabatically, in which case $x_i \to m_i/M_H$. In the case of spin, $\mathcal{M}^\mu$ is defined to include the on-shell spinor factors.

A simple computation then gives $F_M(t) \sim t^{-1} \log t$ (where the logarithm arises from the $x \sim 1$ integration) since we have assumed a scale invariant kernel. The inverse factor of t^{-1} comes from the off-shell quark propagation. For an n-body state, n-1 quark lines are off-shell, giving the result (IVC. 2). Notice that the minimum field description gives the leading asymptotic behavior.

We can also see how these results follow from simple dimensional analysis. After iteration of the interaction kernel, we are dealing with the scattering of a lepton on n_H near-mass-shell quarks each sharing a finite fraction of the momentum of the initial and final hadron. This amplitude which has $n = 2n_H + 2$ external legs and dimensions $[\text{length}]^{n-4}$, then must scale as $[\sqrt{t}]^{4-n}$ at fixed angle (t/s fixed, $|t| \to \infty$) if the internal interactions are scale-free and the coupling constants are dimensionless. This then gives the scaling (IVC. 2) for form factor.

The finiteness of the Bethe-Salpeter wavefunction is crucial for the above derivation. The coefficient of the asymptotic power dependence and mass scale of the meson form factor is set by the value of

$$\psi_p(x_\mu=0) = \int \frac{d^4k}{(2\pi)^4}\, \psi_p(k) \qquad \text{(IVC. 4)}$$

which we require to be finite. This requires, at minimum, that $\psi_p(k)$ converges in the ultraviolet faster than $k^{-4} \log^{-1-\epsilon} k^2$, with $\epsilon > 0$.

There are a number of arguments which imply that $\psi_p(x)$ is in fact regular at $x_\mu \sim 0$. A quite general proof by Ezawa and Nishijima (1974) shows that the existence of a composite field operator for a meson and the assumption that it lies on a Regge trajectory requires $\psi_p(0) < \infty$. Similarly, computations of weak and electromagnetic decays in current algebra are based on the finiteness of the wavefunction at the origin. These arguments, however, do not give an insight into how this result can arise dynamically.

Important progress has been made on the dynamical requirements of the wavefunction condition by Appelquist and Poggio (1974). They show that for the case of asymptotic freedom theories without infrared complications, the asymptotic ultraviolet behavior of the full Bethe-Salpeter kernel (including the self energy insertions on the incoming legs) is exactly one logarithm more convergent at large relative momentum than indicated by ladder approximation (scale invariance). They can then show that the Bethe-Salpeter wavefunction is finite at the origin up to a calculable logarithm, $[\log(x)]^d$, where d depends on the coupling constant. Assuming that the wavefunction has no anomalous behavior when one quark leg goes on the mass shell (we discuss this further, below), then one can show that $F_M \sim t^{-1}$ (modulo calculable logarithms).

We should emphasize here that the use of ladder approximation instead of the full Bethe-Salpeter kernel is misleading for the determination of asymptotic behavior in renormalizable theories, although this has been the historical approach. In this case the wavefunction has a power-law singularity which depends on the coupling constant, which in turn must be restricted ad hoc by hermiticity and normalization requirements. However, such behavior is unstable upon the addition of any additional contribution from the full kernel, e.g., a crossed-ladder graph, and cannot be obtained as the smooth limit of a regulated theory (e.g., dimensional regulation or the use of a Pauli-Villars spectrum). Furthermore, the ladder approach is inconsistent because some operators like the electromagnetic current and energy-momentum tensor do not have the correct (canonical) dimensions. The ladder equation difficulties are analogous to the mathematically-singular behavior of the Dirac wavefunction for the Coulomb potential for $r \to 0$. The physical wavefunction is in fact regular at the origin if the finite mass or size of the source or radiative corrections are taken into account.

In the case of quantum electrodynamics, the full Bethe-Salpeter kernel including radiative corrections undoubtedly falls faster than the simple ladder approximation, again arguing for a finite wavefunction at the origin. The true asymptotic dependence of the QED kernel to all orders in perturbation theory is not rigorously known, but neglecting higher order binding corrections, the form factor of positronium is known to obey the dimensional counting rule—modulo powers of log (t).

Composite Systems and Renormalizable Theories

An important approach to the study of the asymptotic properties of composite systems is the investigation of those renormalizable field theories (such as

asymptotic freedom theories) which insure conformal or scale invariance at short distances. A straightforward calculational technique is to assume that the full Bethe-Salpeter kernel has the effective scaling $(q^2)^{-\epsilon}$. The scale-invariant limit $\epsilon \to 0^+$, corresponding to a renormalizable theory, is taken at the end of the calculations. The results given by Ezawa (1974), Brodsky and Farrar (1974)(using the iteration method), and Alabiso and Schierholz (1974) (which include an analysis of the three particle wavefunction) are consistent (modulo finite powers of log t) with dimensional counting.

A very interesting ansatz for the quark-quark interaction has been recently proposed by Ezawa and Polkinghorne (1974). They assume that the effective Bethe-Salpeter kernel for $k_1 + k_2 \to k_3 + k_4$ is of the form $\gamma_\mu K \gamma^\mu$ where

$$K = \frac{1}{q^2} \prod_{i=1}^{4} \left[\frac{k_i^2}{k_i^2 + q^2} \right]^n , \qquad n>0 \quad . \tag{IVC.5}$$

This form is "asymptotically scale free," i.e.: is only scale-invariant when q^2 and all the external masses k_i^2 are large together. This form has the following advantages:

(a) The Bethe-Salpeter wavefunction and form factors rigorously satisfy the dimensional counting conditions without cumulative logarithmic effects for any $n > 0$.

(b) The Landshoff "pinch" contribution (see below) is suppressed below the interchange and single gluon exchange contributions if $n > 1/16$. The fixed angle dimensional counting scaling law then (IVB.9) holds rigorously.

(c) The p_T^{-4} scale-invariant contributions to inclusive large p_T hadron reactions become suppressed below p_T^{-8} for $n > 1/4$.

(d) Bjorken scaling is obtained for electroproduction with large multiplicities in the photon fragmentation region.

(e) The form (IVC.5), which suppresses the role of on-shell quarks may be relevant to the question of quark confinement. The ultimate origin of this effective interaction remains unknown.

Recently there has been considerable progress employing the more formal tools of the operator product expansion, the renormalization group, and dimensional regularization to analyze the asymptotic properties of composite systems. It has been shown by Shei (1974), Borenstein (1975), and Tiktopolos (1974) that for various renormalizable theories, excluding vector gluon and gauge theories, the asymptotic behavior of the on-mass-shell form factors is rigorously related to the short-distance behavior of the theories. In particular, if the Gell-Mann-Low eigenvalue conditions are satisfied (ultraviolet-stable fixed points) then the asymptotic behavior of the form factor has power behavior $(-q^2)^{-\eta}$ where η can be related to the anomalous dimensions of the particle's field. A phenomenology of form factors can thus be based on these anomalous dimensions.

The intriguing question is then whether the anomalous dimension of an interpolating field for a hadron can be related to its degree of compositeness. Let us restrict ourselves to the conformal invariant or asymptotically free theories where the product of elementary fields at short distances has the canonical scaling of free fields. In particular, this guarantees Bjorken scaling in deep inelastic scattering. The asymptotic freedom theories automatically yield Bjorken scaling modulo logarithmic corrections since the interactions become weaker at short distances. Thus the short distance behavior of the Bethe-Salpeter wavefunction

$$\Psi_P(x) = \langle 0 | T\left(\psi\left(\frac{x}{2}\right)\psi\left(-\frac{x}{2}\right)\right) | P \rangle \qquad \text{(IVC.6)}$$

is controlled at $x^2 \to 0$ by the canonical dimensions of the quark fields. This in turn determines the scaling of the momentum space wavefunction $\Psi_P\left(k_1^2, k_2^2\right)$ in the "light-cone" limit $k_1^2 \to \infty$, $k_2^2 \to \infty$, where the mass of both logs become asymptotic.

However, the dominant contribution to the asymptotic behavior of the form factor involves contributions where one constituent leg is close to the mass shell. Thus we instead require the <u>form factor</u> limit of $\Psi_P\left(k_1^2, k_2^2\right)$ which is $k_1^2 \to \infty$, with k_2^2 <u>fixed</u>. In the case of renormalizable scalar-constituent field theories, such as ϕ^3 in six dimensions, and ϕ^4 in four dimensions, Menotti (1974b) has, in fact, shown that the only asymptotic scaling behavior of the complete wavefunction which gives consistent results for both Fig. IVC.4a and the convolution of the wavefunction shown in Fig. IVC.4b is that of uniform scaling behavior in both the light-cone and form-factor limits. Thus, in these scalar field theories the asymptotic momentum space Bethe-Salpeter wavefunction in both limits and the form factor of the composite system are controlled by the short-distance scaling behavior of the product of free fields. In the absence of anomalous dimensions of the constituent fields one thus obtains the dimensional counting prediction (IVC.2), modulo the usual finite power of a logarithm; this is consistent with the Appelquist-Poggio result.

The formal analysis of the composite particle form factor in spinor field theories is considerably more involved, and thus far theories with vector interactions are not completely understood because of possible infrared complications. The most complete analyses have been done by Ciafaloni and Ferrara (1974) and by Callan and Gross (1974). It should be emphasized that in the case of the spinor theories, the light-cone limit and form-factor limits of the Bethe-Salpeter wavefunction <u>do not</u> give the same scaling results. See P. Menotti (1974a, 1974b,

1975). The light-cone limit $\Psi_P\left(k_1^2, k_2^2\right)$, $k_1^2 \to \infty$, with k_2^2/k_1^2 finite will reflect the dimension of the constituent spinor field (and thus will fall one power faster in k_1^2 relative to the spinless case because the dimension of a spin 1/2 field is $[\text{length}]^{-3/2}$ while the dimension of a spin 0 field is $[\text{length}]^{-1}$). However, as shown explicitly by Ciafaloni and Ferrara, in a spinor theory with scalar interactions, the form factor limit is controlled by the large $x \cdot p$ behavior of the coordinate wavefunction. This is the same asymptotic behavior as in a renormalizable theory with spinless constituents and again the dimensional counting result (IVC.2) is recovered for the meson form factor, independent of the constituent spin. The results are, thus, as expected. The analysis of Ciafaloni and Ferrara (1974) is based on explicit solutions to the Dyson-type bootstrap equation for the propagator of the fundamental quark fields, which is however, obtained by replacing the full Bethe-Salpeter kernel with an effective focal potential with an equivalent scaling behavior. Their solution requires the coupling constant and anomalous dimensions to vanish as a dimensional regulator goes to zero. The composite particles in this theory are effectively weakly-bound, with scale-invariant constituent interactions and thus conform to the dimensional counting analysis.

In the recent work of Callan and Gross (1974), which applies renormalization group techniques to the analysis of the Bethe-Salpeter wavefunction, the difference between the light-cone and form-factor limits of $\Psi\left(k_1^2, k_2^2\right)$ can be traced to the presence of a zero-mass singularity which arises when one fermion leg goes on-shell. These authors also show that the leading contribution to the form factor for a meson with spin 1/2 constituents derives from the disconnected contribution to the vertex function rather than the connected contribution shown in Fig. IVC.5 which arises from insertions into the cross graph kernel, etc.

This agrees again with the dimensional counting analysis which relates the latter contributions to the higher field components in the wavefunction.

The derivation of dimensional counting which utilizes the iteration of the kernel in Eq. (IVC. 3) and the wavefunction condition (IVC. 4) makes it clear that the spin of the constituents is irrelevant if the kernel is scale-invariant, since the connected amplitude M^{μ} always has the same dimensional scaling. The condition (IVC. 4) in the spin case actually refers to the coefficient of on-shell spinors, $\psi^{+-}(x)$ as defined in the Salpeter formalism. The wavefunction $\psi^{+-}(x)$ has similar short distance properties and scaling as the scalar Bethe-Salpeter wavefunction. (See Brodsky and Farrar (1975).)

Thus we see that despite the diversity of the above methods, the physics is identical: the scaling of the amplitudes in these theories is equivalent to that obtained in the weak binding approximation. The scattering effectively occurs on nearly free constituent particles which share a finite fraction of the hadronic momenta.

Infrared Effects

As we have seen a natural realization of the dimensional counting rules for the form factors of composite systems may be the asymptotic freedom theories. However, because of the yet unknown and perhaps critical effects of infrared behavior, a rigorous application of the asymptotic freedom gauge theories with vector gluon or gauge interactions has yet to be given. The simplest application of the renormalization group method to on-shell amplitudes fails due to the potential mass-zero singularities of such theories. The most familiar example of such phenomena is the fermion form factor in massive QED; summing leading logarithms from the infrared region in each order of perturbation theory, one

obtains (Appelquist and Primack, 1970; Sudakov, 1956; Jackiw, 1968, 1969)

$$F(q^2) \sim \exp\left[-\frac{\alpha}{2\pi^2}\log^2(-q^2/\mu^2)\right] \qquad \text{(IV.C. 7)}$$

where μ^2 depends on the photon mass and external leg masses. One can use this form to successfully parametrize the hadron form factors. However, in such a model there is then no connection with short distance behavior or evident reason for Bjorken scaling. Note that it is incorrect to use (IVC. 7) which is derived from on-shell quarks as the constituent quark form factor, which is to be interpolated with a composite hadron "body" form factor, since the quark legs can be effectively far-off shell inside the hadron. Thus, there is considerable uncertainty on the effects of the infrared region on the form factors. However, there is an optimistic point of view. As discussed by Brodsky and Farrar (1975) and by Appelquist and Poggio (1974) (see also Tiktopolos (1974)), the fact that a hadron may be taken to be neutral with respect to the charges of the gauge group leads to an explicit cancellation of the infrared divergences in perturbation theory. Further as we have noted, the quark legs are off-the-mass shell and thus regulate the theory in the infrared so that wavelengths larger than the size of the system are not effective. Additionally, if we take the gluons as color octets and hadrons as color singlets, then gluon emission changes quantum numbers and is not soft; there is thus no reason why an eikonal-like exponentiation or serious modification of the hadronic scaling laws should occur in such models.

Quark Confinement, Large Transverse Momentum and Form Factors

An implicit assumption in the use of the quark-parton model is that the interactions at short distances are unaffected by quark confinement. The usual view is that the confinement of quarks is basically a large distance phenomenon

which operates over distance scales of order 1 fm. This assumption can be partially justified by the success of the quark-parton model in electroproduction, but since it plays such a central role in most treatments of large-transverse momentum processes, it is important to achieve more theoretical understanding.

There have been many theoretical approaches. For example, Bjorken (1973b) and Coon (1974) have shown in the context of simple potential models that closely spaced bound state levels can mimic a continuum of free states in deep inelastic scattering. The currently popular "bag" models (Chodos et al., 1974a, b; Bardeen et al., 1974) represent dynamical attempts to build in the intuitive notion that quarks can essentially be treated as free particles in their short-distance behavior while being confined within hadronic matter. Jaffe (1974) has argued that Bjorken scaling can be obtained in a simplified version of the MIT bag model.

In a theory with quark confinement, the momentum space quark propagator has no physical particle pole as is evident from the fact that in configuration space the propagator has only finite support. Simple quark-parton diagrams are therefore strictly defined only in terms of the propagation within the space-time envelope of the hadron and the usual Feynman rules only apply for quark lines which are far off mass shell. The massive quark model (MQM) proposed and developed by Preparata (Preparata, 1974) heroically attempts to take into account the complicated consequences of this fact. For deep inelastic lepton scattering, the usual "handbag" diagram is replaced in this model by allowing for a J=1 final-state-confining interaction of the quarks. The effective quark propagator has no pole but is peaked at small masses and falls off exponentially along the p^2 real axis. Despite many complexities, the model can be shown to give parton-like behavior.

For large-angle hadron hadron scattering in the MQM the actual systems that are interchanged always have hadronic quantum numbers. In spite of the fact that the diagrams contain an extra internal loop the amplitudes calculated in this model have the same power law scaling behavior as in the CIM discussed previously, and the cross sections agree with dimensional counting.

For inclusive reactions, the predictions of the MQM are again not too dissimilar from those of the CIM. A fit to the reaction $pp \rightarrow \pi +$ anything in the kinematic regimes of the CCR and CP collaboration (Preparata 1974) argues for the presence of at least two terms. In the MQM, one of these falls as p_T^{-8} and the other as p_T^{-10}. At small x_T and very high energies where $\bar{q}q \rightarrow 2$ fireball cane be important ($s > 10^4$ GeV^2) the model also predicts a scale-invariant p_T^{-4} contribution. More details of the phenomenology of the MQM should be sought in the review of Preparata (1974).

The consequences of quark confinement are not fully understood, to say nothing of the mechanism. The intuitive feeling that large transverse momentum phenomena should be insensitive to quark confinement has not been fully confirmed, especially in gauge theories with infrared singularities. The fact that the MQM has many features in common with simple quark parton models and the CIM in spite of vastly different mathematical formalism remains large mysterious.

Throughout the discussion we have assumed that the quark confinement mechanism does not affect the short distance properties of the Bethe-Salpeter wavefunction nor the asymptotic form factor.

In the MIT "Bag" model (A. Chodos et al.,1974a) one can expect that the form factor is controlled asymptotically by a mechanism similar to that of the momentum partition model. After one quark receives the momentum transfer

q, a single vector gluon exchange (possibly with a rather weak coupling constant) is required to restore the motion of both quarks along the final direction p+q. Thus the dimensional counting result would be obtained. Intuitively, it is expected that the bag boundary itself would not be effective to cause the momentum transfer between between quarks. On the other hand, Schiff (1970) has considered a model for a meson in which the quark and antiquark in the rest system satisfy the free Dirac equation inside a spacial boundary. Initial and final states are then obtained by appropriate Lorentz boosts, and it is found, surprisingly, that the form factor falls as $(q^2)^{-1}$ for large momentum transfer.

In the massive quark model of Preparata, which explicitly deals with the quark confinement problem, the meson form factor is assumed to fall asymptotically as $(-q^2)^{-3/2}$, which is, as we have seen is consistent with the data. However, this result is derived by using the Drell-Yan-West relation, and assuming (from a crossing requirement and data) that $F_{2\pi}(x) \sim (1-x)^2$ for $x \sim 1$. However, as emphasized by Ezawa (1974), the DYW relation should be modified in the case of spin 1/2 constituent Bethe-Salpeter models, and thus there is no compelling theoretical reason for a $(q^2)^{-3/2}$ law.

In the model of Bohm and Krammer (1974), quarks are always taken to have very large free mass; thus $|q^2| \ll 4M^2$. The quark-quark interaction is taken to be a four-dimensional hadronic oscillator with a $\gamma_5 \otimes \gamma_5$ Dirac structure. The assumption that the form factor can be built up by resonances leads to an excellent phenomenological fit to the pion form factor and the asymptotic falloff $F \quad (q^2) \sim -0.33\ \mathrm{GeV}^2/q^2$.

Dimensional Counting and Large-Transverse Momentum Exclusive Processes

Most of the discussion given in this section for form factors of composite systems in renormalizable theories also holds for exclusive processes in the fixed θ_{CM} limit. In general, the amplitude for the scattering of composite particles has the form

$$\mathcal{M}_{AB \to CD} = \int \psi^A_{BS}\, \psi^B_{BS}\, \mathcal{M}_n \psi^C_{BS}\, \psi^D_{BS}\, \pi d^4k \qquad \text{(IVC.8)}$$

where $\mathcal{M}_n$ is the connected amplitude for the scattering of the n elementary active constituents. If the Bethe-Salpeter wavefunctions are finite, the scaling of $\mathcal{M}_n$ at large momentum transfer controls the scaling behavior of $\mathcal{M}_{AB \to CD}$. With the usual state normalization $\langle p' | p \rangle = 2E\, \delta^3(\vec{p} - \vec{p}')$ the amplitude $\mathcal{M}_n$ has dimension $[\text{length}]^{n-4}$. If there is no external scale and no infrared problem, then we can write at fixed angle

$$\mathcal{M}_n \sim (\sqrt{s})^{n-4} \qquad \text{(IVC.9)}$$

The dimensional counting/automodality results (IVB.9-IVB.11) thus follow. Some comparisons with experiment are presented in Section IVB.

The crucial question for the validity of the counting rules is the possible origin of infrared effects or an external scale in $\mathcal{M}_n$. The possible corrections to (IVC.9) from anomalous dimensions of the quark fields or the accumulation of logarithmic factors are not known, except that they should be small in some sense if the contributions to Bjorken scaling in deep inelastic lepton scattering are small.

The general validity of the counting rules for hadronic scattering is, however, complicated by the possible contribution of multiple-scattering Glauber-like diagrams. The importance of these diagrams, which in fact contain linear

infrared divergences, was discussed by Landshoff (1974b). For example in $pp \to pp$, each quark of one proton can scatter elastically and near the mass shell on a quark of the other hadron through the same angle θ_{CM} with a finite fraction of the proton's momentum.

If the underlying quark-quark interaction for near on shell quarks is scale-invariant, then the amplitude is only suppressed by a phase-space factor,

$$A_{LAND} \sim (i\, s^{-3/2})^{L-1} \qquad \text{(IVC. 10)}$$

where L is the number of q-q scatterings. For pp scattering L=3 and the contribution of this diagram to the differential cross section

$$\left.\frac{d\sigma}{dt}\right|_{LAND} \sim \frac{1}{s^8} f(\theta_{CM}) \qquad \text{(IVC. 11)}$$

which would be expected to dominate the dimensional counting, s^{-10}, contribution. Empirically, this falloff is too slow. Explicit calculation of the Landshoff diagrams has been given by Cvitanovic (1974) using Feynman parameters and by Brodsky and Farrar (1975) using infinite momentum techniques. Appelquist, Coleman, and Quinn (1974) have shown that, in a renormalizable field theory, the Landshoff diagrams are the only ones with linear infrared divergences.

There have been numerous speculations about the possible suppression of the Landshoff diagrams. Clearly, any mechanism which eliminates scale-invariant quark-quark scattering between quarks of different hadron as empirically required by the absence of a scale-invariant term in the large p_T inclusive data, will also eliminate these multiple-scattering contributions. Polkinghorne (1974) and Appelquist and Poggio (1974) have proposed an on-shell infrared suppression factor and Ezawa and Polkinghorne (1974) have demonstrated a simple

model in which the dimensional counting rules are rigorously correct. This is discussed in detail in Section IVC. As a final empirical note, Farrar and Wu (1975) have shown that the Landshoff diagram cannot account for the angular distribution in present pp elastic scattering data.

LIST OF FIGURES FOR SECTION IVC

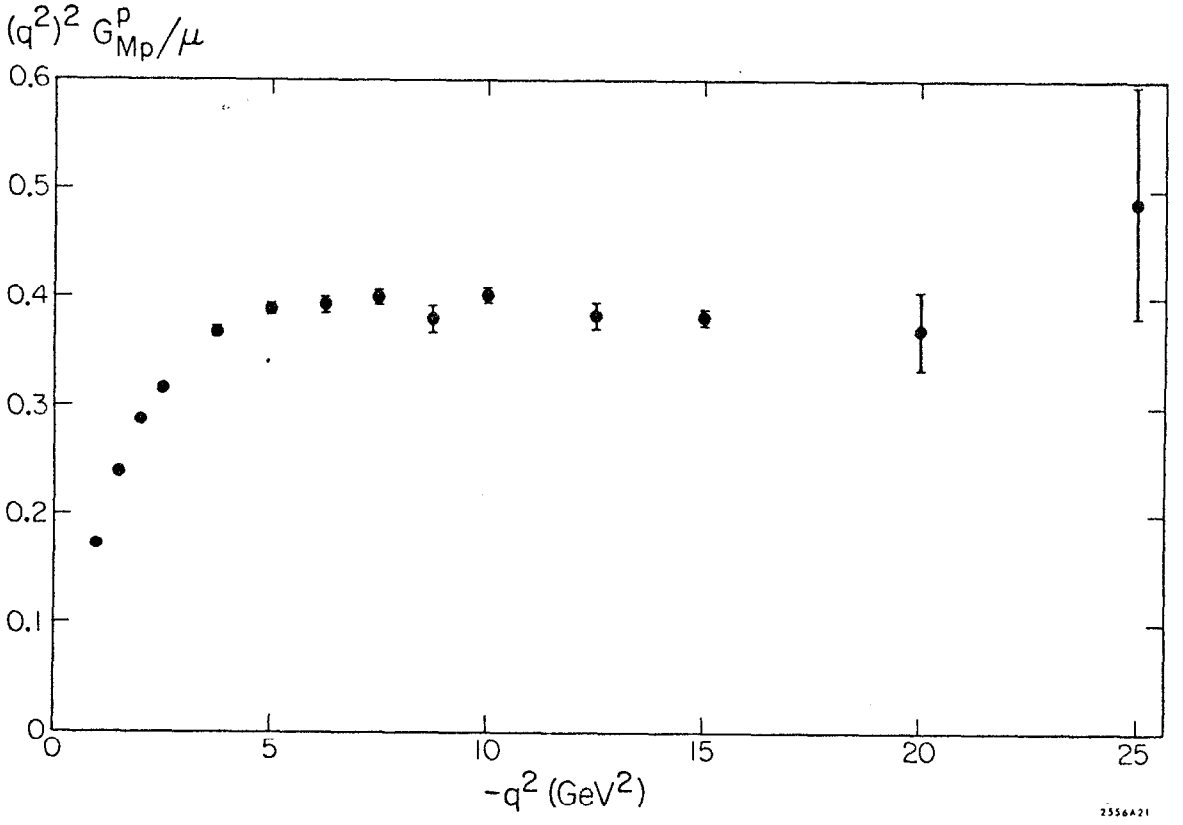

FIG. IVC.1

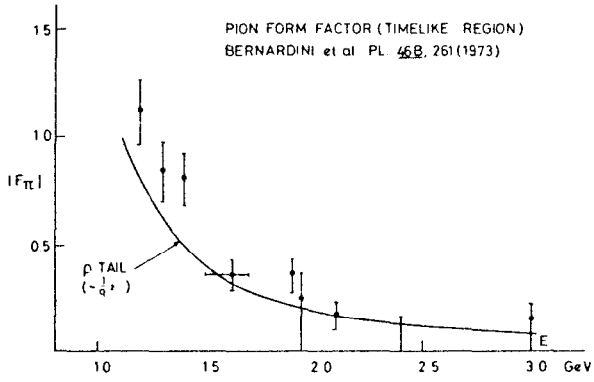
PION FORM FACTOR (TIMELIKE REGION)
BERNARDINI et al PL. 46B, 261 (1973)
1.5
1.0
0.5
|Fπ|
ρ TAIL
(~ 1/Q²)
E
1.0
1.5
2.0
2.5
3.0 GeV

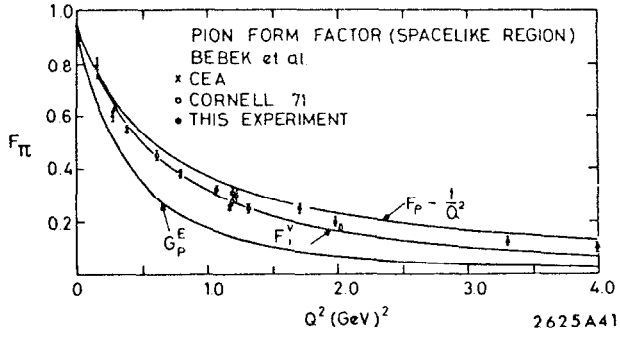
PION FORM FACTOR (SPACELIKE REGION)
BEBEK et al
x CEA
o CORNELL 71
• THIS EXPERIMENT
1.0
0.8
0.6
0.4
0.2
Fπ
Fρ ~ 1/Q²
F₁ᵛ
G_E^p
0
1.0
2.0
3.0
4.0
Q² (GeV)²
2625A41

FIG. IVC.2

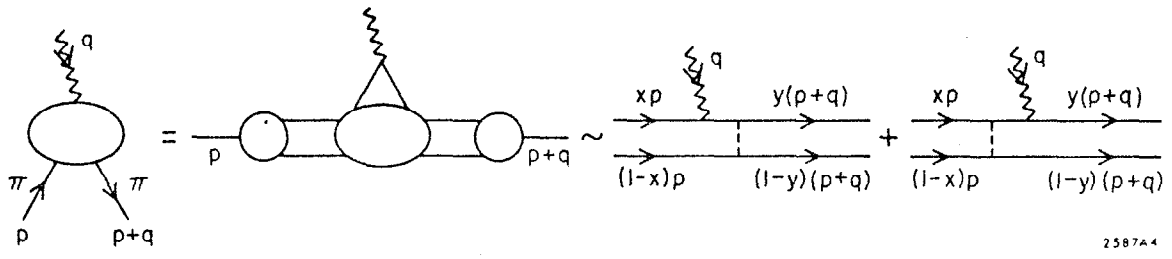

FIG. IVC. 3

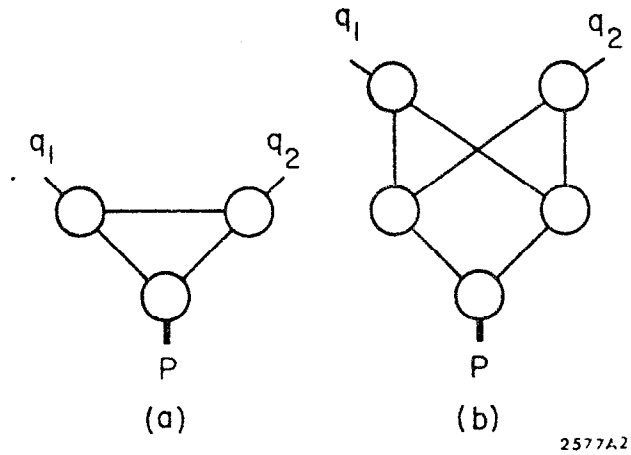

FIG. IVC.4

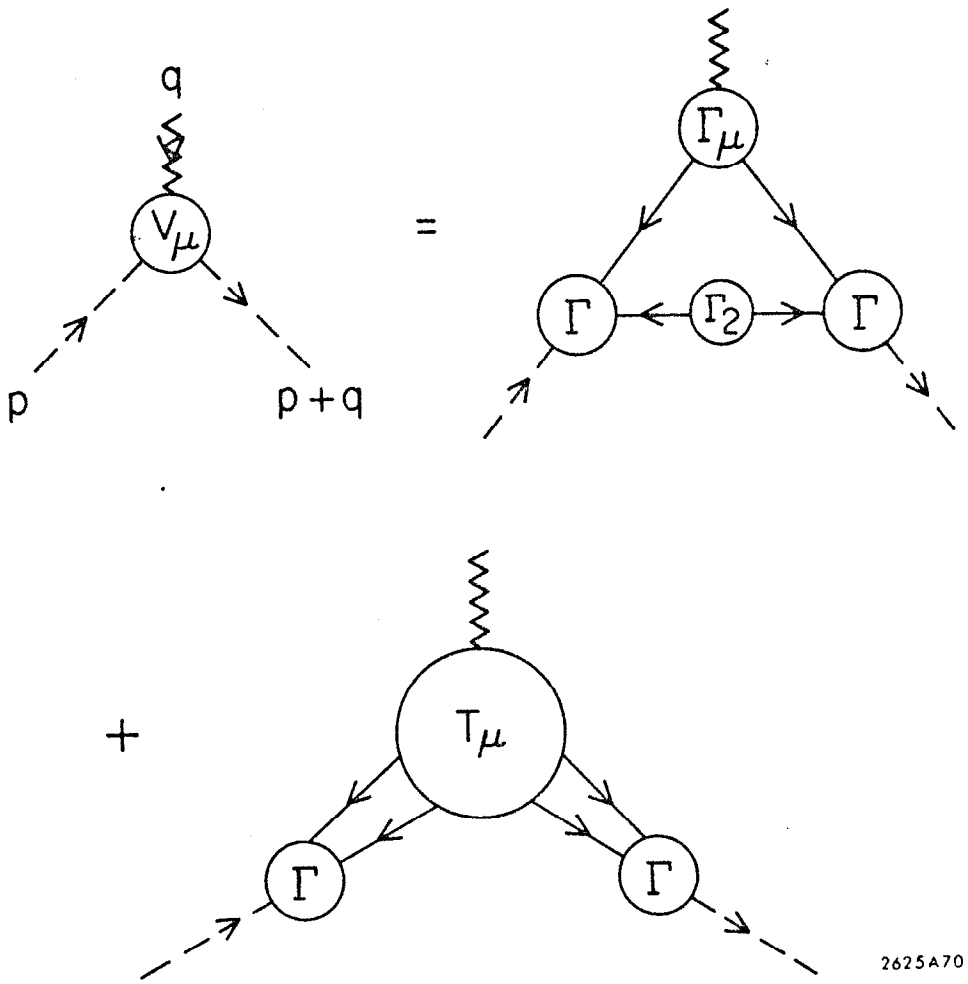
q
V_μ
p
p+q
=
Γ_μ
Γ
Γ_2
Γ
+
T_μ
Γ
Γ
2625A70

FIG. IVC.5

D. Soft Gluon Theories

These theories differ from the "hard" gluon theories, exemplified by the Wu-Yang model as extended by Abarbanel, Drell, and Gilman (1969), in that the exchange of soft gluons strongly modifies a single large t exchange (Fried, Gaisser and Kirby, 1970, 1971). This damping effect grows with momentum transfer and actually controls the large angle behavior. There are several versions of the model which use this same basic physical picture of the large t scattering process, and they seem to be very similar but differ in calculational details. The elastic scattering amplitude for pp $\rightarrow$ pp is of the form

$$\frac{d\sigma}{dt} = \left(\frac{d\sigma}{dt}\right)_{\text{Born}} \left[\exp\ 4\gamma\left(f(t) + f(u) - f(4m^2 - s)\right)\right] , \qquad \text{(IVD. 1)}$$

where the nucleon form factor at large t is given by

$$G(t) \propto \exp\left[\gamma\ f(t)\right] \quad . \qquad \text{(IVD. 2)}$$

The Born term due to the hard scattering interaction is usually taken to arise from a low spin (1 or 0) meson exchange. In the original model of Fried and Gaisser (1970), γ was taken to be constant and the function $f(t)$ was shown to behave as $\ell n\ t$. In the model of Contagouris et al. (1974), γ grows as $\ell n\ s$. This double log behavior was shown to arise in perturbation theory by Halliday, Huskins, and Sachrajda (1974a, b), who have clarified the basic properties required so that the above form holds. This double log was previously found to occur in the form factor in a calculation by Sudahov (1956) see Eq. (IVC. 7) and can be related to the soft photon forms of Yennie et al. (1961).

Since the effects of soft gluon damping become more important at large t, these theories can explain the large difference between the angular distributions of pp (K^+p) and $\bar{p}p$ (K^-p), for example. This is in sharp contrast to hard gluon

exchange theories that require single gluon exchange to dominate at large t and hence would have the cross sections equal.

The predictions of these theories for inclusive reactions is based on the same physical picture, in which neutral vector mesons are radiated and then decay to mesons. The inclusive cross sections achieve the form

$$E \frac{d\sigma}{d^3p} = H(x_T)\, s^{-n(x_T)} \quad , \qquad \text{(IVD. 3)}$$

where in the approximate calculation of Fried and Gaisser, $n = 2+4\gamma x_T$. This behavior is in agreement with the trends of the data, but it does not Feynman scale for $x_T \to 0$, see Fried (1974).

These theories give rise to a breaking of Bjorken scaling in deep inelastic lepton scattering but this can be made undetectably small at present energies. The associated multiplicities have also been discussed by Fried and Gaisser (1973a, b) and their results can be put in the general form discussed by Savit (1973). The recent work of Contagouris et al. (1974) is an ambitious attempt to fit a large amount of data with the few parameters in this type of model. One of the main questions is whether a natural and simple explanation of the particle ratios in inclusive scattering can be achieved.

Perhaps the most fundamental approach is that persued by Halliday, Huskins, and Sachrajda (1974a, b) who use perturbation theory on a vector gluon field theory to extract the asymptotic behavior extending the deep inelastic scattering work of Gribov and Lipatov (1972). The behavior of the form factor and exclusive scattering at fixed angle was found to be very similar to the above formula but the inclusive cross section was found to behave somewhat differently. At fixed x_T, it was found that many particles could be found with large p_T values, and additional logarithmic behavior arose at small x_T. The associated

production was found to be widely spread in p_T, with large p_T particles produced which were not correlated strongly with or against the large p_T trigger. Again Bjorken scaling is not satisfied in these theories. In contrast to scalar ϕ^3 theories that predict a finite multiplicity, vector theories yield a multiplicity that grows like a fractional power of ℓn s and in general depend on the p_T of the trigger.

It must be emphasized, however, that summing only the leading (double) logarithms in perturbation theory may not be an accurate guide to the true asymptotic behavior. A skeptic could well claim that the exponential sum of double logarithms sums to a negligible contribution compared to the remaining terms. This should be contrasted with the infrared problem in quantum electrodynamics, where Yennie, Frautshi and Suura (1961) demonstrated the exponentiation of all log λ dependence as a factor of the matrix element. A related problem occurs on the Regge behavior of the models. Halliday and Huskins (1975) have shown that for $p\bar{p} \rightarrow \pi^+\pi^-$, the sum of leading logarithms gives an exponential of double logarithms times an elementary Born term (fixed pole at j=1/2). Thus the procedure does not produce a moving pole, which would be expected in the complete amplitude.